



Topological mapping of neutrophil cytochrome b epitopes with phage-display libraries  
by James Barton Burritt

A thesis submitted in partial fulfillment of the requirements for the degree of Doctor of Philosophy in  
Microbiology

Montana State University

© Copyright by James Barton Burritt (1995)

Abstract:

Cytochrome b (Cyt b) of human neutrophils is the central component of the microbicidal NADPH-oxidase system. However, the folding topology of this integral membrane protein remains undetermined. Topological features of Cyt b were obtained by determining the epitopes of monoclonal antibodies (mAbs) 44.1 and 54.1, specific for the p22-phox and gp91-phox Cyt b chains, respectively. Two random-sequence bacteriophage peptide libraries were used as sources of surrogate epitopes for each of the mAbs. Recombinant DNA technology was used to construct the M13KBst phage vector used in the production of one such library. M13KBst offers the benefits of high copy replicative form, large plaque formation, and a kanamycin resistance gene. The vector also has a pair of noncomplimentary BstXI restriction sites positioned near the 5' end of the PIII gene. Insertion of foreign DNA between the BstXI sites allows phage surface-display of the protein corresponding to the foreign DNA. The J404 nonapeptide library produced with the M13KBst vector contains  $5 \times 10^8$  unique phage, each expressing a different peptide sequence fused to the amino terminus of the pIII capsid protein. Phage selected by mAb 44.1 displayed the consensus peptide sequence, GGPQVXPI, which is nearly identical to 181GGPQVNPI188 of p22-phox. A second method of antibody-mediated peptide selection using mAb 44.1 suggested the epitope bound by this mAb may contain both the 181GGPQVNPI188 and 29TAGRF33 regions of p22-phox and suggests phage-display library analysis may be used to identify discontinuous segments of Cyt b juxtaposed by tertiary structure as well as simple linear epitopes. Phage selected by mAb 54.1 displayed the consensus sequence, PKXAVDGP, which resembles 382PKIAVDGP389 of gp91-phox. Western blotting demonstrated specific binding of each mAb to the respective Cyt b subunit and selected phage peptides. In flow cytometric analysis, mAb 44.1 bound only permeabilized neutrophils, while 54.1 did not bind intact or permeabilized cells. However, mAb 54.1 immunosedimented detergent solubilized Cyt b in sucrose gradients. These results suggest the 181GGPQVNPI188 segment of p22-phox is accessible on its intracellular surface, but the 382PKIAVDGP389 region on gp91-phox is not accessible to antibody, and probably not on the protein surface.

**TOPOLOGICAL MAPPING OF NEUTROPHIL CYTOCHROME B  
EPITOPES WITH PHAGE-DISPLAY LIBRARIES**

by

**James Barton Burritt**

A thesis submitted in partial fulfillment  
of the requirements for the degree

of

Doctor of Philosophy

in

Microbiology

MONTANA STATE UNIVERSITY  
Bozeman, Montana

May, 1995

D318

B9451

**APPROVAL**

of a thesis submitted by

James Barton Burritt

This thesis has been read by each member of the thesis committee and has been found to be satisfactory regarding content, English usage, format, citations, bibliographic style, and consistency, and is ready for submission to the College of Graduate Studies.

5/25/95  
Date

*Alvin J. Isaacs*  
Chairperson, Graduate Committee

Approved for the Major Department

5/25/95  
Date

*Alvin J. Isaacs*  
Head, Major Department

Approved for the College of Graduate Studies

7/8/95  
Date

*Ed Brown*  
Graduate Dean

**TOPOLOGICAL MAPPING OF NEUTROPHIL CYTOCHROME B  
EPITOPES WITH PHAGE-DISPLAY LIBRARIES**

**James Barton Burritt**

Advisor: Algirdas J. Jesaitis, Ph.D.

Montana State University  
1995

Abstract

Cytochrome *b* (Cyt *b*) of human neutrophils is the central component of the microbicidal NADPH-oxidase system. However, the folding topology of this integral membrane protein remains undetermined. Topological features of Cyt *b* were obtained by determining the epitopes of monoclonal antibodies (mAbs) 44.1 and 54.1, specific for the p22-*phox* and gp91-*phox* Cyt *b* chains, respectively. Two random-sequence bacteriophage peptide libraries were used as sources of surrogate epitopes for each of the mAbs. Recombinant DNA technology was used to construct the M13KBst phage vector used in the production of one such library. M13KBst offers the benefits of high copy replicative form, large plaque formation, and a kanamycin resistance gene. The vector also has a pair of noncomplimentary *Bst*XI restriction sites positioned near the 5' end of the PIII gene. Insertion of foreign DNA between the *Bst*XI sites allows phage surface-display of the protein corresponding to the foreign DNA. The J404 nonapeptide library produced with the M13KBst vector contains  $5 \times 10^8$  unique phage, each expressing a different peptide sequence fused to the amino terminus of the pIII capsid protein. Phage selected by mAb 44.1

displayed the consensus peptide sequence, GGPQVXPI, which is nearly identical to  $^{181}\text{GGPQVNPI}^{188}$  of p22-*phox*. A second method of antibody-mediated peptide selection using mAb 44.1 suggested the epitope bound by this mAb may contain both the  $^{181}\text{GGPQVNPI}^{188}$  and  $^{29}\text{TAGR}^{33}$  regions of p22-*phox* and suggests phage-display library analysis may be used to identify discontinuous segments of Cyt b juxtaposed by tertiary structure as well as simple linear epitopes. Phage selected by mAb 54.1 displayed the consensus sequence, PKXAVDGP, which resembles  $^{382}\text{PKIAVDGP}^{389}$  of gp91-*phox*. Western blotting demonstrated specific binding of each mAb to the respective Cyt *b* subunit and selected phage peptides. In flow cytometric analysis, mAb 44.1 bound only permeabilized neutrophils, while 54.1 did not bind intact or permeabilized cells. However, mAb 54.1 immunosedimented detergent solubilized Cyt *b* in sucrose gradients. These results suggest the  $^{181}\text{GGPQVNPI}^{188}$  segment of p22-*phox* is accessible on its intracellular surface, but the  $^{382}\text{PKIAVDGP}^{389}$  region on gp91-*phox* is not accessible to antibody, and probably not on the protein surface.

**STATEMENT OF PERMISSION TO USE**

In presenting this thesis in partial fulfillment of the requirements for a doctoral degree at Montana State University, I agree that the Library shall make it available to borrowers under rules of the Library. I further agree that copying of this thesis is allowable only for scholarly purposes, consistent with "fair use" as prescribed in the U.S. Copyright Law. Requests for extensive copying or reproduction of this thesis should be referred to University Microfilms International, 300 North Zeeb Road, Ann Arbor, Michigan 48106, to whom I have granted "the exclusive right to reproduce and distribute my dissertation for sale in and from microform or electronic format, along with the right to reproduce and distribute my abstract in any format in whole or in part."

Signature



Date

6/7/05

## TABLE OF CONTENTS

Chapter	Page
1. INTRODUCTION .....	1
Phagocyte NADPH-Oxidase System .....	1
Diseases of an Ineffective NADPH-oxidase .....	4
The Respiratory Burst .....	7
Superoxide Anion .....	10
Hydrogen Peroxide .....	10
Hydroxyl Radical .....	11
Myeloperoxidase .....	11
Degranulation .....	12
Oxygen-independent Microbicidal Factors .....	15
Formylpeptide Receptor and Signal Transduction .....	15
Oxidative Damage by Neutrophils .....	20
Cytochrome b <sub>558</sub> .....	22
Epitope Mapping .....	24
Synthetic Peptide Libraries .....	26
Random Sequence Phage-display Peptide Libraries .....	29
Filamentous Bacteriophages .....	29
Natural Distribution .....	31
Characteristics .....	32
Phage proteins: Capsid Components .....	34
Phage Proteins: DNA Synthesis .....	38
Phage Proteins: Virion Assembly .....	40
Control of Gene Expression .....	42
Transcription .....	42
Translation .....	43
Phage Biology .....	44
Lysogeny .....	46
Filamentous Bacteriophage in Molecular Biology .....	46
Production and Use of a Phage-Display Peptide Library ...	47
Other Uses of Phage-display Technology .....	57
Point by point aims of the Dissertation .....	59
Goals and Experimental Design .....	60
References Cited .....	62
2. NONAPEPTIDE PHAGE-DISPLAY LIBRARY CONSTRUCTED WITH NOVEL M13 VECTOR .....	77
Abstract .....	77
Introduction .....	79
Materials and Methods .....	81

**TABLE OF CONTENTS-continued**

Chapter	Page
Reagents . . . . .	81
Construction of M13KBst . . . . .	81
Production of Library . . . . .	83
Results . . . . .	87
Vector Construction . . . . .	87
Library Production . . . . .	94
Discussion . . . . .	101
References Cited . . . . .	107
3. TOPOLOGICAL MAPPING OF NEUTROPHIL CYTOCHROME B EPITOPES WITH PHAGE-DISPLAY LIBRARIES . . . . .	111
Abstract . . . . .	111
Introduction . . . . .	113
Materials and Methods . . . . .	116
Reagents . . . . .	116
Epitope library and bacterial strains . . . . .	116
Affinity purification . . . . .	116
Phage amplification . . . . .	117
Sequencing phage . . . . .	118
Large scale purification of selected phage . . . . .	119
Neutrophil preparation and FACS analysis . . . . .	119
Western blotting . . . . .	120
Cyt <i>b</i> Immunosedimentation . . . . .	121
Results . . . . .	123
Identification of Monoclonal Antibody Epitopes . . . . .	123
Immunological Analysis . . . . .	125
Discussion . . . . .	138
References Cited . . . . .	143
4. IDENTIFICATION OF A DISCONTINUOUS CYTOCHROME B EPITOPE WITH A NONAPEPTIDE PHAGE-DISPLAY LIBRARY . . . . .	148
Abstract . . . . .	148
Introduction . . . . .	150
Materials and Methods . . . . .	152
Reagents . . . . .	152
Colony-lift Immunological Screening . . . . .	152
Mutant Phage Construction . . . . .	153
Western Blot of Mutant . . . . .	155
Western Blot to Show Effect of TAGRF Sequence . . . . .	156

**TABLE OF CONTENTS-continued**

<b>Chapter</b>	<b>Page</b>
Results .....	157
Discussion .....	165
References Cited .....	172
5. CONCLUSION .....	174
References Cited .....	183
APPENDIX .....	185

## LIST OF TABLES

Table	Page
1. Known NADPH-oxidase Subunit Proteins . . . . .	3
2. Filamentous (Ff) Phage Proteins . . . . .	35
3. Recombinant Phage-display Vectors . . . . .	48
4. Minimum Inhibition Concentration (MIC) Values for M13KBst and pUC119.K-borne APT Genes . . . . .	94
5. Deduced Amino Acid Sequences of Random Peptides Displayed on Unfractionated J404 Library Members . . . . .	98
6. Deduced Amino Acids of in-First Two Positions in Random Region of Unfractionated J404 Library . . . . .	100
7. Deduced Amino Acid Sequence of Peptides on Phage Clones Selected by Immunological Screening . . . . .	158
8. Deduced Unique Peptide Sequences of Phage Selected by Binding to F-actin . . . . .	177
9. Deduced Amino Acid Sequences of p47- <i>phox</i> - binding Phage Displaying Sequences of Homology with Cyt b . . . . .	179
10. One Letter Abbreviations for the Amino Acids . . . . .	186
11. One Letter Abbreviations for Nucleosides . . . . .	187
12. Synthetic Oligonucleotides Used . . . . .	188
13. Procedure for Sequencing M13 and fd Phage . . . . .	189
14. Procedure for Producing "Starved" K91 cells . . . . .	191

## LIST OF FIGURES

Figure	Page
1. Components of the NADPH-oxidase System . . . . .	5
2. Salient Features of the Signal Transduction Events following Stimulation of the Formylpeptide Receptor . . . . .	17
3. Affinity Purification of Phage on Column . . . . .	56
4. Agarose Gel Analysis of DNA During Oligonucleotide-directed Mutagenesis . . . . .	88
5. Agarose Gel Analysis of Mutant Phage Clones Which Demonstrate Cutting by <i>Bst</i> XI . . . . .	89
6. Nucleotide Sequence Analysis of Mutations Which Create M13KBst . . . . .	91
7. Agarose Preparative Gel for Harvest of the 1.4 kBp <i>Pst</i> I Fragment of pUC119.K Containing the APT Gene . . . . .	92
8. Agarose Gel Analysis of M13KBst DNA in Preparation of J404 Library Construction . . . . .	95
9. Representation of Deduced Amino Acids in Random Nonapeptides of Unfractionated J404 Library Members . . . . .	99
10. Selection of Phage from a Phage-Display Library by Affinity Chromatography . . . . .	127
11. Hexapeptide and Nonapeptide Sequences Selected on mAb Affinity Matrices . . . . .	128
12. Location of Similarity Between Antibody-selected Phage Sequences and Primary Structure of Cyt b . . . . .	129
13. Specificity of mAb for Cyt <i>b</i> and Phage pIII Proteins . . . . .	130
14. FACS Analysis of Neutrophils Stained with mAb 44.1 . . . . .	132

**LIST OF FIGURES-continued**

<b>Figure</b>		<b>Page</b>
15.	Specific Phage Block mAb 44.1 Binding to Permeabilized Neutrophils . . . . .	134
16.	FACS Analysis of Neutrophils Stained with mAb 54.1 . . . . .	135
17.	Immunosedimentation of mAbs with Detergent- solubilized Cyt <i>b</i> . . . . .	136
18.	Colony-lift Immunological Screening of Phage Expressing Peptides Recognized by mAb 44.1 . . . . .	160
19.	Western Blotting of Putative Epitope Regions Recognized by mAb 44.1 . . . . .	161
20.	Western Blot Analysis Illustrates Perturbing Effect of Specific Peptides for mAb 44.1 Epitopes . . . . .	164
21.	Model of Comparison Between Hypothetical Phage-displayed Consensus Epitope for mAb 44.1 and Native p22- <i>phox</i> Epitope . . . . .	168

## ABSTRACT

Cytochrome *b* (Cyt *b*) of human neutrophils is the central component of the microbicidal NADPH-oxidase system. However, the folding topology of this integral membrane protein remains undetermined. Topological features of Cyt *b* were obtained by determining the epitopes of monoclonal antibodies (mAbs) 44.1 and 54.1, specific for the p22-*phox* and gp91-*phox* Cyt *b* chains, respectively. Two random-sequence bacteriophage peptide libraries were used as sources of surrogate epitopes for each of the mAbs. Recombinant DNA technology was used to construct the M13KBst phage vector used in the production of one such library. M13KBst offers the benefits of high copy replicative form, large plaque formation, and a kanamycin resistance gene. The vector also has a pair of noncomplimentary *Bst*XI restriction sites positioned near the 5' end of the PIII gene. Insertion of foreign DNA between the *Bst*XI sites allows phage surface-display of the protein corresponding to the foreign DNA. The J404 nonapeptide library produced with the M13KBst vector contains  $5 \times 10^8$  unique phage, each expressing a different peptide sequence fused to the amino terminus of the pIII capsid protein. Phage selected by mAb 44.1 displayed the consensus peptide sequence, GGPQVXPI, which is nearly identical to  $^{181}\text{GGPQVNPI}^{188}$  of p22-*phox*. A second method of antibody-mediated peptide selection using mAb 44.1 suggested the epitope bound by this mAb may contain both the  $^{181}\text{GGPQVNPI}^{188}$  and  $^{29}\text{TAGR}^{\text{F}33}$  regions of p22-*phox* and suggests phage-display library analysis may be used to identify discontinuous segments of Cyt *b* juxtaposed by tertiary structure as well as simple linear epitopes. Phage selected by mAb 54.1 displayed the consensus sequence, PKXAVDGP, which resembles  $^{382}\text{PKIAVDGP}^{389}$  of gp91-*phox*. Western blotting demonstrated specific binding of each mAb to the respective Cyt *b* subunit and selected phage peptides. In flow cytometric analysis, mAb 44.1 bound only permeabilized neutrophils, while 54.1 did not bind intact or permeabilized cells. However, mAb 54.1 immunosedimented detergent solubilized Cyt *b* in sucrose gradients. These results suggest the  $^{181}\text{GGPQVNPI}^{188}$  segment of p22-*phox* is accessible on its intracellular surface, but the  $^{382}\text{PKIAVDGP}^{389}$  region on gp91-*phox* is not accessible to antibody, and probably not on the protein surface.

## CHAPTER ONE

### INTRODUCTION

#### Phagocyte NADPH-Oxidase System

The NADPH-oxidase system of phagocytic cells is a plasma membrane redox system that produces reactive oxygen metabolites important for the destruction of invading microbes. A heterodimeric membrane-bound cytochrome b (Cyt b), comprised of the subunits gp91-*phox* and p22-*phox*, functions as the central component of the multi-subunit oxidase system. The result of this system is the transfer of singlet electrons from a reduced flavin moiety to an oxygen acceptor bound to Cyt b and accessible to the exterior aspect of the cell. On the external surface of the cell or within the phagocytic vacuole, the reduced oxygen, in the form of superoxide anion ( $O_2^-$ ), undergoes subsequent redox conversions to form other microbicidal oxidants important for the destruction of the microbe (7).

Neutrophils are unique among phagocytic cells in their ability to respond to chemoattractant stimuli and deliver a microbicidal response within seconds. They are well equipped for this role by possessing elaborate mechanisms of sensory detection, adhesion, migration, and microbicidal potential. In the circulating neutrophil, the anti-microbial mechanisms are inactive, and the components of the NADPH-oxidase remain in a disassembled configuration. However, within seconds following appropriate

stimulation by a variety of stimuli including chemoattractants, rapid assembly of the oxidase promotes the immediate production of superoxide and other necessary compounds for neutralization of most pathogens.

When the neutrophil is stimulated by a defined chemical signal, the sequence of the microbicidal responses are sequentially orchestrated. For example, less than 1 nanomolar concentrations of the bacterial product, fMet-Leu-Phe (fMLF), is capable of stimulating chemoattractant migration. However, production of superoxide generally does not take place until this compound is present in concentrations greater than 10 nM. Concentrations of fMLF sufficient for superoxide generation are probably only encountered in the neutrophil following engulfment of a microorganisms. Therefore, deployment of the microbicidal ordnance does not occur before it can be applied directly to the pathogen.

Activation of the cell to produce superoxide can be initiated by a number of events, and leads to a rapid increase of phagocyte oxygen consumption, known as the respiratory burst (7). The burst occurs immediately following assembly of several oxidase components of the oxidase on the cytosolic aspect of the cell membrane. Translocated factors include p47-*phox*, p67-*phox*, and Rac (45,49,121,147). The NADPH-oxidase components are tabulated in Table 1, and the assembled NADPH-oxidase is schematically represented in Figure 1. Exposure of the neutrophil to a variety of extracellular substances is known to activate the oxidase; cytokines, bacterial products, chemoattractants, aggregated immunoglobulins, activated complement factors, and inflammatory products are known examples. These substances cause signal

transduction activity of the cytosol by way of membrane transduction mechanisms (13), resulting in the production of superoxide. Direct activation of the oxidase with arachidonic acid (32,102), sodium dodecyl sulfate (21), and phosphatidic acid has been shown in cell free systems suggesting additional mechanisms of NADPH-oxidase activation.

Table 1. Known NADPH-oxidase Subunit Proteins

Protein	Location <sup>a</sup>	Deficiency in CGD <sup>b</sup>	Relative Molec. Wt. <sup>c</sup>	Chromosome (Ref.) Location
p22- <i>phox</i>	plasma membrane	yes	22 kDa	16 q24 (40,115)
gp91- <i>phox</i>	plasma membrane	yes	91 kDa	X p 21.1 (130)
p47- <i>phox</i>	cytosol	yes	47 kDa	7 q 11.23 (160)
p67- <i>phox</i>	cytosol	yes	67 kDa	1 q 25 (93)
Rap1A	plasma membrane	unknown	22 kDa	? (123)
Rac	cytosol	unknown	24 kDa	? (38)

<sup>a</sup> Location in unactivated human neutrophils.

<sup>b</sup> Chronic Granulomatous Disease

<sup>c</sup> Determined by SDS-PAGE (88).

In the absence of oxygen, which normally functions as the terminal electron acceptor for this system, an alternative mechanism(s) appears to ensure the maintenance of electron flow. This oxygen-independent activity is not dependent on the availability of p47-*phox* and can be measured with diaphorase, a dye reductase (31). In this case, assembly of the NADPH-oxidase components does not result in the

production of superoxide but may ensure other microbicidal neutrophil functions linked to the oxidase. Interleukin-4 has been shown to affect the oxidase in porcine macrophages and manifests an inhibitory effect on the mRNA level of the gp91-*phox*, but not p22-*phox* (164). Though the role of membrane carbohydrate groups in the activation of the oxidase is unclear, 20% membrane desialylation in neutrophils prevents activation of oxidase activity despite normal phagocytosis and hexose monophosphate shunt (HMP) activity associated with the active oxidase (152).

Following ingestion of a microbe by a neutrophil, the respiratory burst and degranulation constitute the hallmark of the neutrophil immune response. The two processes act independently, but are complimentary in the microbicidal response.

#### Diseases of an Ineffective NADPH-oxidase

Several diseases result from genetic anomalies which affect components of the NADPH-oxidase. The frequency of these diseases is about one in one million and familial patterns suggest classic Mendelian inheritance. Conditions associated with the diseases manifest primarily in the skin, lungs, lymph nodes, bone, and liver. The etiology of each disease is a mutation of the gene encoding a subunit of the NADPH-oxidase system, and diseases characterized at this time have involved either the gp91-*phox*, p22-*phox*, p47-*phox*, or p67-*phox* subunits. The genetic defect that affects gp91-*phox* accounts for about 55% of cases of disease, and is X-linked. The locus for this gene maps in close proximity to the locus for Duchenne muscular dystrophy, and some cases have been reported of unfortunate individuals affected by both diseases.

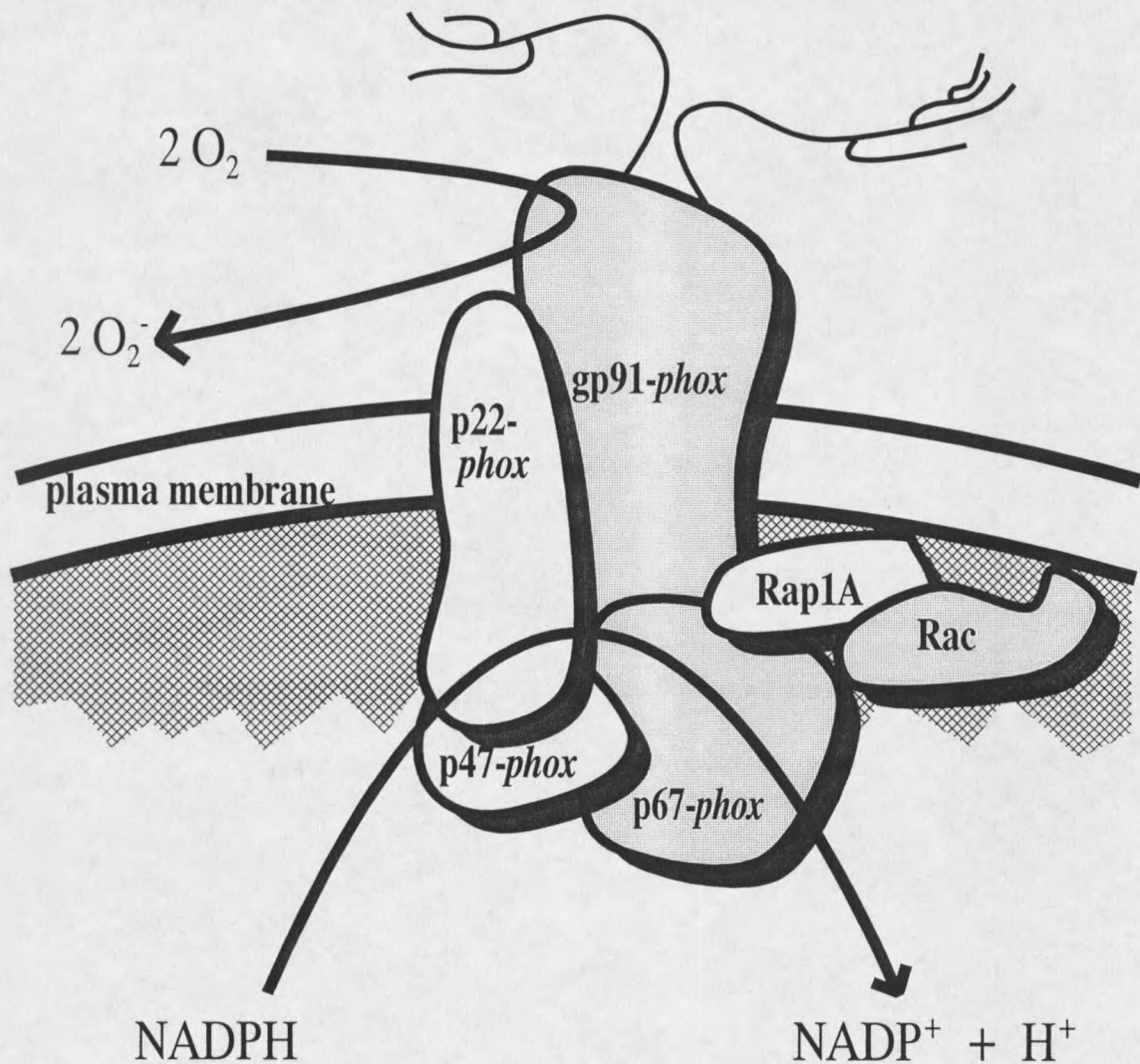


**Figure 1.** Components of the assembled NADPH-oxidase System. Cytochrome b<sub>558</sub> is comprised of p22-phox and gp91-phox. Cytosolic factors are Rac, p47-phox and p67-phox. Rap 1A is associated with the plasma membrane. This model reflects the activated complex as it exists during the oxidation of NADPH and subsequent reduction of molecular oxygen which generates the superoxide anion.

Inheritance for all other currently known diseases associated with the oxidase is autosomal recessive. These heterogeneous diseases of the NADPH-oxidase, regardless of the underlying genetic lesion, are known as chronic granulomatous disease (CGD) (12,33,39,91,94,140,147).

Patients with diseases of the NADPH-oxidase exhibit an abnormal inflammatory response when challenged by bacterial and fungal pathogens. The functional result in each case is a failure of the respiratory burst and attendant microbicidal activity, predisposing the affected individual to repeated life-threatening infections and granulomatous lesions. Because of the inability of neutrophils in these patients to kill, but not ingest microbes, persistence of microorganisms in endocytic vesicles of accumulated phagocytic cells appears to be associated with the granulomatous lesions which typify the disease. The granulomas themselves contain giant multinucleated cells, resulting from the fusion of macrophages with monocytes. These cells are sometimes distended with lipid material, reminiscent of some lipid storage diseases. The granulomas may become enlarged to the point that strictures in the digestive and urinary tracts result, precluding the normal passage of waste.

Microorganisms most often associated with infections in CGD patients belong to the genera, *Staphylococcus*, *Pseudomonas*, *Aspergillus*, some *Candida*, *Nocardia*, and many Gram negative rods belonging to the Enterobacteriaceae group. Catalase-negative organisms such as the lactobacilli and streptococci are generally not associated with infections of CGD patients. These organisms lack heme synthesis and are unable to produce heme proteins which reduce molecular oxygen to water. The

metabolic systems of these organisms reduce oxygen to hydrogen peroxide and release it into the medium. The inability of these organisms to produce catalase prevents them from degrading the self-generated hydrogen peroxide, which then is able to complement the deficiency in cells of CGD patients. Therefore, hydrogen peroxide produced by the streptococci is available to the microbicidal machinery of the neutrophil, and is ultimately used in destruction of the organism.

Despite the morbidity and mortality associated with CGD (12,91), molecular and genetic analysis in human cases has allowed discovery and examination of several components required for the functional oxidase complex.

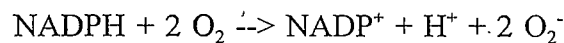
Gene therapeutic measures which address deficiencies in CGD patients are limited at this time. However, some progress toward this goal has been reported recently, primarily by the use of retroviral gene delivery systems (95,98,119).

### The Respiratory Burst

The respiratory burst of neutrophils is the sudden increase in oxidative metabolism that occurs during the ingestion of microorganisms. This event takes place as molecular oxygen is consumed and reactive oxygen metabolites are produced. Under anaerobic conditions, both the respiratory burst and microbicidal effect are abrogated. The burst can result from any of a variety of appropriate stimuli in functional neutrophils. These stimuli activate the NADPH-oxidase system in an event which is not perturbed by classic inhibitors of mitochondrial metabolism, such as cyanide and azide. These unusual properties of neutrophils were first reported in 1933

(8), when they were described as the "extra respiration of neutrophils." It was concluded at that time that the event represented an unusual mechanism of microbial killing which involved oxygen metabolites.

Once triggered, the respiratory burst is fueled by energy derived from the hexose monophosphate shunt. A diffusible proton/electron carrier such as NADP<sup>+</sup> delivers the metabolic electron-proton pair from the HMP to the cytochrome system and electron transport chain on the cytosolic aspect of the cell membrane. The protons are deposited in the periplasmic space to establish and maintain the proton motive force (PMF), and the electrons are similarly displaced to the external surface of the cell by the NADPH-oxidase, where it reduces molecular oxygen to form superoxide. The overall reactions of the electron transport can be summarized as:



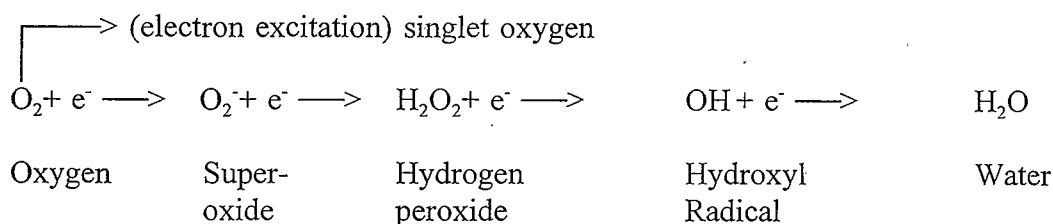
The result of this event is the production of superoxide anion on the external surface of the cell which neutralizes the positively charged PMF, causing a membrane depolarization which is greatest at 40 seconds following maximal cell stimulation. This burst-associated depolarization is not found to occur in neutrophils of CGD patients, supporting the belief that superoxide is at least partially responsible for depolarization.

A significant limitation to the study of the NADPH-oxidase system has been the difficulty with which components of this system can be extracted in a functional

form from the neutrophils. In 1985, it was reported that superoxide production could be studied in cell-free systems when using anionic detergents such as arachidonic acid or sodium dodecyl sulfate when combined with cytosolic and membrane fractions extracted from neutrophils (21,32,102). By many indications, these *in vitro* reactions closely parallel events of the oxidase in the cell, and have therefore made the cell-free assay a useful representation of the system. This technique has led to the understanding of several features of component localization and interaction. Furthermore, because components can be introduced into a system which occurs naturally within the cell membrane, the influence of novel compounds and conditions can easily be tested. Recently, the production of recombinant proteins in baculovirus or bacterial expression systems has proven to be an advancement in the study of this and other multiprotein systems. An active NADPH-oxidase in a cell-free system has been constructed solely from cloned and expressed proteins (128).

Molecular oxygen is the obligate electron acceptor of the NADPH-oxidase when reactive oxygen intermediates are produced. Under normal conditions, molecular oxygen may be regarded as being kinetically (but not thermodynamically) inert, and therefore, unlikely to form compounds without participation of a catalyst (81). This property of oxygen results because electrons in molecular oxygen occur in paired spin configurations of opposite polarity. However, if oxygen is reduced by a low-potential oxidant, the addition of an additional electron results in the superoxide free radical with unusual properties.

Superoxide Anion Superoxide anion is capable of dismutation (oxidation-reduction) which results in the formation of a number of highly reactive oxygen species. Substances such as singlet oxygen, hydrogen peroxide, hydroxyl radical, and water are formed as shown below:



In an aqueous environment, superoxide lacks the necessary toxicity to be significantly microbicidal by itself. However, much of the reactivity of superoxide may take place in hydrophobic microenvironments within the cell membrane. In this setting, superoxide can act as a strong base and is capable of reactive nucleophilic attack. However, microorganisms which produce the enzyme superoxide dismutase are able to neutralize this substance, and are therefore protected from its toxic properties.

Hydrogen Peroxide Hydrogen peroxide is produced rapidly by dismutation of superoxide in stimulated neutrophils (81). Hydrogen peroxide is less reactive with many biological compounds than the hydroxyl radical and hypochlorous acid. Therefore, hydrogen peroxide demonstrates a greater penetrating ability than the more reactive compounds which tend to be consumed rapidly upon diffusion. For this reason, hydrogen peroxide may be the most microbicidal of the reactive oxygen compounds found in inflamed joint fluids and exudates where large amounts of

proteinaceous fluids occur. Sensitivity of bacteria to superoxide is usually dictated by the lack of microbial catalase and the glutathione reductase system, both of which act as peroxide scavengers. Neutrophils themselves are protected from the toxic effects of hydrogen peroxide by these mechanisms. The availability of hydrogen peroxide is crucial for the activity of myeloperoxidase (below).

Hydroxyl Radical The hydroxyl radical is one of the most reactive oxygen radicals known, and may be utilized in the burst oxidase repertoire of microbicidal compounds (81). It is also possible that the hydroxyl radical is produced as a result of the activity of myeloperoxidase (below). At this time, however, convincing demonstration of the importance of the hydroxyl radical in a microbicidal response has not been reported.

### Myeloperoxidase

Neutrophils contain all of their myeloperoxidase (MPO) within azurophilic storage granules. Therefore, the action of myeloperoxidase upon ingested microorganisms constitutes a union of degranulation and burst oxidase mechanisms. The activity of MPO can also be exerted beyond the periplasm, as diffusion, direct application, or cell lysis may present this enzyme outside the cell membrane (81). MPO constitutes as much as five percent of the neutrophil dry weight, and its inherent green color produces the characteristic green appearance of purulent material. The primary MPO transcript contains a 41 residue leader sequence and undergoes cleavage

by a signal peptidase and other post-translational modifications to produce subunits of 12 and 57 kDa (109). The native enzyme is a heterotetramer, comprised of two protomers, each of which contains a heavy and light subunit. Both heme and carbohydrate groups are coordinated by the large subunits.

As myeloperoxidase is released by the azurophilic granules into the phagosome during degranulation, it reacts with hydrogen peroxide and halide ions to form primarily hypochlorous acid, but other hypohalogenous acids, chloramine, aldehydes, and possibly singlet oxygen and hydroxyl radical (81). The toxic activity of these compounds to biological material in the phagosome generally belongs to either of the groups; oxidation or halogenation. The effect of these processes includes tyrosine and unsaturated fatty acid halogenation; oxidation of sulfhydryl groups, iron-sulfur centers and heme proteins; oxidative decarboxylation, deamination, and peptide cleavage; and lipid peroxidation. Surprisingly, individuals with nonfunctional MPO systems do not appear to be predisposed to infectious conditions. Perhaps this fact demonstrates the complementarity of various facets of the immune response, and the ability to rely on compensatory mechanisms in some instances.

### Degranulation

The granulocytes are comprised of three groups of leukocytes: neutrophils, eosinophils, and basophils. All three cell types harbor vesicular organelles or storage granules which contain materials important in the inflammatory response. The vesicles give these cells the typical granular appearance and the descriptive term for this group

of cells. Each of the granulocytes contains several different types of granules, but each contains a different predominant type. The cell types can be distinguished by Wright stain, according to the appearance of the specific (dominating) granule. On Wright stained blood smears, the specific granules of eosinophils stain strongly with the acidic stain eosin, and appear red. Those of basophils stain with a basic dye in the Wright stain, producing a dark blue color; and those of neutrophils show neutral staining, and assume a light pink color.

Degranulation refers to the redistribution of granule contents as the granule membranes fuse with other cellular membranes. Target membrane surfaces usually include either the phagosomal vacuoles or the plasma membrane. During this process, contents are deposited either within target phagosomes, or into the periplasmic space. Degranulation of the neutrophil usually takes place concomitantly with activation of the NADPH-oxidase, as pre-packaged microbicidal factors are introduced either into the phagosome containing ingested microbes, or into the periplasmic space in order to act upon adjacent target structures. Trafficking of the cellular granules to the phagosome or the plasma membrane may depend upon events associated with phagocytosis or activation of the neutrophil in the absence of phagocytosis, respectively.

It has long been recognized that exudate fluids associated with inflammatory processes contained many constituents of inflammatory cells. However, recent evidence suggests these products are actively deposited by degranulation and secretion, rather than by cellular lysis. Therefore, the process of degranulation may be regarded

as an important mechanism whereby cells which accumulate during the inflammatory response perform an active, rather than a passive role in presenting microbicidal compounds.

Neutrophils contain three types of granules: specific, azurophilic, and a group of less numerous heterogenic granules. Following phagocytosis, the fusion of each granule type with the phagosome appears to follow sequential order. This may allow granule contents to act in the phagolysosome in a manner which augments the pH optima for the presented enzymes. The compounds contained within each granule type and the prospective functions of the compounds have been the subject of considerable interest. Primary constituents of the azurophilic granules include defensin-like proteins, peroxidase, lysozyme, serine proteases such as elastase and cathepsin b, and acid phosphatase. Specific granules contain lactoferrin, histamine, collagenase, vitamin B binding proteins, and are a reservoir of plasma membrane proteins such as alkaline phosphatase, receptors such as fMLF and cytochrome b; and other granules contain acid phosphatases, glycolytic enzymes, acid proteinases, and gelatinase (64).

Because neutrophils can release the repertoire of antimicrobial compounds outside the cell membrane independently of phagosome formation, they are capable of destroying fungal elements and other organisms too large for ingestion. Unfortunately, normal tissue cells may also be damaged by inappropriately stimulated neutrophils in this way. In response to these non-ingestible targets, neutrophils attach to adjacent surfaces where they deposit the contents of the host-defensive granules and products of the respiratory burst. The term "frustrated phagocyte" has been used to describe these

cells which attack objects too large for ingestion by phagocytosis.

### Oxygen-independent Microbicidal Factors

Elucidation of the deficiencies associated with the NADPH-oxidase in CGD patients reduced the level of interest in other oxygen-independent microbicidal constituents of neutrophil. However, the clinical heterogeneity of CGD patients and observations that some pathogens were apparently destroyed by the cells of CGD patients suggested that other mechanisms of neutrophil-associated immune surveillance were involved. This led to the discovery of a number of compounds which exert the microbicidal effect independently of the reactive oxygen compounds (50). These include the cationic peptide-like compounds called defensins which share strong similarity to constituents of the insect immune system (44). Collectively, these oxidase-independent defensive factors constitute an important means of protection in several situations. For example, the activity of oxygen-independent microbicidal functions are critically important in cases where the NADPH-oxidase is impaired, as in CGD, or when molecular oxygen is not available to the neutrophil. Such conditions include sites of infection lacking adequate perfusion of oxygenated blood, and settings in which microbial challenge occurs concomitantly with severe cyanosis such as bacterial pneumonia.

### Formylpeptide Receptor and Signal Transduction

An enigmatic process of cell signalling is the mechanism by which many

different extracellular stimuli can be received, resulting in the engagement of appropriate effector systems, yet only limited avenues of communication exist between molecular systems within the cell. The specificity by which varied signal transduction systems are routed relies on exquisite linkage of involved cellular factors. Such factors include specific enzyme systems, and on the timing, concentration, and species of small substances mobilized or activated in response to the signal. These small substances are referred to as second messengers, and include cAMP, diacyl glycerol,  $\text{Ca}^{2+}$ , and inositol triphosphate ( $\text{IP}_3$ ).

The chemical responses which begin with the exposure of the neutrophil to bacterial products and result in cell adherence, aggregation, migration, the respiratory burst, and degranulation have received significant attention (27,96). Many of the signal transduction events associated with neutrophil activation have been revealed, yet perhaps many more remain obscure. Information about signal transduction in neutrophils has illuminated similar mechanisms in other cells.

The formylpeptide receptor (FPR) and associated signal transduction cascade is a well-characterized receptor-mediated chemical signaling system in human neutrophils and is involved in many microbicidal events (Figure 2). The gene encoding the FPR was cloned and sequenced, and the transcript was deduced to contain 350 amino acids and seven membrane-spanning domains predicted by hydrophathy analysis (19). Two other receptors, the C5a anaphylatoxin receptor and the platelet activating factor (PAF) receptor, have also been characterized in neutrophils (107). These receptors have sequence homology to the FPR and appear to share routes of neutrophil activation.

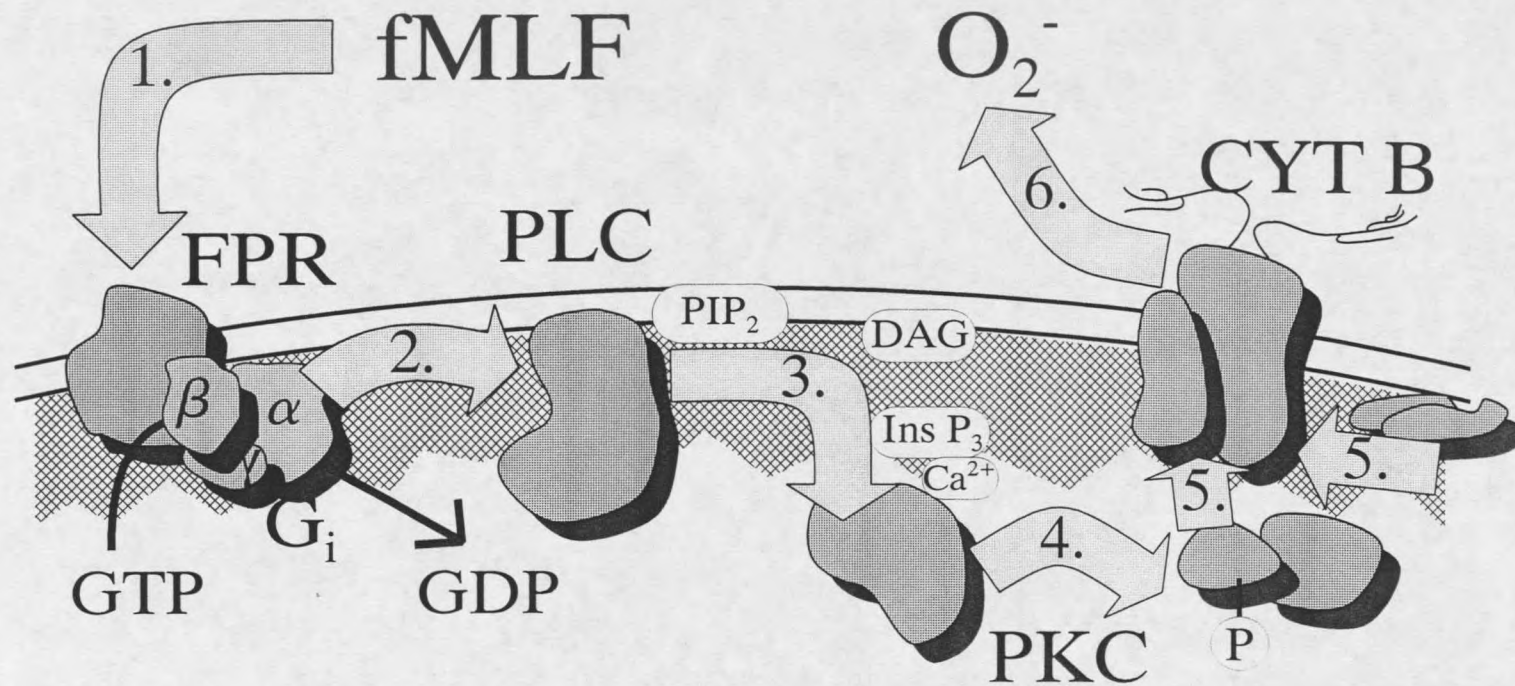


**Figure 2.** Salient features of signal transduction events leading to NADPH-oxidase activation following stimulation of the formylpeptide receptor. Step 1 depicts the binding of a formylpeptide such as f-met-leu-phe (fMLF) to the formyl peptide receptor (FPR) on the external aspect of the cell membrane. This event triggers the exchange of GDP for GTP by the heterotrimeric G-protein, G<sub>i</sub>, and activation of membrane bound phospholipase C (PLC) by the activated G-protein α subunit (step 2). The activated PLC then cleaves the membrane constituent, phosphoinositol diphosphate PIP<sub>2</sub>, producing diacylglycerol (DAG) and inositol triphosphate (Ins P<sub>3</sub>) as shown in step 3. Both DAG and Ins P<sub>3</sub> are capable of activating the phosphorylation of selected cytosolic proteins through the activation of protein kinase C (PKC) (step 4). The phosphorylation of proteins such as p47-*phox* and perhaps other cytosolic components appears to be involved in the assembly (step 5) of the NADPH-oxidase and attendant electron transfer, resulting in superoxide generation on the external surface of the cell (step 6).

The signal transduction initiated by each of these receptors converge at a cytosolic component which binds the internal aspect of the associated receptor. This component belongs to a group of about 25 known human heterotrimeric guanine-binding regulatory proteins, known as G-proteins.

G-proteins couple sensory and effector molecular systems in many cell types. The G-protein associated with FPR is known as  $G_{12}$  (28), and belongs to a group of related G-proteins which are sensitive to a toxin produced by the bacterium, *Bordetella pertussis* (155). This G-protein is a heterotrimer, comprised of the  $\alpha$ ,  $\beta$  and  $\gamma$  subunits. The mechanism of pertussis toxin sensitivity in these proteins appears to involve ADP-ribosylation of a cysteine residue near the carboxyl terminus of the alpha subunit of this G-protein. This modification interrupts or prevents the binding of the G-protein to the receptor.

The result of the signal transduction in the neutrophil FPR system includes many of the microbicidal functions, but for the present purpose, discussion will focus on activation of the respiratory burst. FPR binds effector formylpeptides with nanomolar affinity on the exterior surface of the cell membrane, causing a conformational change in the cytosolic regions of the receptor. This change influences the activation of  $G_i$  probably by the binding of GTP. The GTP-bound (active) form of  $G_{1\alpha}$  signals a membrane bound phospholipase C (PLC) (108), and perhaps less importantly, phospholipase D and  $A_2$  (27). PLC activation is dependent upon the presence of nanomolar levels of  $Ca^{2+}$  and activation of this enzyme is possible simply by increasing the  $Ca^{2+}$  concentration to the millimolar range. This result indicated  $Ca^{2+}$

levels alone may regulate PLC activation. However, recent evidence suggests the activation of PLC in these studies may have involved exogenous ATP, involving the recently identified ATP receptor on the surface of the cell (27). The PLC catalyzes the cleavage of the membrane constituent, phosphoinositol bisphosphate (PIP<sub>2</sub>). Enzymatic products of PIP<sub>2</sub> are equimolar amounts of diacyl glycerol (DAG) and inositol triphosphate (InsP<sub>3</sub>). Both DAG and InsP<sub>3</sub> act as second messengers which activate protein kinase C (PKC), either directly in the case of DAG, or indirectly as InsP<sub>3</sub> causes additional Ca<sup>2+</sup> release and subsequent PKC activation. Both the PLC and PKC enzymes exist as multiple isoenzyme forms, suggesting a heterogeneity of signals can be relayed by these components during signal transduction. The PLC, and to a lesser extent PKC (27), are variably sensitive to the activity of calcium. The alpha (calcium-sensitive) isoform predominates in human neutrophils, and upon activation, this PKC causes phosphorylation of serine and threonine residues of target proteins. Recent evidence suggests an additional target of activation by activated G<sub>i</sub> is the enzyme phosphatidylinositol 3-kinase, which is capable of initiating signal transduction by tyrosine phosphorylation (27).

A number of components of the NADPH-oxidase system include serine and threonine residues which may be substrates for PKC phosphorylation. For example, serine residues #303, 304, 320, and 328 of p47-*phox* have been reported as such targets (11). The result of FRP stimulation and subsequent signal transduction may therefore be phosphorylation of target oxidase components, required for assembly of the active NADPH-oxidase and production of superoxide.

### Oxidative Damage by Neutrophils

Antimicrobial functions of the NADPH-oxidase system offer continuous protection from many types of infection. The system targets the invading microbe with an antimicrobial response which usually causes minimal host injury. Under ideal conditions, precise regulation by complex interaction of at least six proteins prevents inappropriate activation of the system and serious damage to host tissues (33,127,147). However, the inappropriate generation of superoxide or inability to appropriately metabolize this anion radical contributes to tissue damage and inflammatory disease. The morbidity due to the deleterious interaction of neutrophil-generated toxic oxidants and injured tissue can be severe.

Noninfectious conditions which recruit and activate neutrophils may be exacerbated by neutrophil-generated toxic oxygen metabolites. Such conditions include arthritis, myocardial infarction, sunburn, ischemia-reperfusion, and hypertension. In these settings, neutrophil-generated oxidants damage tissues directly (101), and in the absence of a microbial target, neutrophil involvement appears primarily injurious. Important oxidants produced by activated neutrophils include superoxide anion ( $O_2^-$ ), hydrogen peroxide ( $H_2O_2$ ), hypochlorous acid (HOCl), and the hydroxyl radical ( $HO^\cdot$ ).

Recently, a novel interaction between superoxide and nitric oxide (NO) has been shown to produce peroxynitrite ( $ONOO^-$ ) which can result in the nitration of protein tyrosine groups. This effect is particularly debilitating to the motor neurons in patients suffering from amyotrophic lateral sclerosis (ALS). The etiology of ALS

involves a defect of the superoxide dismutase (SOD) enzyme which normally scavenges superoxide, resulting in a two-fold increase of superoxide at selected sites. The increased availability of superoxide in the microenvironment of the motor neurons reacts with neuron-generated nitric oxide which is produced normally to maintain synaptic plasticity. The resulting reaction between superoxide and nitric oxide produces the ONOO<sup>-</sup> radical, accelerating tyrosine nitration and attendant destruction of the single neuron which innervates muscle fibers (10). The destructive effects of tyrosine nitration are also believed to be associated with many types of inflammatory disorders, particularly in endothelial cells (9).

Each oxidant produced as a result of NADPH-oxidase causes a specific effect on cellular systems and supporting tissues. The result of these effects is the destruction of some enzymes and metabolic pathways, DNA damage, and malignant transformation (26). Superoxide dismutase and scavengers of the hydroxyl radical, such as catalase, dimethyl sulfoxide, dimethylthiourea, and mannitol, have proven protective not only to the oxidative damage of reperfusion injury, but also prevent the accumulation of neutrophils attendant with inflammation and reperfusion injury (165). Neutrophil depletion or pretreatment with monoclonal antibodies which block phagocyte attachment to the ICAM-1 molecule and subsequent emigration (79), signify the role of neutrophils in changes of microvascular permeability and reperfusion injury. These data suggest neutrophils are at least partially the cause and not an effect of reperfusion injury (65).

Cytochrome  $b_{558}$ 

Flavocytochrome b (Cyt b) (a.k.a., flavocytochrome *b*, cytochrome  $b_{558}$ , cytochrome  $b_{559}$ , cytochrome  $b_{245}$ ) is the central redox component of the NADPH-oxidase system of human neutrophils (39,150). Cyt b is a heterodimeric integral membrane protein comprised of two subunits, gp91-*phox* and p22-*phox* (114). The two subunits copurify on wheat germ agglutinin and immobilized heparin affinity columns (113). The p22-*phox* subunit has been selectively purified on hydroxyapatite and DEAE-Sephacel liquid chromatography columns (163).

Cyt b acts as the electron transferase that transfers metabolic electrons across the plasma membrane to the external surface of the cell where molecular oxygen is reduced to form  $O_2^-$ . Cyt b demonstrates the low mid-point potential of -245 mV (139), making it capable of reducing oxygen directly. For this reason, Cyt b is the likely terminal electron donor of the NADPH-oxidase system components. At least two heme groups have been shown to be associated with Cyt b (122), probably coordinated by heme iron atoms to histidine residues within membrane-spanning domains of both subunits (161). The gp91-*phox* subunit of Cyt b is believed to function as the NADPH-binding component of the oxidase (129,156,158). Affinity reductive radiolabeling of gp91-*phox* of human neutrophils with tritiated  $NaBH_4$  suggests the NADPH-binding domain of this subunit may undergo a conformational change during oxidase activation (124). The large subunit of Cyt b in bovine neutrophils is also believed to contain a domain for the binding of NADPH, based on the binding of the NADPH analog, azido-NADPH (42). However, reports by Umei *et*

*al.* (157,158), based on binding studies with  $^{32}\text{P}$ -labeled NADPH (156), or the NADPH 2',3'-dialdehyde derivative suggest the NADPH binding component of the oxidase may be a protein distinct from *gp91-phox*. The glycosylation of the large subunit is mainly N-acetyl-glucosamine and galactose, the extent of which depends on the type of cell (107).

Despite intense research on the NADPH-oxidase system for several decades, the molecular basis of CGD and the architecture of the assembled oxidase complex is not well understood due to a lack of knowledge about the interaction of protein subunits. Examination of the assembled complex outside the cell is difficult, owing to the instability of interactions between subunits and accessory groups during purification. That Cyt b acts as a flavin-dependent electron transferase is well accepted, and some evidence suggests that Cyt b itself (*gp91-phox*) may contain a flavin-binding domain (85,129,141). However, the existence of flavin proteins that couple with Cyt b to form superoxide suggests that the identification of the flavin-binding component in the cellular oxidase remains undefined.

As with other multicomponent systems, Cyt b probably coordinates interactions with other proteins, dictated by well-defined interactive sequences of the molecule (125). For example, Rap1a, and perhaps *p47-phox* (48,49), was shown to bind a region of Cyt b in a phosphorylation-dependent manner (18). Rap1a was found to copurify with heparin ultrogel purified Cyt b (123), though the molecular mechanism of the Rap1a association with Cyt b has not been determined. Additionally, the carboxyl terminus of *gp91-phox* which includes the  $^{558}\text{RGVHFIF}^{564}$  amino acid

sequence has been shown to be important in activation (127).

Because Cyt b is the primary, if not the sole NADPH-oxidase redox component, regions of Cyt b exposed to the cytosol probably function as important docking and interactive sites for the assembled oxidase complex (18). However, the inability to apply X-ray crystallography and nuclear magnetic resonance (NMR) structural methods to this integral membrane protein, implies that little is known about its structure. For this reason, the emphasis of this research has been placed upon the topology of Cyt b by epitope mapping. We have defined the exact location in the primary structure of Cyt b for two epitopes recognized by Cyt b subunit-specific mAbs. We then examined the location of the epitopes with respect to the sidedness of the neutrophil plasma membrane by FACS analysis. In this way, predictions could be made regarding the topology of this molecule.

### Epitope Mapping

In 1973, Anfinsen showed that the amino acid sequence of a protein provides information to direct its correct three-dimensional structure (4). Yet, after twenty years, the ability to predict the structure of a protein from its amino acid sequence still eludes us. For many proteins, including most integral membrane proteins such as Cyt b, application of powerful structural methods such as X-ray crystallography and NMR are not yet possible. Therefore, protein modeling must rely on identification of surface domains and functional and structural features of the molecule. Epitope mapping has provided a means by which surface features of a protein can be determined.

Epitope mapping includes a number of methods to determine the relative location of antibody binding on a molecule. Some epitope mapping data only provides resolution of the epitope to a protein subunit, or domain of a subunit (142). Synthetic peptides have been used to raise antibodies specific to a smaller region of a protein (54,71,106), and synthetic peptides have been used to block specific interactions between components of a system (15,106,142,154). Epitope mapping with anti-peptide antibodies has been used to determine the regions of viral proteins which contain neutralizing epitopes (133). Epitope mapping has also been carried out by producing a series of bacterial mutants which express various deletions of a protein. The mutants can then be sequentially screened and analyzed to locate the portion of a protein necessary for recognition by the antibody (5). Similarly, immunologic detection of enzymatic digestion fragments has been used to locate the epitope region of a protein (71).

Not all epitope positions on proteins have been empirically determined. Recently, a pentapeptide recognized by a mAb specific for tissue plasminogen activator was predicted by computer identification of likely epitope regions, and confirmed by molecular methods (58). Thus, computer modeling is one method by which some regions of proteins likely to be involved in antigenic determinants can be predicted based solely on primary structure.

The methods of epitope mapping listed above usually do not permit determining the region of antibody binding to fewer than 20-30 amino acids. Furthermore, the methods generally do not reveal individual amino acid residues

important in protein interactions. However, large collections of short peptide sequences (peptide libraries) have been used in some cases to narrow the resolution of interactive regions of proteins to the level of individual amino acids.

### Synthetic Peptide Libraries

Peptide libraries have been used as a source of interactive amino acid sequences, and permit the determination of amino acid residues critical for interaction in a variety of biological systems. The library is utilized by probing the peptide collection with a prospective ligand thought to involve affinity interactions with proteins. The ligand is then evaluated for bound peptides, and the sequences of the peptides, if present, are determined (70,73,90,162).

Synthetic peptide libraries have been produced as collections of random oligopeptides bound to solid supports (25,134), or synthetic peptides in solution called combinatorial libraries (117,118). An advantage of the peptide library over site-specific mutagenesis (86) and synthetic peptide inhibition studies (82), is that novel peptide sequences which interact with a system can be identified without preexisting information about the interactive regions of a protein. The peptide library, therefore, is a source from which interactive peptides can be recovered and identified.

Peptide libraries consisting of bound sequences include up to  $10^7$  unique peptides, and combinatorial libraries may contain up to five orders of magnitude more (118). The greater the diversity of the library, the better the likelihood that rare binding peptides long enough to mimic a particular interactive sequence are present.

The number of peptides in a library necessary to represent any possible sequence of a given length can be predicted by:

$$x = 20^n$$

where  $x$  represents the number of peptides in the library,  $n$  refers to the number of residues in the random sequence, and twenty reflects the number of different amino acids in each position. For example, a theoretical synthetic peptide library containing all possible heptapeptides (seven-mers) must contain at least  $20^7$  or  $1.3 \times 10^9$  unique sequences, and a library of one million sequences would probably contain all quadrapeptides, but not all pentapeptides. Therefore, the large number of peptides in a library constitutes an essential feature concerning its potential usefulness.

A novel peptide library of D-amino acids was reported by Lam *et al.*, from which peptides containing D-amino acids were affinity selected that demonstrated higher affinities for a chosen ligand than identical sequences containing L-amino acids (89). While the natural relevance of interactive peptides containing D-amino acids is questionable, such information may include pharmacological significance (41).

A drawback of synthetic peptide libraries is that once binding sequences are recovered, some difficulty is attendant with determining the amino acid sequences for a number of different recovered peptides (90,110). An interesting method of determining the sequence of bead-bound peptides selected by fluorescence-activated cell sorting was described by Needels, *et al* (110). In this system, all peptides of the

library are bound to individual beads (~10  $\mu\text{m}$  diameter) which also express an oligonucleotide coding for the peptide. After the beads are affinity-selected by a chosen ligand, the sequence of the selected peptide is determined by PCR-amplification of the coexisting oligonucleotide. The sequence of the PCR-amplified DNA can then be determined by standard methods (136). An additional shortcoming of the synthetic peptide library is that because the amount of any given peptide in the library is quite small, binding peptide sequences, once identified, must be synthesized individually before they can be evaluated experimentally.

The production of a nonrandom peptide library was reported by Geysen *et al.*, which encompassed all 208 possible overlapping hexapeptides included in the 213 amino acid sequence of the VP1 protein subunit of the foot and mouth disease virus (55). Despite the fact that the antibody tested in this system was a polyclonal preparation raised against the purified protein subunit of the virus, a seven amino acid region of the subunit was found to be immunodominant, as this segment was bound by the majority of the antibodies in the preparation. This result illustrates the importance of certain immunodominant regions of proteins which elicit the humoral response. A different strategy to produce a similar nonrandom library of protein fragments was carried out by producing a library of DNase I digestion products of the 4.3 kb dystrophin cDNA. The fragments were then expressed in the pTEX expression vector (151), and clones expressing immunoreactive proteins were compared to those expressing proteins not recognized by the anti-dystrophin antibody. The epitope-containing region of the dystrophin antibody was thus deduced, and found to lie within

a segment of the protein spanning about 35 amino acids.

### Random Sequence Phage-display Peptide Libraries

A pioneering report which provided a foundation for the method on which this dissertation is based was done by Reidharr-Olson and Sauer using combinatorial cassette mutagenesis (CCM) (125). This study addressed the structurally allowable amino acid substitutions at specific positions in the alpha helix 5 region of the  $\lambda$  repressor. The report illustrated the biological selection of specific amino acids or classes of amino acids in interactive positions of a protein. Thus, CCM was used to biologically create novel peptide sequences from which rare interactive peptide sequences could be recovered and determined. This provided an avenue by which vast libraries of peptides could be produced nonselectively, and used as a source of interactive sequences for any molecular system of the investigator's choosing. While some efforts in producing such libraries were carried out using bacteria as the displaying particle, the greatest utility appears to be the production of libraries of random peptides expressed on the surface of filamentous bacteriophage (146). The primary considerations involved with the production and use of the phage-display peptide library (PDPL) are listed in a subsequent section of this chapter.

### Filamentous Bacteriophages

The filamentous bacteriophages, from which the phage-display library is based,

comprise a few dozen viruses which exclusively infect specific genera of Gram negative bacteria (105). The filamentous bacteriophages described in this research bind a receptor on the fertility (F) pilus to initiate infection. Other groups of filamentous phage recognize a receptor on other types of pili, or other sites on the surface of the cell (105). The phage exhibit a unique slender and filamentous morphology, and contain a genome which is a circular single-stranded molecule, comprising about seven kilobases of DNA. The virion includes a protein coat consisting of five structural proteins. No lipid-containing component has been found associated with the virion.

Utility of the PDPL lies in several desirable characteristics of the filamentous bacteriophage. Progeny phage are liberated from infected cells, and accumulate in the suspending medium to produce titers as high as  $10^{11}$  plaque forming units per ml (pfu/ml). Concentrating virions as high as  $10^{13}$  pfu/ml is easily accomplished by precipitation with polyethylene glycol, centrifugation, and resuspending the phage pellet in a small volume of buffer (146). Therefore, an entire library of  $10^9$  sequences can be represented in a few microliters of phage suspension. This characteristic of the phage library makes possible the exposure of small amounts of a chosen ligand to the entire repertoire of peptides in the library. Isolated phage bearing peptides of interest can be amplified in a matter of hours by replicating the displaying phage in *E. coli* to produce enough phage-displayed peptide for analysis by a variety of molecular methods. The sequence of a phage-displayed peptide is deduced by sequencing the relevant region of the single stranded phage genome which codes for the peptide (136).

The filamentous bacteriophages do not lyse or significantly alter the basic functions of the host cellular metabolism beyond the production of progeny phage. Therefore, the relationship may be regarded as parasitic. Progeny phage are produced by infected cells by a process known as extrusion as nascent virions are encased in capsid proteins as single-stranded virions pass through the cell membrane. This extrusion of phage is tolerated by the host which is capable of maintaining continuous cell divisions, albeit at a slightly longer doubling times.

Natural Distribution Very few organisms have been found which do not have associated viruses that infect them specifically. The viruses which infect bacteria (bacteriophage, or phage) demonstrate remarkable diversity (105). Those which infect Gram negative bacteria have been well characterized, owing to the ease by which they can be replicated, and their potential uses in molecular biology. Many important discoveries regarding DNA replication were made at the Cold Spring Harbor Laboratories in New York, by Zinder, Delbrück, Luria, Hershey, and others, while studying a number of bacteriophage groups (1).

The filamentous bacteriophage represent a group of bacterial viruses which are long and slender. The F-specific filamentous phages which infect *E. coli* are so named because of the bacterial F pilus where they attach prior to infection. Iike phage infect a different strain of *E. coli* which produce N pili. Examples of filamentous phages, listed with the genus of host organism are: *Salmonella*- If, X; *Vibrio*- v6; *Xanthomonas*- Cf; *Pseudomonas*- Pf; *Escherichia*- Ike Ff (fd, M13, f1) (105).

Characteristics Filamentous phage have a width of about six to seven nanometers and a length of one to two micrometers, making the virion about 200 times as long as wide. Wild-type Ff phages average 890 nm in length (105). The number of nucleotides per major coat protein molecule varies between 1 and 2.4. The length of the virion can be quite variable, and is determined by the size of the genome packaged within. This allows flexibility of genome length, as truncated phage particles are produced by deletion mutants, and longer particles are produced by phage harboring genomes containing up to several kilobases of additional (foreign) DNA. As high as five percent of phage particles exist as multimers of unit length genomes. X-ray diffraction patterns of oriented phage fibers have shown the f1, fd, M13, I<sub>ke</sub>, and I<sub>f1</sub> phages display a five-fold screw axis helical symmetry (99). However, none of the Ff filamentous phage have been analyzed by detailed X-ray crystallographic studies.

Filamentous phage are resistant to temperatures of 65° C for 30 minutes and many proteolytic enzymes, including trypsin and Pronase. However, they are sensitive to Nagarse, ficin, subtilisin, papain, shear forces, and chaotropic agents (105). The single-stranded phage genome is particularly sensitive to ionizing radiation. The PIII gene product has been shown to be important in the stability of the phage in extremes of heat, salt concentration, and pH.

Mature filamentous phage particles do not exist within the infected host cell. Phage morphogenesis occurs as viral DNA is extruded through the plasma membrane of the host. The virally encoded structural proteins are targeted to the plasma membrane of the host for uptake by progeny during extrusion. Two phage structural

proteins are translated as precursor proteins and inserted into the cell membrane by means of a leader peptide which is subsequently cleaved. Neither the host membrane nor cellular function is severely affected as a result of infection and replication of the infecting phage. This association enables a culture which is infected by a filamentous phage to continue cell growth and division, albeit at a lower rate. The slower growth rate of infected cells allows the detection of isolated phage clones in the plaque assay (61).

The phage virion contains a circular DNA genome enclosed in a slender protein sheath comprised of five structural proteins. The single stranded genome contains about 6.5 kilobases of DNA. The packaging signal of the genome includes the nucleotide sequence which appears to result in a hairpin structure. The walls of the sheath are formed by ca. 2700 copies of the major coat protein (pVIII), and the virion termini contain structural proteins specific for respective ends. The first phage terminus to extrude from the infected host cell displays five copies each of the minor coat protein (pIII) and the gene VI product (pVI). The opposite end of the virion contains three to five copies each of pVII and pIX. Thus, the termini of the virion are distinguishable morphologically, structurally, by electron microscopy, immunologically, and functionally.

The entire nucleotide sequence for each of the Ff phage types has been determined (159), and therefore the amino acid sequence of each of the ten gene products is known. However, with the exception of the pV protein (below), little three-dimensional information beyond the primary structure of each protein is

available. The structural proteins encoded by the Ff group of filamentous phage are: pVIII, pIII, pVI, pVII, and pIX. Because of the structural concerns of phage-display technology, they will be covered individually in sufficient detail to describe their functions or locations on the virion. The three proteins involved in DNA synthesis, pII, pX, and pV; and the two proteins involved in virion assembly, pI and pIV, will also be briefly discussed. The ten Ff phage-encoded proteins are tabulated in Table 2.

Phage proteins: Capsid Components The pIII protein is the minor coat protein. The mature protein is 403 residues in length, making it the largest of the phage encoded structural gene products. Following transcription by host machinery, the pIII proprotein is inserted into the host plasma membrane where the 18 residue leader peptide is cleaved by the host signal peptidase I. Five copies of the protein are incorporated into the end of virion which first passes through the host plasma membrane during assembly. The protein is required for virion stability and attachment to the prospective host prior to infection.

Three domains are evident in the pIII protein. The carboxyl third of the molecule is required for assembly, and contains a 23-amino acid region which anchors the molecule into the cell membrane prior to assembly (105). This domain also functions to attach the protein to the virion. Subtilisin cleaves the protein, liberating the amino two-thirds of the molecule, producing a noninfectious virion (59). The amino domain cleaved by subtilisin can be used to pretreat uninfected cells, and block attachment of phage. This result provides strong evidence that this region contains the

antireceptor for attachment to the host, though the structure of the antireceptor has not been determined.

Table 2. Filamentous (Ff) Phage Proteins<sup>a</sup>

Protein	Copies per virion	Amino acid residues	Signal peptide	Phage-display	Function
pI	none	348	no	no	assembly
pII	none	410	no	no	synthesis
pIII	5	423	18 residues	yes	structural
pIV	none	425	no	no	assembly
pV	none	87	no	no	synthesis
pVI	5	112	no	no	structural
pVII	3-4	33	no	no	structural
pVIII	~2700	73	23 residues	yes	structural
pIX	3-4	32	no	no	structural
pX	none	111	no	no	synthesis

<sup>a</sup> Includes the M13, fd, and f1 phage, for which the nucleotide sequence is very similar (159).

The pIII protein contains two glycine rich domains, each containing permutations of an EGGGS peptide sequence. These regions appear to be required for specific host phenotype changes following infection. Expression of the altered host phenotype results either when the cell is infected by the filamentous phage or when expressing a plasmid-borne pIII gene. In either case, the cell becomes sensitive to

deoxycholate, loses cytosolic components, becomes resistant to the homologous phage type, is unable to form mating pairs, and becomes resistant to colicins (166).

On SDS-PAGE gels (88), the pIII protein migrates with an apparent mass of approximately 65 kDa (16,17,57,63,74,159), despite the actual molecular weight of 42.6 kDa (46). The weight discrepancy appears to be due to the high glycine content and extended structure of the pIII protein (46,53,159).

Smith first showed that foreign DNA inserted in frame near the 5' end of the pIII gene produces infectious phage with a fusion protein expressed on the pIII protein, with no apparent loss of pIII function (144). However, deletions near the amino terminus of the pIII protein cause progeny phage which are noninfectious (105). The ability to express foreign proteins at the amino terminus of the pIII protein without loss of function provides a basis of phage-display technology.

About 2700 copies of the pVIII protein comprises the entire protein sheath along the sides of the filamentous phage. The amino acid sequence of the pVIII protein has been determined (159), and suggests the mature protein is 50 residues long. A 23 residue leader peptide directs the emerging translation product to the cell membrane. The leader peptide is subsequently cleaved by the host-encoded signal peptidase I, leaving the amino terminus of the protein on the extracellular surface of the membrane. The pVIII protein of M13 differs from fl and fd by a single amino acid (159).

A large degree of alpha helical structure is noted for the pVIII subunit monomers, reflecting the conformation of the subunits as they exist in the plasma

membrane of the host, prior to assembly (135). The helical arrangement of the protein cannot be duplicated in artificial medium suggesting conformational adjustment occurs during production. A hydrophobic central region of the pVIII protein is flanked by an acidic N-terminal and a basic C-terminal domain.

The pVI protein consists of 112 residues, is hydrophobic, and contains a predominance of leucine and isoleucine residues (159). It is incorporated into the same virion terminus as the pIII protein during assembly. A signal peptide is not translated with this protein as with the pVIII and pIII proteins, though a region of hydrophobic residues is present to provide a possible membrane anchor prior to assembly. The function of the pVI protein has not been determined, yet recent evidence suggests the pIII and pVI proteins form a complex, referred to as the proximal cap, that survives phage disruption by sodium deoxycholate and chloroform (53). The pVI protein is thought to exist in an equimolar ratio with pIII.

The pVII and pIX proteins are found in the virion terminus opposite the end containing the pIII and pVI proteins. The length of the pVII and pIX proteins are 33 and 32 residues, respectively. Like the pVI protein, neither pVII nor pIX is produced with a leader peptide, but each contains a hydrophobic region which probably serves as a membrane anchor prior to assembly. The functions of the pVII and pIX proteins has not been determined. The pVII and pIX proteins appear to be equal in number, probably 3 or 4 copies of each are present in intact virions (53).

Phage Proteins: DNA Synthesis Phage encoded proteins pII and pX are required for DNA synthesis. pII has nuclease-topoisomerase activity in the presence of  $Mg^{2+}$ , and functions by relaxing supercoiled replicative form of the phage in order for DNA replication to take place. Amber mutations in the PII gene do not result in an imbalance of phage proteins and death of the host, a characteristic found to occur in all other phage genes. Amber mutations in the pII gene merely prevent the replication of the phage, and intracellular RF is eventually lost due to dilution by host division. The pII protein has also been shown to be required for the production of single stranded DNA, though this mechanism is not known. The pII enzyme is specific for filamentous phage replicative form, cleaving the DNA between nucleotides 5781 and 5782. The nucleotide sequence in this region is cgttcttaa\tagtggact, and therefore, the recognition site for the enzyme is not palindromic. *In vitro* studies suggest that when pII enzyme is accompanied by DNA polymerase III holoenzyme, *rep* helicase, and *E. coli* DNA-binding protein I, single-stranded DNA molecules of positive polarity are produced. These molecules are presumably intended as genomes of progeny phage, and support the role of pII in the production of progeny genomes.

The nucleotide sequence of gene X is entirely included in the gene II open reading frame. Furthermore, the two genes are in the same reading frame. Transcription of gene X begins at an initiation AUG 300 codons downstream of the gene II initiation codon, and the two genes share a stop codon. Thus, pX is identical to the carboxyl third of the pII protein. The pX protein contains its own N-formyl methionine and is therefore not produced as a proteolytic cleavage product of pII.

Amber mutations within the pX gene which inhibit pX, but not pII synthesis, indicate replication of the phage is completely dependent upon the presence of pX. The function of pX has not been determined.

The 87 amino acid product of gene V is required for the formation of single-stranded DNA genomes. Within infected cells, about 1300 subunits of the pV protein are associated with each newly synthesized single-stranded phage genome. It is believed that the monomers associate with the DNA immediately following synthesis. The unusual property of binding between pV and single-stranded polynucleotides has prompted intensive research for several decades.

Following infection of the cell by phage genome, host DNA polymerase converts the single-stranded genome into a double-stranded RF molecule. The RF molecule produces additional single-stranded genomes by rolling circle replication (56), which in turn serve as templates for additional double-stranded RF molecules. This process continues during the early stages of replication while the concentration of pV protein is low, producing several hundred copies of RF molecules in each infected cell. As the concentration of the pV protein begins to rise, nascent single-stranded DNA molecules are bound by the pV protein subunits and prevented from becoming RF molecules. Thus, following the initial buildup of RF molecules, single-stranded forms are sequestered for use as progeny genomes and encapsidation. This mechanism represents an elegant means whereby the distribution of DNA forms within the infected cell is regulated solely by concentration of a phage-encoded protein. During virion assembly, the phage genome extrudes through the wall of the infected host as

coat protein subunits are exchanged for the pV subunits. The pV protein is therefore not included in the mature phage particle.

The pV protein has been crystallized and a three dimensional structure has been suggested (103). The crystallized molecule includes homodimers of the protein which associate by a hydrophobic interface that prevents aqueous solvent access. These dimers are also formed in physiological salt concentration, and appear to associate with the single-stranded DNA by one or more of the five tyrosine residues. Nitration of the tyrosine residues with tetranitromethane reduces the affinity to DNA (80). Tyrosine residues #26, 41, and 56 can be protected from chemical modification by this compound when pretreated with DNA, suggesting tyrosine residues play an important role in the binding of DNA, presumably by intercalating with the nucleotide bases. The single cysteine residue of the pV protein also appears to provide an important role in the binding to DNA, as treatment with mercury interferes with the interaction (3).

Phage Proteins: Virion Assembly The pI protein is not part of the virion and not involved in DNA synthesis. Temperature sensitive mutants of this gene suggest the pI protein is required for phage assembly. The protein appears to be associated with the host thioredoxin metabolism and may facilitate assembly of progeny phage by altering membrane permeability. Membrane permeabilization induced by over-expression of pI causes excessive loss of intracellular ions and cell death. Therefore, the very low levels of pI expression in infected cells is necessary to ensure maintenance of the host. The precise mechanism by which the pI protein is involved

in phage assembly has not been determined, however, it appears to associate with the pIV protein.

Gene I has been cloned (69), and cells carrying recombinant plasmids which express this gene rapidly halt macromolecule synthesis and die, presumably as a loss of energy metabolism due to membrane permeability. Cell-killing is not noted in hosts containing a construct with an amber mutation in the 3' third of the gene, suggesting the carboxyl component of the protein contains the bacteriocidal factor. A stretch of 20 hydrophobic amino acids in the carboxyl third of the protein may function as a membrane insertion sequence, and may be responsible for cell death when over-expressed.

The mature pIV protein locates to the periplasm of the infected cell, and forms homomeric multimers (77) that are required for assembly of progeny phage (105). The proprotein is processed by cleavage of a signal sequence, and expression of high amounts of the protein from cloned constructs suggests it is lethal to the cell.

Many Gram negative bacteria encode proteins with a high degree of similarity to the pIV protein of filamentous phage (131). The function of these bacterial proteins is to form channels across the cell membrane specific for a cellular component. The best characterized is the pullulase export pathway of *Klebsiella oxytoca* (120). Recent study of these transport pathways in bacteria suggests the pIV phage protein acts in a similar manner, and aggregates in the periplasmic space, possibly in conjunction with the pI protein, to form channels specific for the assembly and transport of progeny phage.

Control of Gene Expression Complex regulation of phage gene products is required to produce some phage proteins in several log excesses above others. This regulation is especially critical because many of the phage proteins are toxic to the host, and relative excesses can rapidly lead to cell death. Critical regulatory events at both the levels of transcription and translation are responsible for this control.

Transcription RNA processing in the filamentous phage is surprisingly complex. Many promoters have been identified in the phage genome by sequence analysis, and *in vitro* and *in vivo* studies (105). The RNA species have different stabilities, and therefore the populations of RNA change with respect to time following infection. Phage RNA forms in the infected cell suggest significant post transcriptional processing occurs. Variable strengths of promoters are observed, and the number of promoters exceeds the number of terminators, which causes overlapping transcription in several places. *In vivo* activity of several terminators and promoters differs from *in vitro* activity, suggesting host encoded transcriptional factors play an additional roll in transcriptional regulation.

Preservation of 3' regions of RNA transcripts relative to 5' degradation offers an additional means of regulating the prevalence of some RNA species. For example, the 3' end on one major transcript includes the genes for the single stranded DNA binding protein (pV) and the major capsid protein (pVIII), both of which are required in large amounts. Partly as a result of this, two percent of the total cellular RNA may code for the major capsid protein (pVIII) alone, and the message encoding pV can also

be found in large amounts relative to RNA species encoding other phage proteins. The need for greater amounts of these proteins reflects the requirement of several thousand subunits of each pVIII and pV per progeny virion. Conversely, the very low requirement and cell tolerance for pIV and pI is reflected by a low stability in the 5' regions of message which encode these proteins.

Taken together, these mechanisms of transcriptional regulation allow a gradient of RNA species which encode the phage proteins. Factors which affect the cascade effect of transcription are i) the stability gradients of RNA species, ii) the position of the genes relative to promoters and terminators, and iii) the numbers and positions of the promoters and terminators relative to the genes. These effects have been referred to as the cascade mechanisms of transcriptional regulation (47).

While these factors provide an elegant explanation for the complex regulation of the transcription, they do not explain phage gene regulation in its entirety. For instance, because gene VII is located between genes V and VIII in the phage genome, the levels of gene VII protein would be expected to be midway between the two, according to the proximity of the promoter. However, the pVII is found in low levels in the infected cell, suggesting regulation at the level of translation augments the constraints imposed by transcription.

Translation Translation of the filamentous phage proteins has been studied as a function of the binding between RNA transcripts and ribosomes. In ribosome-protection experiments (72), phage RNA transcripts are allowed to bind to ribosomes

and the complexes are challenged by nucleases. Residual RNA fragments, corresponding to regions of the RNA which were protected by the ribosome, are then sequenced and the identity of the gene which corresponds to the transcript is determined. In this way, it was determined that the transcripts encoded by genes V, VIII, and VI contained the strongest ribosome-binding sequences within the promotor regions (72), corresponding to the transcripts producing the highest levels of protein expression *in vitro*. The transcripts of gene V and VIII were also bound by eukaryotic ribosomes in rabbit reticulocyte expression systems (92), suggesting a probable correlation between the binding affinity of the promotor region and translation level of the protein *in vivo*.

Phage Biology The infection event of a host bacterium by a filamentous phage involves two steps; adsorption, and subsequent entry of the phage genome into the host cell. Infection of a host bacterium is initiated by adsorption of the phage to the host F pilus. As many as 12 host encoded gene products and several regulatory genes of the F episome are involved with this process. Mutant bacteria which contain the F episome but are resistant to infection have also been found to lack normal pili production.

Adsorption is the only step of infection which is energy independent, and is presumed to take place immediately following collision between the receptor and antireceptor. Because the adsorption of phage to the host cell is dependent upon the collision frequency, efficient adsorption rates are noted when host cells are

concentrated to greater than  $5 \times 10^9$  cfu/ml (153). For this reason, it is advantageous to prepare host cells for infection by first 'starving' an early log-phase  $F^+$  culture in 80 mM NaCl and concentrating it by centrifugation. The purpose of starving the culture is to allow the cells to better tolerate the concentration process and to allow them to better tolerate storage at  $4^\circ$  C for several days. Efficient adsorption of phage to host pili is dependent upon ion concentration but not ion species in the suspending medium. One hundred millimolar NaCl, NaNO<sub>3</sub>, Na<sub>2</sub>SO<sub>4</sub>, KCl, NH<sub>4</sub>Cl, CaCl<sub>2</sub>, MgCl<sub>2</sub>, and MgSO<sub>4</sub> all allow maximal adsorption (153). There appears to be no pH optimum between five and eight for adsorption, and temperature governs the attachment only to the degree that it affects the viscosity and diffusion rate in the suspending medium. Temperatures above  $37^\circ$  C can cause inactivation of the receptor-antireceptor complex, and denaturation of the complex takes place at  $42^\circ$  C (153).

Several theories of phage entry have been suggested, though none have been convincingly demonstrated. Most evidence supports that phage pIII protein triggers a shortening of the pilus upon attachment. For this reason, the pilus contraction model was proposed (100). According to this theory, the contracting pilus brings the phage particle in close proximity to the surface of the bacterial cell, allowing the entire virus to enter through the cell membrane near the base of the pilus. This view is supported by electron microscopy which suggests the pili of infected cells are shorter (72), and because both nucleic acid and protein subunits of the infecting phage may be incorporated in progeny. It is also possible that the pilus functions as a docking site for the phage, and once attachment has taken place, entry into the cell may take place

at a nearby, but distinct location. The genome of filamentous phage is not sensitive to DNase at any stage, suggesting the phage genome does not exist in an unprotected state at any time during infection.

Lysogeny F-specific filamentous phages do not lysogenize in the host chromosome. In situations where phage infect or replicate inefficiently, low yields of progeny may be produced. While this situation may resemble lysogeny, low levels of progeny production by the majority of cells in the infected culture usually dispels a true lysogenic condition. However, another filamentous phage, Cf1t, infects and lysogenizes the plant pathogen *Xanthomonas citri*. *X. citri* infected by this phage show turbid plaques, produce phage at low titers, and demonstrate chromosomal DNA which can be probed by phage specific sequences on Southern blot (87).

#### Filamentous Bacteriophage in Molecular Biology

The filamentous phage demonstrate characteristics which make them useful in molecular biology. Either single or double stranded forms of the phage genome can be extracted from cultures of infected host bacteria. Production of mature phage by an infected bacterium takes place as progeny are extruded through the cell wall of the host. Intact progeny phage bearing single-stranded genomes accumulate in the culture supernatant making them a convenient source of DNA for primed synthesis DNA sequencing (136) and oligonucleotide-directed mutagenesis (86). Double-stranded replicative form (RF) virus genomes are produced in the infected cells by rolling circle

replication (56). The RF can be extracted and manipulated in a manner similar to bacterial plasmids, and therefore serve as a recipient molecule for the ligation of foreign double-stranded DNA inserts (6).

Production and Use of a Phage-Display Peptide Library Phage-display technology was pioneered by Dr. G. P. Smith at the University of Missouri in Columbia, Missouri. Smith *et al.* first published reports of libraries of phage-expressed peptides used for epitope mapping in 1988 (116,137). These libraries, and soon others (34,37), contained random peptides which are expressed as fusion proteins on the surface of the phage virion, rather than free in solution or immobilized on a solid support. The peptides of the phage-display library are not produced synthetically, but rather, the random or degenerate nucleotide sequences encoding them are. These random oligonucleotides are ligated into a phage vector capable of displaying the product of the DNA insert as a fusion with a capsid subunit (146).

The PDPL is produced by recombinant DNA technology by first creating a pair of restriction sites near the 5' end of the phage capsid PIII or PVIII gene. The sites are cleaved by the appropriate restriction endonuclease, and the synthetic oligonucleotide containing three random bases for each random amino acid to be expressed is ligated into the cleaved vector. The recombinant DNA is then transfected into electrocompetent *E. coli* cells (43), and following incubation of the transfected culture, the many unique progeny phage which constitute the library are collected by precipitation (146). A list of reported phage display vectors which have been used to

express PDPLs is included in Table 3. A number of different strategies have been

**Table 3.** Recombinant Phage-display Vectors<sup>a</sup>.

Vector	Fusion with Capsid Protein	Parent Phage	Antibiotic Resistance	Restriction Site(s) <sup>b</sup>	Refer.
fUSE5	III	fd	tetracycline	<i>Sfi</i> I	(116,137)
fAFF1	III	(fUSE5)	tetracycline	<i>Bst</i> XI	(34)
M13LP67	III	M13	ampicillin	<i>Eag</i> I, <i>Kpn</i> I	(37)
fdH	VIII	fd	none	<i>Hpa</i> I	(60)
M13KBst	III	M13	kanamycin	<i>Bst</i> XI	(23)
m666	III	M13	none		(52)
PC89	VIII	f1	none	<i>Eco</i> RI, <i>Bam</i> HI	(51)
M13-PL6	III	M13	kanamycin	<i>Kpn</i> I, <i>Bst</i> XI	(112)

<sup>a</sup> For reference a of phagemid vectors, see (146).

<sup>b</sup> The restriction sites were specifically created to allow cloning of the foreign DNA intended to code for the fusion protein on the capsid subunit indicated.

developed for creating inserts for the phage-display vectors which code for random peptides. All methods used thus far have involved some means of eliminating the opal and ochre stop codons from the random region of synthetic oligonucleotides by eliminating adenine from the last position of the codon. Several other libraries have utilized equal amounts of all four nucleotides in each of the other two positions of the codon. In order to get a more even distribution of all codons, Jellis *et al.* (75) utilized a mixture of 19% of each guanine and cytosine and 31% of each adenine and thymine in the second position of the codon, and in the third position, 39% guanine and

cytosine and 22% thymine.

A difficulty in creating a nucleotide sequence which will base pair with the random region of the degenerate insert has prompted several solutions. This was first addressed by including the degenerate regions within an oligonucleotide which contained sequence to which PCR primers could be annealed. The strand complimentary to the degenerate regions could be filled in by polymerase chain reaction (PCR), using the random sequence as the template (137). The restriction-compatible ends could then be created by cleaving the double-stranded product, which contained the recognition sequence of an appropriate restriction endonuclease. Because the large numbers of identical coding strands possible by PCR were not desired, a more logical means of addressing this problem was reported in which the oligonucleotide encoding the degenerate region also included at the 3' end, a region which would flip back to base-pair with a complimentary region forming a hairpin (24). The 3' terminus of the construct, then acts to prime synthesis of the entire complimentary strand during *in vivo* DNA polymerization. Both ends of the resulting double-stranded cassette could then be cleaved with the appropriated restriction endonuclease to produce ligation-compatible insert termini. Both of these methods suffer to some extent by the fact that the use of a restriction endonuclease to create a ligation-compatible insert termini also cleaves restriction sites within the random region. This results in loss of those inserts containing restriction sites and the reduction of the complexity of the library by the protein sequences which would have been coded for by oligonucleotides containing inherent restriction cleavage sequences.

The method adopted for use in the construction of our J404 PDPL was first described by Cwirla *et al.* (34), and subsequently used to create other PDPLs. According to this method, three oligonucleotides are synthesized, one of which contains the degenerate region, and each of the other two anneal to the nonrandom sequence at the respective end of the degenerate oligonucleotide, creating the double-stranded ligation-compatible termini of the insert. The region in the central portion of the insert is single stranded, since no strand complimentary to the random region has been created. This form has been referred to as a "gapped duplex" because it is a single-stranded segment of DNA, flanked by double-stranded regions which contain ligation compatible ends. This form of insert can be ligated to the cleaved vector to produce covalently closed circular molecules which can be transfected directly (34) into electrocompetent cells (43,146), or the single stranded region can be filled in with a mixture of the four nucleoside triphosphates and a polymerase such as T4 DNA polymerase or Sequenase<sup>®</sup> enzyme.

An additional strategy for producing a strand complimentary to the random region was reported using an oligonucleotide which would base-pair to the entire oligonucleotide encoding the random region. This was accomplished by using an antisense oligonucleotide containing deoxyinosine bases which can indiscriminately base-pair with any nucleotide in the random regions of the insert (37). The flanking regions of this strand were synthesized with specific bases to base pair with the constant regions of the degenerate oligonucleotide. In this way, the entire double-stranded insert construct with restriction site-compatible ends could be produced by

annealing just two oligonucleotides. However, it is not clear what the fate of the negative strand containing the inosine bases is once transfected into the electrocompetent host (G. P. Smith, personal communication).

The phage particles of a PDPL differ from each other only by i) the nucleotide sequence of the random DNA insert within the phage capsid protein gene, and ii) the peptide product of the random DNA, covalently fused to the amino terminus of the capsid protein. Members of the PDPL each express five copies of the unique peptide, which is displayed in an accessible location on the phage surface and free to interact with other components in the suspending medium. The length of the random peptide region is predetermined by the length of the synthetic DNA insert, but usually has not exceeded 15 residues. However, a PDPL expressing peptides containing 38 random amino acids was reported (76). Each library contains at least as many unique phage particles as there are different peptide sequences, and each clone of the library is usually amplified to give about  $10^6$  copies of each clone. The phage which constitute the library are then concentrated to give  $10^{13}$ - $10^{14}$  clones per milliliter of solution (146). In this way, the entire library may be represented in only a few microliters of solution, facilitating the exposure of small amounts of a potential ligand to all possible binding phage-expressed sequences.

Peptide sequences of the library which bear similarity to natural interactive regions of a protein are accessible on the phage surface for interaction with a chosen ligate. The technique exploits the large number of peptide sequences available in the library, some of which mimic the natural region of a protein involved in an affinity

interaction. The rare binding phage-displayed peptides can be affinity purified, along with the expressing phage, without *a priori* information of peptide sequences involved in the affinity interactions of the system. Once isolated, any unique peptide in the library can be propagated as part of the phage on which it is expressed, and the amino acid sequence can be deduced from the nucleotide sequence insert of the phage genome (136,146). This technology has been used to determine the epitopes recognized by monoclonal antibodies (20,24,34,37,76,78,97,104,126,137,138) and sequences involved in protein-protein interactions (14,35,37,76,83,112,132,145).

The chemical diversity of PDPLs parallels that of synthetic peptide libraries. Libraries containing one billion unique oligopeptides expressed on phage have been reported (14). While the diversity of the phage-display library is significantly less than that of the combinatorial libraries, our data suggests the ability of the PDPL to identify interactive sequences appears at least as good as that of synthetic peptide libraries, based on the length of interactive peptide sequences identified.

Predicting the size of a PDPL needed to contain all possible peptides of a specified length is slightly different than the method for predicting the numbers of members in a synthetic peptide library. This is because biological peptide libraries such as the PDPL are created by linking nucleic acid codons instead of amino acids. The number of possible codons (sixty-four) is greater than the number of amino acids (twenty) because of redundancy of the genetic code. Therefore, it takes more oligonucleotides to code for all peptides of a given length than it would take polypeptides to make all peptides the same length, because several different

oligonucleotides would code for the same peptide. In the construction of our J404 library, as with most other PDPLs, the third position of the codon was restricted to only G or T bases, reducing the number of codons by a factor of two. This adjustment also precludes both the ochre and opal stop codons, and allows a more equal representation of all codons. Thus, the formula for predicting the number of PDPL members necessary to represent any possible peptide of a given length can be predicted by:

$$x = 32^n$$

where x represents the number of peptides in the library, n refers to the number of residues in the random sequence, and thirty-two reflects the number of different codons encoding amino acids at each position of the random peptide. Slightly different strategies for producing degenerate inserts have been reported (75,76).

Amenities of the filamentous phage as a vehicle for the expression of peptides and proteins include a) the small phage size allows library solutions of much higher titer to be produced ( $10^{13}$  pfu/ml) than bacterial suspensions, b) filamentous phage can be kept at 4° C in simple buffer solutions containing azide for several years, c) each displaying phage contains all necessary mechanisms for producing more of the expressed polypeptide, d) the result of a single infectious event can be easily detected by the naked eye in a plaque assay (61), allowing isolated phage clones expressing a single peptide to be propagated in pure culture, e) the single-stranded DNA genome of

the phage includes the nucleotide sequence encoding the expressed polypeptide and can be determined by conventional dideoxy sequencing (136).

A variety of PDPLs have been created, reflecting the many intended uses. The first libraries consisted of random hexapeptides expressed near, but not adjacent at the amino terminus of the five copies of the pIII protein (116,137). A library of M13 phage displaying a 15 residue random peptide was produced in which the random segment was linked by a hexaproline tether to discourage interaction of the random region with the native pIII protein (37). A library of hexapeptides was expressed at the very amino terminus of the pIII protein to avoid possible confounding effects of native pIII residues on both sides of the random regions (34). The J404 PDPL produced as part of this research is such a library, and comprises 500 million phage expressing random nonapeptides tethered at the very amino terminus of the pIII protein. The random region is linked by a flexible glycine residue, and two proline residues included to discourage helical association of the unique region with the native pIII protein. Efficacy of the library has been demonstrated in several system (22,36). A library of random 38-mer peptides was produced to allow greater randomness not only of the primary structure of the displayed peptide, but secondary structure as well (76).

Another means of expressing the random peptide is to flank the region with cysteine residues (66,67). In this way, the assumed structure of the random peptide is that of a constrained loop. Certain binding motifs have been identified using libraries of constrained, but not unconstrained peptide libraries. An example of a binding motif

determined only by use of a constrained library is the well characterized RGD binding sequence of integrin interactions (84,112). Phage which displayed the constrained peptide sequence, GGCRGDMFGC, were found to be internalized in cultured human laryngeal epithelial cells, illustrating the functional conformation of the displayed RGD sequence (62). Apparently the torsional constraint of the peptide backbone in the constrained peptide is required for binding by some ligands. The majority of these phage-display constructs were expressed as part of the pIII capsid protein.

The pVIII protein has also been used to express foreign peptides on the surface of filamentous phage. An advantage of using the pVIII protein for peptide display is that each phage contains about 2700 surface-accessible copies of the pVIII protein; and therefore, more copies of each peptide exist to interact with a ligand. A disadvantage of using the pVIII protein to display foreign proteins is that inserts of greater than five amino acids preclude correct assembly of the phage. A solution to this problem is to co-infect the host *E. coli* with a helper phage which encodes a wild-type pVIII protein, or express the wild-type protein on a plasmid in the infected cell. In this way, the progeny phage contain two populations of the pVIII protein; a small fraction expresses the foreign protein or peptide fusion product, and the remainder are wild-type subunits, necessary for correct virion assembly.

The phage-display library was used by exposing a chosen ligand to the vast number of different phage in the library, each of which express five copies of a unique peptide on the capsid surface (Figure 3). In this way, the ligand is brought into contact with the many different peptide sequences, and those which interact with the

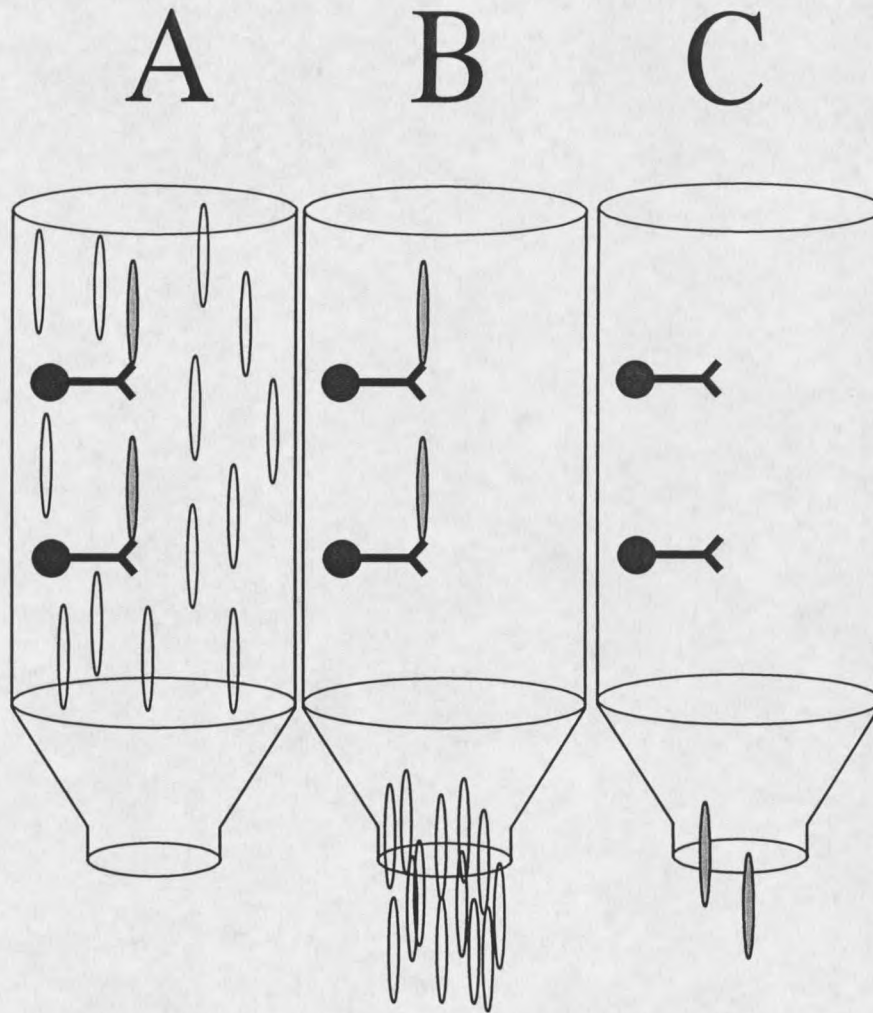


**Figure 3.** Affinity purification of phage-display library members bearing peptides bound by monoclonal antibodies (mAbs) on an immunoaffinity column. A) mAb of choice is bound to Sepharose beads and exposed to the phage library, B) nonadherent phage are removed from the column by washing the beads with 50 column volumes of wash buffer, C) adherent phage bearing peptides bound by peptides recognized the mAbs are eluted with low pH buffer. For details of immunoaffinity purification, see Chapter 3.

ligand will be bound specifically as indicated in Figure 3A. Once adherent phage have been given the opportunity to bind the ligate, nonadherent phage clones bearing peptides which were not bound are washed from the system by ca. 50 column volumes of phage buffer (Chapter 3), as illustrated in Figure 3B. After nonadherent phage have been removed, the interaction between the ligand and specifically bound phage is disrupted with four column volumes of a low pH (pH 2.2) buffer (Figure 3C). The pH of the eluate is then neutralized, and the phage are infected back in specially prepared *E. coli* cells for amplification and subsequent repassage on the column. Generally, three cycles of selection are alternated by two rounds of amplification before clones are propagated as isolated plaques for sequence analysis.

The goal of this work was to (i) construct a recombinant bacteriophage vector from M13mp18 which would be amenable for PDPL production, (ii) using the recombinant vector, produce a library of sufficient complexity to determine the epitopes recognized by monoclonal antibodies raised against human neutrophil flavocytochrome  $b_{558}$  (Cyt b), (iii) characterize the binding of the mAbs to purified Cyt b, or native Cyt b in intact and saponin-permeabilized human neutrophils so that predictions, based on the data, could be made about the topology of Cyt b.

Other Uses of Phage-display Technology Many efforts of protein engineering rely on the ability to test novel amino acid sequences or protein domains, or alter the specificity of protein-protein interactions. Filamentous phage have utility in displaying novel peptides and protein segments because they are able to produce and display the

polypeptide encoded by most any nucleotide sequence within liberal size constraints. These phage can tolerate ca. one kilobase of foreign DNA in the 5' end of the pIII gene and foreign protein displayed on the pIII protein is for the most part unconstrained. For these reasons, phage-display vectors have become popular as expression systems for novel protein arrangements. For example, the entire trypsin (29), or beta-lactamase (149) enzyme has been expressed in a functional form on the surface of M13 or fd, respectively. Random mutagenesis can thus be targeted to the region of the protein which imparts catalytic activity, and mutant progeny can be screened by simple affinity selection for clones which bind an immobilized substrate of choice. A phage-display construct was produced in which the Jun protein, involved in high-affinity leucine-zipper interactions, was used to select proteins from a library of randomized Fos mutants in order to locate protein binding pairs that demonstrate binding affinities higher than those that occur naturally (30).

Antibody libraries have been created as antibody fragments of random binding specificities displayed on the surface of filamentous phage (68). As with the PDPLs, the genome of each antibody-expressing phage contains the gene encoding the antibody, and therefore, the ability to produce large amounts of the antibody in pure culture. Libraries were created by cloning *in vitro* hypermutated, PCR-amplified cDNA corresponding to antibody V regions genes obtained from unimmunized human splenocytes (111) into a specially prepared phage-display vector (143). An antibody, or set of antibodies, can be selected from the library by immobilizing the desired "antigen" and recovering phage clones displaying variable antibody regions which bind

the intended ligand. This process may be regarded as an *in vitro* immune response. A library of phage-displayed antibodies specific for the C5 complement was produced by immunizing mice with rC5a, extracting splenic mRNA from the immunized mice, and cloning the cDNA into the pComb3 antibody expression vector (2). In this way, monoclonal antibodies specific for both active and inactive C5 were obtained.

In some cases, the phage vector is unable to present the antibody in a correctly folded conformation. For this reason, a system has been devised in which the chaperons, GroES (Hsp10) or GroEL (Hsp60) are co-expressed in the infected bacterial host to give a 200-fold increase in infectious, antibody-expressing phage clones (148). This has allowed improved folding of the antibody fragments and a greater overall titer (but not diversity) of the antibody library.

#### Point-by-point Aims of the Dissertation

Topological epitope mapping of the human neutrophil Cyt b by random PDPL analysis includes the following objectives:

- 1) construct a bacteriophage vector which can be used for the production of a PDPL
- 2) produce a PDPL of sufficient diversity to determine the epitopes recognized by Cyt b-specific mAbs
- 3) probe the library to select phage clones bearing peptides which resemble the natural epitope of the Cyt b-specific mAbs, determine the sequences of the selected phage, and locate regions in the primary structure of Cyt b which resemble the sequences of the consensus selected phage-displayed peptides
- 4) characterize the binding of the Cyt b-specific mAbs to the native, denatured,

and detergent solubilized Cyt b to determine the location of the Cyt b epitopes relative to the plasma membrane of the neutrophil.

### Goals and Experimental Design

The long-term goal of this research is to understand the molecular basis of the NADPH-oxidase system. The means by which this dissertation addresses the goal is by the examination of the topology of Cyt b using PDPL epitope mapping. The attempt to define topological structures of Cyt b to learn about the oxidase system reflects many current approaches to biomedical research; that structure-based molecular approaches toward the mechanisms of disease provide a functional rationale for pharmacologic therapies and preventative measures. Therefore, future strategies of therapy for CGD patients and those suffering the results of NADPH-oxidase-induced damage depends upon revealing important structural features of this system. A cardinal example which exemplifies this rationale is the understanding of the structure-function relationships of DNA, and how molecular genetics flourished as a result.

The primary goals of this dissertation are a) to construct a phage-display library to be used in the identification of Cyt b-specific mAb epitopes, b) to determine the amino acid residues of Cyt b which are recognized by the mAbs c) to analyze physical accessibility of the Cyt b epitopes on the native and denatured Cyt b molecule. The ability to determine the accessibility of specific epitope regions of the Cyt b molecule and to evaluate the sidedness of these locations relative to the plasma membrane provides structural information about Cyt b, and therefore, the assembled NADPH-oxidase.

The results which reflect the dissertation goals are summarized below. A 500 million clone PDPL was produced using recombinant DNA techniques, and used to show the  $^{181}\text{GGPQVNPI}^{188}$  segment of p22-*phox* is accessible on the intracellular surface of the plasma membrane in neutrophils, but the  $^{382}\text{PKIAVDGP}^{389}$  region on gp91-*phox* is not accessible to antibody on either aspect of the membrane, and is probably not on the protein surface. Furthermore, epitope mapping for mAb 44.1 suggest the two regions of p22-*phox*, which include the peptide segments  $^{29}\text{TAGR}^{33}$  and  $^{181}\text{GGPQVNPI}^{188}$ , may be associated by tertiary structure of the molecule and comprise a more complete natural epitope recognized by this mAb. The epitope recognized by mAb 54.1, which includes the  $^{382}\text{PKIAVDGP}^{389}$  segment of gp91-*phox*, may also be of particular significance, as the region which includes this epitope may be the site of interaction with another component of the oxidase system, or the binding site for either NADPH or flavin groups.

Mapping of structural features in the NADPH-oxidase system as described with PDPLs may justify further efforts by this method. Additional mAbs, other interactive proteins, and different strategies of the libraries may all offer a greater understanding of the interaction of components in this and other multiple-subunit systems.

References Cited

1. 1966. Phage and the Origins of Molecular Biology. Cold Spring Harbor Laboratory, Long Island.
2. **Ames, R. S., M. A. Tornetta, C. S. Jones, and P. Tsui.** 1994. Isolation of neutralizing anti-C5a monoclonal antibodies from a filamentous phage monovalent Fab display library. *J. Immunol.* **152**:4572-4581.
3. **Anderson, E., Y. Nakashima, and W. Konigsberg.** 1975. Photo-induced cross-linkage of gene 5 protein and bacteriophage fd DNA+. *Nucleic Acids Res.* **2**:361-371.
4. **Anfinsen, C. B.** 1973. Principles that govern the folding of protein chains. *Science* **181**:223-230.
5. **Arsenault, H. and J. M. Weber.** 1993. Mapping of the mAb73 epitope on Ad2 E1A proteins with random peptide libraries and deletion mutants. *FEMS Microbiol. Lett.* **114**:37-40.
6. **Ausubel, F., R. Brent, R. Kingston, D. Moore, J. G. Seidman, J. Smith, and K. Struhl.** 1995. *Current Protocols in Molecular Biology.* Greene Publishing Assoc. and Wiley-Interscience, New York.
7. **Badwey, J. A. and M. L. Karnovsky.** 1980. Active oxygen species and the functions of phagocytic leukocytes. *Ann. Rev. Biochem.* **49**:695-726.
8. **Baldrige, C. W. and R. W. Gerard.** 1933. The extra respiration of phagocytosis. *Am. J. Physiol.* **103**:235-236.
9. **Beckman, J. S., T. W. Beckman, J. Chen, P. A. Marshall, and B. A. Freeman.** 1990. Apparent hydroxyl radical production by peroxynitrite: Implications for endothelial injury from nitric oxide and superoxide. *Proc. Natl. Acad. Sci. USA* **87**:1620-1624.
10. **Beckman, J. S., M. Carson, C. D. Smith, and W. H. Koppenol.** 1993. ALS, SOD, and peroxynitrite. *Nature* **364**:584.
11. **Benna, J. E., L. P. Faust, and B. M. Babior.** 1994. The phosphorylation of the respiratory burst oxidase component p47-phox during neutrophil activation. *J. Biol. Chem.* **269**:23431-23436.
12. **Berendes, H., R. A. Bridges, and R. A. Good.** 1957. Fatal granulomatosis of childhood: clinical study of a new syndrome. *Minn. Med.* **40**:309-312.

13. **Birnbaumer, L.** 1990. Transduction of receptor signal into modulation of effector activity by G proteins: The first 20 years of so... *FASEB J.* **4**:3068-3078.
14. **Blond-Elguindi, S., S. E. Cwirla, W. J. Dower, R. J. Lipshutz, S. R. Sprang, J. F. Sambrook, and M. -J. H. Gething.** 1993. Affinity panning of a library of peptides displayed on bacteriophages reveals the binding specificity of BiP. *Cell* **75**:717-728.
15. **Bloom, J. W., J. D. Bettencourt, and G. Mitra.** 1993. Epitope mapping and functional analysis of three murine IgG1 monoclonal antibodies to human tumor necrosis factor- $\alpha$ . *J. Immunol.* **151**:2707-2716.
16. **Boeke, J. D., P. Model, and N. D. Zinder.** 1982. Effects of bacteriophage  $\phi$ 1 gene III protein on the host cell membrane. *Mol. Gen. Genet.* **186**:185-192.
17. **Boeke, J. D., M. Russell, and P. Model.** 1980. Processing of filamentous phage pre-coat protein. *J. Mol. Biol.* **144**:103-116.
18. **Bokoch, G. M., L. A. Quilliam, B. P. Bohl, A. J. Jesaitis, and M. T. Quinn.** 1991. Inhibition of Rap1A binding to cytochrome b-558 of NADPH oxidase by phosphorylation of Rap1A. *Science* **254**:1794-1796.
19. **Boulay, F., M. Tardif, L. Brouchon, and P. Vignais.** 1990. Synthesis and use of a novel N-formyl peptide derivative to isolate a human N-formyl peptide receptor cDNA. *Biochem. Biophys. Res. Commun.* **168**:1103-1109.
20. **Böttger, V. and E. B. Lane.** 1994. A monoclonal antibody epitope on keratin 8 identified using a phage peptide library. *J. Mol. Biol.* **235**:61-67.
21. **Bromberg, Y. and E. Pick.** 1985. Activation of NADPH-dependent superoxide production in a cell-free system by sodium dodecyl sulfate. *J. Biol. Chem.* **260**:13539-13545.
22. **Burritt, J. B., M. T. Quinn, M. A. Jutila, C. W. Bond, K. W. Doss, and A. J. Jesaitis.** 1994. Random sequence peptide library analysis of neutrophil flavocytochrome b structure. *Mol. Biol. of the Cell* **5**:121a.(Abstract)
23. **Burritt, J. B., M. T. Quinn, M. A. Jutila, C. W. Bond, and A. J. Jesaitis.** 1995. Topological mapping of neutrophil cytochrome b epitopes with phage-display libraries. *J. Biol. Chem.* (In Press)
24. **Christian, R. B., R. N. Zuckermann, J. M. Kerr, L. Wang, and B. A. Malcolm.** 1992. Simplified methods for construction, assessment and rapid screening of peptide libraries in bacteriophage. *J. Mol. Biol.* **227**:711-718.

25. **Chu, Y. -H., L. Z. Avila, H. A. Biebuyck, and G. M. Whitesides.** 1993. Using affinity capillary electrophoresis to identify the peptide in a peptide library that binds most tightly to vancomycin. *J. Org. Chem.* **58**:648-652.
26. **Cochrane, C. G.** 1992. Mechanisms of Cell Damage by Oxidants, p. 149-162. In A. J. Jesaitis and E. A. Dratz (eds.), *Molecular Basis of Oxidative Damage by Leukocytes*. CRC Press, Boca Raton, Ann Arbor, London, Tokyo.
27. **Cockcroft, S.** 1992. G-protein-regulated phospholipases C, D and A2-mediated signalling in neutrophils. *Biochim. Biophys. Acta* **1113**:135-160.
28. **Cockcroft, S. and B. D. Gomberts.** 1985. Role of guanine nucleotide binding protein in the activation of polyphosphoinositide phosphodiesterase. *Nature* **314**:534-536.
29. **Corey, D. R., A. K. Shiau, Q. Yang, B. A. Janowski, and C. S. Craik.** 1993. Trypsin display on the surface of bacteriophage. *Gene* **128**:129-134.
30. **Cramer, R. and M. Suter.** 1993. Display of biologically active proteins on the surface of filamentous phages: A cDNA cloning system for selection of functional gene products linked to the genetic information responsible for their production. *Gene* **137**:69-75.
31. **Cross, A. R., J. L. Yarchover, and J. T. Curnutte.** 1994. The superoxide-generating system of human neutrophils possesses a novel diaphorase activity. Evidence for distinct regulation of electron flow within NADPH oxidase by p67-*phox* and p47-*phox*. *J. Biol. Chem.* **269**:21448-21454.
32. **Curnutte, J. T.** 1985. Activation of human neutrophil nicotinamide adenine dinucleotide phosphate reduced (triphosphopyridine nucleotide, reduced) oxidase by arachidonic acid in a cell-free system. *J. Clin. Invest.* **75**:1740-1743.
33. **Curnutte, J. T.** 1993. Chronic granulomatous disease: the solving of a clinical riddle at the molecular level. *Clin. Immun. and Immunopath.* **67**:S2-S15.
34. **Cwirla, S, E. Peters, R. Barrett, and W. Dower.** 1990. Peptides on phage: a vast library of peptides for identifying ligands. *Proc. Natl. Acad. Sci. USA* **87**:6378-6382.
35. **Dedman, J. R., M. A. Kaetzel, H. Chang Chan, D. J. Nelson, and G. A. Jamieson, Jr.** 1993. Selection of targeted biological modifiers from a bacteriophage library of random peptides. The identification of novel calmodulin regulatory peptides. *J. Biol. Chem.* **268**:23025-23030.

36. **DeLeo, F. R., J. B. Burritt, C. W. Bond, A. J. Jesaitis, and M. T. Quinn.** 1994. Inhibition of the association of p47-phox with neutrophil flavocytochrome b-558 by an novel flavocytochrome b peptide. *Mol. Biol. of the Cell* 5:121a.(Abstract)
37. **Devlin, J., L. Panganiban, and P. Devlin.** 1990. Random peptide libraries: a source of specific protein binding molecules. *Science*. 249:404-406.
38. **Didsbury, J. R., R. J. Uhing, and R. Snyderman.** 1990. Isoprenylation of the low molecular mass GTP-binding proteins rac 1 and rac 2: Possible role in membrane localization. *Biochem. Biophys. Res. Comm.* 171:804-812.
39. **Dinauer, M. C., S. H. Orkin, R. Brown, A. J. Jesaitis, and C. A. Parkos.** 1987. The glycoprotein encoded by the X-linked chronic granulomatous disease locus is a component of the neutrophil cytochrome b complex. *Nature* 327:717-720.
40. **Dinauer, M. C., E. A. Pierce, G. A. P. Bruns, J. T. Curnutte, and S. H. Orkin.** 1990. Human neutrophil cytochrome b light chain (p22-phox). *J. Clin. Invest.* 86:1729-1737.
41. **Dooley, C. T., N. N. Chung, B. C. Wilkes, P. W. Schiller, J. M. Bidlack, G. W. Pasternak, and R. A. Houghten.** 1994. An all D-amino acid opioid peptide with central analgesic activity from a combinatorial library. *Science* 266:2019-2022.
42. **Doussiere, J., G. Brandolin, V. Derrien, and P. V. Vignais.** 1993. Critical assessment of the presence of an NADPH binding site on neutrophil cytochrome *b*<sub>558</sub> by photoaffinity and immunochemical labeling. *Biochemistry* 32:8880-8887.
43. **Dower, W. and S. Cwirla.** 1992. Creating vast peptide expression libraries: electroporation as a tool to construct plasmid libraries of greater than 10<sup>9</sup> recombinants, p. 291-301. In D. Chang, B. Chassy, J. Saunders, and A. Sowers (eds.), *Guide to Electroporation and Electrofusion*. Academic Press, Inc., San Diego, California.
44. **Dunn, P.** 1986. Biochemical aspects of insect immunology. *Ann. Rev. Entomol.* 31:321-339.
45. **Dusi, S. and F. Rossi.** 1993. Activation of NADPH oxidase of human neutrophils involves the phosphorylation and the translocation of cytosolic p67phox. *Biochem. J.* 296:367-371.
46. **Ebright, R., Q. Dong, and J. Messing.** 1992. Corrected nucleotide sequence of M13mp18 gene III. *Gene*. 114:81-83.

47. **Edens, L., R. N. H. Konings, and J. G. G. Schownmakers.** 1978. A cascade mechanism of transcription in bacteriophage M13 DNA. *Virology* **86**:354-367.
48. **El Benna, J., L. P. Faust, and B. M. Babior.** 1994. The phosphorylation of the respiratory burst oxidase component p47<sup>phox</sup> during neutrophil activation. Phosphorylation of sites recognized by protein kinase C and by proline-directed kinases. *J. Biol. Chem.* **269**:23431-23436.
49. **El Benna, J., J. M. Ruedi, and B. M. Babior.** 1994. Cytosolic guanine nucleotide-binding protein Rac2 operates *in vivo* as a component of the neutrophil respiratory burst oxidase. Transfer of Rac2 and the cytosolic oxidase components p47<sup>phox</sup> and p67<sup>phox</sup> to the submembranous actin cytoskeleton during oxidase activation. *J. Biol. Chem.* **269**:6729-6734.
50. **Elsbach, P. and J. Weiss.** 1992. Oxygen-independent Antimicrobial Systems of Phagocytes, p. 603-636. In J. Gallin, I. M. Goldstein, and R. Snyderman (eds.), *Inflammation: Basic Principles and Clinical Correlates*. Raven, New York.
51. **Felici, F., L. Castagnoli, A. Musacchio, R. Jappelli, and G. Cesareni.** 1991. Selection of antibody ligands from a large library of oligopeptides expressed on a multivalent exposition vector. *J. Mol. Biol.* **222**:301-310.
52. **Fowlkes, D. M., M. A. Adams, V. A. Fowler, and B. K. Kay.** 1992. Multipurpose vectors for peptide expression on the M13 viral surface. *BioTechniques* **13**:422-427.
53. **Gailus, V. and I. Rasched.** 1994. The adsorption protein of bacteriophage fd and its neighbour minor coat protein build a structural entity. *Eur. J. Biochem.* **222**:927-931.
54. **García, J., B. García-Barreno, I. Martinez, and J. A. Melero.** 1993. Mapping of monoclonal antibody epitopes of the human respiratory syncytial virus P protein. *Virology* **195**:239-242.
55. **Geysen, M. H., R. H. Meloen, and S. J. Barteling.** 1984. Use of peptide synthesis to probe viral antigens for epitopes to a resolution of a single amino acid. *Proc. Natl. Acad. Sci. USA*
56. **Gilbert, W. and D. Dressler.** 1968. DNA replication: The rolling circle model. *Cold Spring Harb. Symp. Quant. Biol.* **33**:473.
57. **Goldsmith, M. E. and W. H. Koingsberg.** 1977. Adsorption protein of the bacteriophage fd: isolation, molecular properties, and location in the virus: *Biochemistry* **16**:2686-2694.

58. **Gombert, F. O., W. Werz, M. Schlüter, A. Bayer, R. G. Werner, W. Berthold, and G. Jung.** 1994. Pentapeptide identified as a monoclonal antibody binding site in the serine-protease domain of t-PA. *Biol. Chem. Hoppe Seyler* **375**:471-480.
59. **Gray, C. W., R. S. Brown, and D. A. Marvin.** 1981. Adsorption complex of filamentous fd virus. *J. Mol. Biol.* **146**:621-627.
60. **Greenwood, J., Anne E. Willis, and R. N. Perham.** 1991. Multiple display of foreign peptides on a filamentous bacteriophage. *J. Mol. Biol.* **220**:821-827.
61. **Hackett, P., J. Fuchs, and J. Messing.** 1992. *An Introduction to Recombinant DNA Techniques.* Benjamin Cummings, Melno Park, Reading, Don Mills, Wokingham, Amsterdam, Sydney.
62. **Hart, S. L., A. M. Knight, R. P. Harbottle, A. Mistry, H. -D. Hunger, D. F. Cutler, R. Williamson, and C. Coutelle.** 1994. Cell binding and internalization by filamentous phage displaying a cyclic Arg-Gly-Asp-containing peptide. *J. Biol. Chem.* **269**:12468-12474.
63. **Henry, T. J. and D. Pratt.** 1968. The proteins of bacteriophage M13. *Proc. Natl. Acad. Sci. USA* **62**:800-807.
64. **Henson, P. M., J. E. Henson, Fittschen C., D. L. Bratton, and D. W. H. Riches.** 1992. Degranulation and Secretion by Phagocytic Cells, p. 511-539. In J. Gallin, I. M. Goldstein, and R. Snyderman (eds.), *Inflammation: Basic Principles and Clinical Correlates.* Raven Press, New York.
65. **Hernandez, L. A., M. B. Grisham, B. Twohig, K. E. Arfors, J. M. Harlan, and D. N. Granger.** 1987. Role of neutrophils in ischemia-reperfusion-induced microvascular injury. *Am. J. Physiol.* **253**:H699.
66. **Hoess, R. H.** 1993. Phage display of peptides and protein domains. *Curr. Opin. Struct. Biol.* **3**:572-579.
67. **Hoess, R. H., A. J. Mack, H. Wallton, and T. M. Reilly.** 1994. Identification of a structural epitope by using a peptide library displayed on filamentous bacteriophage. *J. Immunol.* **153**:1-6.
68. **Hoogenboom, H. R. and G. Winter.** 1992. By-passing immunisation: Human antibodies from synthetic repertoires of germline V-H gene segments rearranged in vitro. *J. Mol. Biol.* **227**:381-388.

69. **Horabin, J. I. and R. E. Webster.** 1986. Morphogenesis of f1 filamentous bacteriophage increased expression of gene I inhibits bacterial growth. *J. Mol. Biol.* **188**:403-413.
70. **Houghten, R. A., C. Pinilla, S. E. Blondelle, J. R. Appel, C. T. Dooley, and J. H. Cuervo.** 1991. Generation and use of synthetic peptide combinatorial libraries for basic research and drug discovery. *Nature* **354**:84-86.
71. **Imajoh-Ohmi, S., K. Tokita, H. Ochiai, M. Nakamura, and S. Kanegasaki.** 1992. Topology of cytochrome b558 in neutrophil membrane analyzed by anti-peptide antibodies and proteolysis. *J. Biol. Chem.* **267**:180-184.
72. **Jacobson, A.** 1972. Role of F pili in the penetration of bacteriophage f1. *J. Virol.* **10**:835-843.
73. **Jayawickreme, C. K., G. F. Graminski, J. M. Quillan, and M. R. Lerner.** 1994. Creation and functional screening of a multi-use peptide library. *Proc. Natl. Acad. Sci. USA* **91**:1614-1618.
74. **Jazwinski, M., R. Marco, and A. Kornberg.** 1973. A coat roptein of the bacteriophage M13 virion participates in membrane-oriented synthesis of DNA. *Proc. Natl. Acad. Sci. USA* **70**:205-209.
75. **Jellis, C. L., T. J. Cradick, P. Rennert, P. Salinas, J. Boyd, T. Amirault, and G. S. Gray.** 1993. Defining critical residues in the epitope for a HIV-neutralizing monoclonal antibody using phage display and peptide array technologies. *Gene* **137**:63-68.
76. **Kay, B. K., N. B. Adey, Y. -S. He, J. P. Manfredi, A. H. Mataragnon, and D. M. Fowlkes.** 1993. An M13 phage library displaying random 38-amino-acid peptides as a source of novel sequences with affinity to selected targets. *Gene* **128**:59-65.
77. **Kazmierczak, B. I., D. L. Mielke, M. Russel, and P. Model.** 1994. pIV, a filamentous phage protein that mediates phage export across the bacterial cell envelope, forms a multimer. *J. Mol. Biol.* **238**:187-198.
78. **Keller, P. M., B. A. Arnold, A. R. Shaw, R. L. Tolman, F. Van Middlesworth, S. Bondy, V. K. Rusiecki, S. Koenig, S. Zolla-Pazner, P. Conard, E. A. Emini, and A. J. Conley.** 1993. Identification of HIV vaccine candidate peptides by screening random phage epitope libraries. *Virology* **193**:709-716.
79. **Kelly, K. J., W. W. Jr. Williams, R. B. Colvin, and J. V. Bonventre.** 1994. Antibody to intracellular adhesion molecule 1 protects the kidney against ischemic injury. *Proc. Natl. Acad. Sci. USA* **91**:812-816.

80. **King, G. C. and J. E. Coleman.** 1987. Two-dimensional  $^1\text{H}$  NMR of gene 5 protein indicates that only two aromatic rings interact significantly with oligodeoxynucleotide bases. *Biochemistry* **26**:2929-2937.
81. **Klebanoff, S. J.** 1992. Oxygen Metabolites from Phagocytes, p. 541-588. In J. Gallin, I. M. Goldstein, and R. Snyderman (eds.), *Inflammation: Basic Principles and Clinical Correlates*. Raven, New York.
82. **Kleinberg, M. E., H. L. Malech, D. A. Mital, and T. L. Leto.** 1994. p21*rac* does not participate in the early interaction between p47-*phox* and cytochrome *b*<sub>558</sub> that leads to phagocyte NADPH oxidase activation *in vitro*. *Biochemistry* **33**:2490-2495.
83. **Koivunen, E., B. Wang, and E. Ruoslahti.** 1994. Isolation of a highly specific ligand for the  $\alpha$ -5,  $\beta$ -1 integrin from a phage display library. *J. Cell Biol.* **124**:373-380.
84. **Koivunen, E., B. Wang, and E. Ruoslahti.** 1994. Isolation of a highly specific ligand for the  $\alpha$ <sub>5</sub> $\beta$ <sub>1</sub> integrin from a phage display library. *J. Cell Biol.* **124**:373-380.
85. **Koshkin, V. and E. Pick.** 1994. Superoxide production of cytochrome b-559: mechanism of cytosol-independent activation. *FEBS Lett.* **338**:285-289.
86. **Kunkel, T., J. Roberts, and R. Zakour.** 1987. Rapid and efficient site-specific mutagenesis without phenotypic selection, p. 367-382. In R Wu and L Grossman (eds.), *Methods in Enzymology Volume 154, Recombinany DNA*. Academic Press, Inc., San Diego, CA.
87. **Kuo, T. -T., Y. -H. Lin, C. -M. Huang, S. -F. Chang, H. Dai, and T. -Y. Feng.** 1987. The lysogenic cycle of the filamentous phage Cf1t from *Xanthomonas campestris* pv. *citri*. *Virology* **156**:305-312.
88. **Laemmli, U. K. and M. Favre.** 1973. Maturation of the head of bacteriophage T4. I. DNA packaging events. *J. Mol. Biol.* **80**:575-599.
89. **Lam, K. S., M. Lebl, V. Krchnak, S. Wade, F. Abdul-Latif, R. Ferguson, C. Cuzzocrea, and K. Wertman.** 1993. Discovery of D-amino-acid-containing ligands with selectide technology. *Gene* **137**:13-16.
90. **Lam, K. S., S. E. Salmon, E. M. Hersh, V. J. Hruby, W. M. Kazmierski, and R. J. Knapp.** 1993. A new type of synthetic peptide library for identifying ligand-binding activity. *Nature* **354**:82-84.

91. **Landing, B. H. and H. S. Shirkey.** 1957. A syndrome of recurrent infection and infiltration of viscera by pigmented lipid histiocytes. *Pediatr.* **20**:431-438.
92. **Legon, S., P. Model, and H. D. Roberston.** 1977. Interaction of rabbit reticulocyte ribosomes with bacteriophage fl messenger RNA and of *E. coli* ribosomes with rabbit globin messenger RNA. *Proc. Natl. Acad. Sci. USA* **74**:2692-2696.
93. **Leto, T. L., K. J. Lomax, B. D. Volpp, H. Nuno, J. M. G. Sechler, W. M. Nauseef, R. A. Clark, J. I. Gallin, and H. L. Malech.** 1990. Cloning of a 67-kD neutrophil oxidase factor with similarity to a noncatalytic region of p60c-src. *Science* **248**:727-730.
94. **Leusen, J. H. W., M. De Boer, B. G. J. M. Bolscher, P. M. Hilarius, R. S. Weening, H. D. Ochs, D. Roos, and A. J. Verhoeven.** 1994. A point mutation in gp91-*phox* of cytochrome *b*<sub>558</sub> of the human NADPH oxidase leading to defective translocation of the cytosolic proteins p47-*phox* and p67-*phox*. *J. Clin. Invest.* **93**:2120-2126.
95. **Li, F., G. F. Linton, S. Sekhsaria, N. Whiting-Theobald, J. P. Katkin, J. I. Gallin, and H. L. Malech.** 1994. CD34<sup>+</sup> peripheral blood progenitors as a target for genetic correction of the two flavocytochrome *b*<sub>558</sub> defective forms of chronic granulomatous disease. *Blood* **84**:53-58.
96. **Lu, D. J., W. Furuya, and S. Grinstein.** 1993. Involvement of multiple kinases in neutrophil activation. *Bld. Cells* **19**:343-351.
97. **Luzzago, A., F. Felici, A. Tramontano, A. Pessi, and R. Cortese.** 1993. Mimicking of discontinuous epitopes by phage-displayed peptides, I. Epitope mapping of human H ferritin using a phage library of constrained peptides. *Gene* **128**:51-57.
98. **Maly, F. E., C. C. Schuerer-Maly, L. Quilliam, C. G. Cochrane, P. E. Newburger, J. T. Curnutte, M. Gifford, and M. C. Dinauer.** 1993. Restitution of superoxide generation in autosomal cytochrome-negative chronic granulomatous disease (A22<sup>0</sup> CGD)-derived B lymphocyte cell lines by transfection with p22<sup>phox</sup> cDNA. *J. Exp. Med.* **178**:2047-2053.
99. **Marvin, D. A.** 1978. Structure of the Filamentous Phage Virion, p. 583-603. In D. T. Denhardt, D. Dressler, and D. S. Ray (eds.), *The Single-Stranded DNA Phages*. Cold Spring Harbor Laboratory, Cold Spring Harbor, NY.
100. **Marvin, D. A. and B. Hohn.** 1969. Filamentous bacterial viruses. *Bacteriol. Rev.* **33**:172-209.

101. **McCord, J. M.** 1992. The Molecular Basis of Oxidative Damage by Leukocytes. p.225-239. CRC Press, Boca Raton, Ann Arbor, London, Tokyo.
102. **McPhail, L. C., P. S. Shirley, C. C. Clayton, and R. Snyderman.** 1985. Activation of the respiratory burst enzyme from human neutrophils in a cell-free system. *J. Clin. Invest.* **75**:1735-1739.
103. **McPherson, A., A. H. J. Wang, F. A. Journak, I. Molineux, F. Kolpak, and A. Rich.** 1980. X-ray diffraction studies on crystalline complexes of the gene 5 DNA-unwinding protein with deoxyoligonucleotides. *J. Biol. Chem.* **255**:3174-3177.
104. **Miceli, R. M., M. E. DeGraaf, and H. D. Fischer.** 1994. Two-stage selection of sequences from a random phage display library delineates both core residues and permitted structural range within an epitope. *J. Immunol. Methods* **167**:279-287.
105. **Model, P and M Russel.** 1988. Filamentous bacteriophages, p. 375-456. In R. Calender (ed.), *The Bacteriophages* vol. 2. Plenum Press, New York.
106. **Molnár, E., R. A. J. McIlhinney, A. Baude, Z. Nusser, and P. Somogyi.** 1994. Membrane topology of the GluR1 glutamate receptor subunit: Epitope mapping by site-directed antipeptide antibodies. *J. Neurochem.* **63**:683-693.
107. **Morel, F., J. Doussiere, and P. V. Vignais.** 1991. The superoxide-generating oxidase of phagocytic cells. *Eur. J. Biochem.* **201**:523-546.
108. **Morris, A. J., G. L. Waldo, J. L. Boyer, J. R. Hepler, C. P. Downes, and T. K. Harden.** 1990. Regulation of Phospholipase C, p. 61-76. In N. M. Nathanson and T. K. Harden (eds.), *G Proteins and Signal Transduction*. Rockefeller University Press, New York.
109. **Nauseef, W. M.** 1986. Myeloperoxidase biosynthesis by a human promyelocytic leukemia cell line: insight into myeloperoxidase deficiency. *Blood* **67**:865-872.
110. **Needels, M. C., D. G. Jones, E. H. Tate, G. L. Heinkel, L. M. Kochersperger, W. J. Dower, R. W. Barrett, and M. A. Gallop.** 1993. Generation and screening of an oligonucleotide-encoded synthetic peptide library. *Proc. Natl. Acad. Sci. USA* **90**:10700-10704.
111. **Nissim, A., H. R. Hoogenboom, I. M. Tomlinson, G. Flynn, C. Midgley, D. Lane, and G. Winter.** 1994. Antibody fragments from a 'single pot' phage display library as immunochemical reagents. *EMBO J.* **13**:692-698.

112. **O'Neil, K. T., R. H. Hoess, S. A. Jackson, N. S. Ramachandran, S. A. Mousa, and W. F. DeGrado.** 1992. Identification of novel peptide antagonists for GPIIb/IIIa from a conformationally constrained phage peptide library. *Proteins* **14**:509-515.
113. **Parkos, C. A., R. A. Allen, C. G. Cochrane, and A. J. Jesaitis.** 1987. Purified cytochrome b from human granulocyte plasma membrane is comprised of two polypeptides with relative molecular weights of 91,000 and 22,000. *J. Clin. Invest.* **80**:732-742.
114. **Parkos, C. A., R. A. Allen, C. G. Cochrane, and A. J. Jesaitis.** 1988. The quaternary structure of the plasma membrane b-type cytochrome of human granulocytes. *Biochim. Biophys. Acta* **932**:71-83.
115. **Parkos, C. A., M. C. Dinauer, L. E. Walker, R. A. Allen, A. J. Jesaitis, and S. H. Orkin.** 1988. Primary structure and unique expression of the 22-kilodalton light chain of human neutrophil cytochrome b. *Proc. Natl. Acad. Sci. USA* **85**:3319-3323.
116. **Parmley, S and G. Smith.** 1988. Antibody-selectable filamentous fd phage vectors: affinity purification of target genes. *Gene* **73**:305-318.
117. **Pinilla, C., J. R. Appel, and R. A. Houghten.** 1993. Synthetic peptide combinatorial libraries (SPCLs): identification of the antigenic determinant of beta-endorphin recognized by monoclonal antibody 3E7. *Gene* **128**:71-76.
118. **Pinilla, C., J. R. Appel, and R. A. Houghten.** 1994. Investigation of antigen-antibody interactions using a soluble, non-support-bound synthetic decapeptide library composed of four trillion ( $4 \times 10^{12}$ ) sequences. *Biochem. J.* **301**:847-853.
119. **Porter, C. D., M. H. Parkar, A. J. Verhoeven, R. J. Levinsky, M. K. L. Collins, and C. Kinnon.** 1994. p22-*phox*-deficient chronic granulomatous disease: Reconstitution by retrovirus-mediated expression and identification of a biosynthetic intermediate of gp91-*phox*. *Blood* **84**:2767-2775.
120. **Pugsley, A. P.** 1993. The complete general secretory pathway in Gram negative bacteria. *Microbiol. Rev.* **57**:50-108.
121. **Quinn, M. T., T. Evans, L. R. Loetterle, A. J. Jesaitis, and G. M. Bokoch.** 1993. Translocation of rac correlates with NADPH oxidase activation. *J. Biol. Chem.* **268**:20983-20987.
122. **Quinn, M. T., M. L. Mullen, and A. J. Jesaitis.** 1992. Human neutrophil cytochrome b contains multiple hemes. *J. Biol. Chem.* **267**:7303-7309.

123. **Quinn, M. T., C. A. Parkos, L. Walker, S. H. Orkin, M. C. Dinauer, and A. J. Jesaitis.** 1989. Association of a ras-related protein with cytochrome b of human neutrophils. *Nature* **342**:198-200.
124. **Ravel, P. and F. Lederer.** 1993. Affinity-labeling of an NADPH-binding site on the heavy subunit of flavocytochrome *b*<sub>558</sub> in particulate NADPH oxidase from activated human neutrophils. *Biochem. Biophys. Res. Commun.* **196**:543-552.
125. **Reidhaar-Olson, J. F. and R. T. Sauer.** 1988. Combinatorial cassette mutagenesis as a probe of the informational content of protein sequences. *Science.* **241**:53-57.
126. **Roberts, D., K. Guegler, and J. Winter.** 1993. Antibody as a surrogate receptor in the screening of a phage display library. *Gene* **128**:67-69.
127. **Rotrosen, D., M. E. Kleinberg, H. Nuno, T. Leto, J. I. Gallin, and H. L. Malech.** 1990. Evidence for a functional cytoplasmic domain of phagocyte oxidase cytochrome b558. *J. Biol. Chem.* **265**:8745-8750.
128. **Rotrosen, D., C. L. Yeung, and J. P. Katlin.** 1993. Production of recombinant cytochrome b558 allows reconstitution of the phagocyte NADPH oxidase solely from recombinant proteins. *J. Biol. Chem.* **268**:14256-14260.
129. **Rotrosen, D., C. L. Yeung, T. L. Leto, H. L. Malech, and C. H. Kwong.** 1992. Cytochrome b-558: the flavin-binding component of the phagocyte NADPH oxidase. *Science* **256**:1459-1462.
130. **Royer-Pokora, B., L. M. Kunkel, A. P. Monaco, S. C. Goff, R. L. Newburger, R. L. Bachner, F. S. Cole, J. T. Curnutte, and S. H. Orkin.** 1986. Cloning the gene for an inherited human disorder-chronic granulomatous disease-on the basis of its chromosomal location. *Nature* **322**:32-38.
131. **Russel, M.** 1994. Mutants at conserved positions in gene IV, a gene required for assembly and secretion of filamentous phages. *Mol. Microbiol.* **14**:357-369.
132. **Saggio, I. and R. Laufer.** 1993. Biotin binders selected from a random peptide library expressed on phage. *Biochem. J.* **293**:613-616.
133. **Saikawa, T., S. Anderson, M. Momoeda, S. Kajigaya, and N. S. Young.** 1993. Neutralizing linear epitopes of B19 parvovirus cluster in the VP1 unique and VP1-VP2 junction regions. *J. Virol.* **67**:3004-3009.

134. **Salmon, S. E., K. S. Lam, M. Lebl, A. Kandola, P. S. Khattri, S. Wade, M. Pátek, P. Kocis, V. Krchnák, D. Thorpe, and S. Felder.** 1993. Discovery of biologically active peptides in random libraries: Solution-phase testing after staged orthogonal release from resin beads. *Proc. Natl. Acad. Sci. USA* **90**:11708-11712.
135. **Sanders, J. C., P. I. Haris, D. Chapman, C. Otto, and M. A. Hemminga.** 1993. Secondary structure of M13 coat protein in phospholipids studied by circular dichroism, Raman, and Fourier transform infrared spectroscopy. *Biochemistry* **32**:12446-12454.
136. **Sanger, F., S. Nicklen, and A. R. Coulson.** 1977. DNA sequencing with chain-terminating inhibitors. *Proc. Natl. Acad. Sci. USA* **74**:5463-5467.
137. **Scott, J. and G. Smith.** 1990. Searching for peptide ligands with an epitope library. *Science*. **249**:386-390.
138. **Scott, J. K., D. Loganathan, R. B. Easley, and W. Gong.** 1993. A family of concanavalin A-binding peptides from a hexapeptide epitope library. *Proc. Natl. Acad. Sci. USA* **89**:5398-5402.
139. **Segal, A. W.** 1988. Cytochrome b245 and its involvement in the molecular pathology of chronic granulomatous disease. *Hematology/Oncology Clinics of North America* **2**:213-223.
140. **Segal, A. W.** 1993. The electron transport chain of the microbicidal oxidase of phagocytic cells and its involvement in the molecular pathology of chronic granulomatous disease. *J. Clin. Invest.* **83**:1785-1793.
141. **Segal, A. W., I. West, F. Wientjes, J. H. A. Nugent, A. J. Chavan, B. Haley, R. C. Garcia, H. Rosen, and G. Scrase.** 1992. Cytochrome b-245 is a flavocytochrome containing FAD and the NADPH-binding site of the microbicidal oxidase of phagocytes. *Biochem. J.* **284**:781-788.
142. **Shih, D. -T., J. M. Edelman, A. F. Horwitz, G. B. Grunwald, and C. A. Buck.** 1993. Structure/function analysis of the integrin  $\beta_1$  subunit by epitope mapping. *J. Cell Biol.* **122**:1361-1371.
143. **Siegel, D. L. and L. E. Silberstein.** 1994. Expression and characterization of recombinant anti-Rh(D) antibodies on filamentous phage: A model system for isolating human red blood cell antibodies by repertoire cloning. *Blood* **83**:2334-2344.
144. **Smith, G. P.** 1985. Filamentous fusion phage. Novel expression vectors that display cloned antigens on the virion surface. *Science* **228**:1315-1317.

145. **Smith, G. P., D. A. Schultz, and J. E. Ladbury.** 1993. A ribonuclease S-peptide antagonist discovered with a bacteriophage display library. *Gene* **128**:37-42.
146. **Smith, G. P. and J. K. Scott.** 1993. Libraries of peptides and proteins displayed on filamentous phage. *Methods Enzymol.* **217**:228-257.
147. **Smith, R. M. and J. T. Curnutte.** 1991. Molecular basis of chronic granulomatous disease. *Blood* **77**:673-686.
148. **Soderlind, E., A. C. S. Lagerkvist, M. Duenas, A. Malmberg, M. Ayala, L. Danielsson, and C. A. K. Borrebaeck.** 1993. Chaperonin assisted phage display of antibody fragments on filamentous bacteriophages. *BioTechniques* **11**:503-507.
149. **Soumillion, P., L. Jespers, M. Bouchet, J. Marchand-Brynaert, G. Winter, and J. Fastrez.** 1994. Selection of  $\beta$ -lactamase on filamentous bacteriophage by catalytic activity. *J. Mol. Biol.* **237**:415-422.
150. **Teahan, C., P. Rowe, P. Parker, N. Totty, and A. W. Segal.** 1987. The X-linked chronic granulomatous disease gene codes for the b-chain of cytochrome b-245. *Nature* **327**:720-721.
151. **Thi Man, N. and G. E. Morris.** 1993. Use of epitope libraries to identify exon-specific monoclonal antibodies for characterization of altered dystrophins in muscular dystrophy. *Am. J. Hum. Genet.* **52**:1057-1066.
152. **Tsan, M. and P. A. McIntyre.** 1976. The requirement for membrane sialic acid in the stimulation of superoxide production during phagocytosis by human polymorphonuclear leukocytes. *J. Exp. Med.* **143**:1308-1316.
153. **Tzagloff, H. and D. Pratt.** 1964. The initial steps in infection with Coliphage M13. *Virology* **24**:372-380.
154. **Uhlinger, D. J., S. R. Tyagi, and J. D. Lambeth.** 1995. On the mechanism of inhibition of the neutrophil respiratory burst oxidase by a peptide from the C-terminus of the large subunit of cytochrome *b*<sub>558</sub>. *Biochemistry* **34**:524-527.
155. **Ui, M.** 1990. G Proteins Identified as Pertussis Toxin Substrates, p. 3-27. In P. Naccache (ed.), *G Proteins and Calcium Signaling*. CRC Press, Boca Raton.
156. **Umei, T., B. M. Babior, J. T. Curnutte, and R. M. Smith.** 1991. Identification of the NADPH-binding subunit of the respiratory burst oxidase. *J. Biol. Chem.* **266**:6019-6022.

157. **Umei, T., K. Takeshige, and S. Minakami.** 1986. NADPH binding component of neutrophil superoxide-generating oxidase. *J. Biol. Chem.* **261**:5229-5232.
158. **Umei, T., K. Takeshige, and S. Minakami.** 1987. NADPH-binding component of the superoxide-generating oxidase in unstimulated neutrophils and the neutrophils from the patients with chronic granulomatous disease. *Biochem. J.* **243**:467-472.
159. **van Wzenbeek, P. M. G. F., T. J. M. Hulsebos, and J. G. G. Schoemakers.** 1993. Nucleotide sequence of the filamentous bacteriophage M13 DNA genome: comparison with phage fd. *Gene* **11**:129-148.
160. **Volpp, B. D., W. M. Nauseef, D. R. Donelson, D. R. Moser, and R. A. Clark.** 1989. Cloning of the cDNA and functional expression of the 47 kilodalton cytosolic component of the human neutrophil respiratory burst oxidase. *Proc. Natl. Acad. Sci. USA* **86**:7195-??.
161. **Widger, W. R., W. A. Cramer, R. G. Herrmann, and A. Trebst.** 1984. Sequence homology and structural similarity between cytochrome b of mitochondrial complex III and the chloroplast b6-f complex: position of the cytochrome b hemes in the membrane. *Proc. Natl. Acad. Sci. USA* **81**:674-678.
162. **Wu, J., Q. N. Ma, and K. S. Lam.** 1994. Identifying substrate motifs of protein kinases by a random library approach. *Biochemistry* **33**:14825-14833.
163. **Yamaguchi, T., T. Hayakawa, M. Kaneda, K. Kakinuma, and A. Yoshikawa.** 1989. Purification and some properties of the small subunit of cytochrome b558 from human neutrophils. *J. Biol. Chem.* **264**:112-118.
164. **Zhou, Y. and M. P. Murtaugh.** 1994. Cloning and expression of the gene encoding the porcine NADPH oxidase light-chain subunit (p22-phox). *Gene* **148**:363-367.
165. **Zimmerman, B. J., M. B. Grisham, and D. N. Granger.** 1990. Role of oxidants in ischemia/reperfusion-induced granulocyte infiltration. *Am. J. Physiol.* **258**:21-22.
166. **Zinder, N. D.** 1973. Resistance to colicins E3 and K induced by infection with bacteriophage f1. *Proc. Natl. Acad. Sci. USA* **70**:3160-3164.

## CHAPTER TWO

### NONAPEPTIDE PHAGE-DISPLAY LIBRARY CONSTRUCTED WITH NOVEL M13 VECTOR

#### Abstract

The identification of peptide sequences bound by biological molecules is possible following affinity purification of peptides expressed by bacteriophage peptide-display libraries. A population of phage constitutes the library, and each unique peptide of the library is expressed on the surface of a different infectious virus particle. Recombinant DNA technology was used to construct a novel bacteriophage vector for the production of such a library. The vector was produced from M13mp18 and offers the benefits of high copy replicative form, large plaque formation, and a kanamycin resistance gene. The vector also has a pair of noncomplimentary *Bst*XI restriction sites positioned near the 5' end of the PIII gene. Insertion of foreign DNA between the *Bst*XI sites allows phage surface-display of the protein corresponding to the foreign DNA. The J404 phage library expressing random nonapeptides was produced by inserting DNA containing a 27 base random sequence oligonucleotide between the *Bst*XI sites of the vector and transfecting the DNA into electrocompetent *E. coli* cells.

The library contains  $5 \times 10^8$  unique phage, each expressing a different nonapeptide sequence fused to the amino terminus of the pIII capsid protein. Inspection of a sample of codons contained in the DNA inserts coding for unique nonapeptide of unfractionated library members suggest the encoded amino acids assume a random distribution.

### Introduction

The activity of many proteins is dependent upon interactions of relatively short regions of specific amino acid sequence. Phage peptide-display libraries have proven a useful tool in the identification of such interactive peptide regions of proteins (3,6,9,12,16,17,21,22,32,33). A phage peptide library is a population of infectious bacteriophage, which can be produced to contain up to one billion unique phage particles, each of which expresses five copies of a different oligopeptide sequence on the capsid surface. A library containing this number of unique peptides theoretically includes all possible six amino acid sequence (32).

Unique peptide sequences of the library can be selected on the basis of their interaction with a chosen ligand without *a priori* information about the critical binding residues. These phage-expressed peptides are displayed on the phage surface in a manner which is accessible to any ligand of choice. Once the peptide is affinity selected, the expressing phage can be propagated, and the amino acid sequence of the unique peptide bound by the ligand can be deduced from the nucleotide sequence of the phage genome (36). This technology has been used to determine the epitopes recognized by monoclonal antibodies (4,6,7,12,16,17,21,23,29,32,33) and sequences involved in protein-protein interactions (3,8,10,12,16,18,26,30,35).

The utility of bacteriophage random peptide-display technology is made possible by 1) the large number of unique amino acid sequences available in the library, 2) recovery of these sequences by affinity selection, 3) and the relative ease by which the selected peptide sequences are determined. This technique allows the

identification of many types of biologically active regions of proteins including sufficient residue matches to give very strong identification of interactive sequences.

We report the detailed construction of a large nonapeptide phage-display library using a novel bacteriophage vector, M13KBst. The vector was created for the production of a phage peptide-display library, and like other vectors tailored for phage peptide library production (7,12,16,21,22,32), M13KBst belongs to the Ff class of filamentous bacteriophages, and specifically infects *E. coli* which harbor the fertility (F<sup>+</sup>) episome. M13KBst differs from other phage library vectors because it possesses all four of the following features: 1) a high copy number replicative form which simplifies production of large amounts of replicative form (RF) DNA necessary for library production, 2) large plaque formation enables accurate quantitation of virions as plaque forming units, 3) a kanamycin resistance gene allows selection of colonies of *E. coli* infected by the phage, and 4) a pair of nonidentical *Bst*XI restriction sites near the 5' end of the PIII phage gene. The *Bst*XI sites allow cleavage of the M13KBst RF DNA with a single endonuclease, producing four-base 3' overhanging ends which are not ligation-compatible (7). This library has been used in the identification of several epitopes recognized by mAbs and interactive regions of proteins.

## Materials and Methods

### Reagents

Tween 20, yeast extract, tryptone, agar, Trizma base, EDTA, agarose, and CsCl were purchased from Sigma Chemical Co. (St. Louis, MO). Sequencing data was obtained using Sequenase<sup>®</sup> version 2.0 sequencing enzyme and additional reagents purchased from United States Biochemical (Arlington, Heights, IL). *Pst*I, *Bst*XI, calf intestinal phosphatase, and T4 DNA ligase were purchased from New England Biolabs (Beverly, MA). Gelase<sup>®</sup> enzyme and reagents were purchased from Epicenter Technologies (Madison, WI). ATP and nucleoside-triphosphates were purchased from Boehringer Mannheim (Indianapolis, IN). Oligonucleotides were synthesized either at Montana State University or by Macromolecular Resources at Colorado State University in Fort Collins, CO. *E. coli* strains K91 and MC1061 were kindly provided by Dr. George P. Smith at the University of Missouri, Columbia.

### Construction of M13KBst

The filamentous phage vector, M13KBst, was constructed for the production of a random nonapeptide library by introducing the following changes to M13mp18 (14). A 1.4 kBp *Pst*I fragment from the pUC119.kan plasmid (15) encoding aminoglycoside 3'-phosphotransferase (APT) (27) was isolated from a preparative agarose gel using Gelase<sup>®</sup> extraction (Epicenter Technologies). The insert containing the APT gene was obtained from 10 µg of CsCl-purified and *Pst*I-digested pUC119.K (15). The digested DNA was loaded into four wells of a 1% (w/v) low melting agarose gel, run for two

hours, and stained with ethidium bromide. Liberation of the 1.4 kBp fragment from the plasmid was evident following electrophoresis and visualization of the bands, and the appropriate bands were excised from the gel for extraction of the DNA using the Gelase enzyme system. The fragment was recovered from the digested gel by ethanol precipitation and lyophilization according to the manufacturer. The DNA fragment was then ligated into the double stranded RF of M13mp18 at the *Pst*I site in the polycloning region using standard techniques (2). The ligation product was then transfected into electrocompetent MC1061 cells to obtain phage containing the APT gene.

Agarose gel analysis was used to follow the DNA products through this and subsequent steps of manipulation. Analyses were performed in 1% high-melting agarose slab TAE gels (40 mM Tris acetate, 2 mM EDTA pH 8.3). Samples of DNA (0.1 to 1  $\mu$ g) in 12  $\mu$ l of water were mixed with four  $\mu$ l of loading buffer (50% glycerol (v/v), 0.2 M EDTA pH 8.3, 0.05% (w/v) bromphenol blue) and separated in individual lanes with 50 volts constant current for 2.5 hours. Gels were stained in 1  $\mu$ g/ml ethidium bromide for three hours and destained in water for two hours followed by photography on a UV transilluminator using Polaroid® type 55 or 57 film.

Oligonucleotide-directed mutagenesis (20) was used to introduce two *Bst*XI restriction sites in the 5' end of the PIII phage gene. Mutagenesis of the PIII gene with the J97 oligonucleotide, 3'-caaGGTAAGAT/GACCgtgaggcgcactttgacaacGGTCAACA/AACCgttttg-5', creates seven point mutations in the phage genome corresponding to underlined bases which create the two *Bst*XI recognition sequences (shown in upper-case letters). The

recognition sequences of the two sites are different, and when cleavage occurs at the position indicated by the (/), the resulting overhanging ends are not compatible for ligation. The resulting DNA contains restriction sites to allow removal of a 31 bp fragment from the vector when cleaved with *Bst*XI, enabling the insertion of synthetic DNA encoding random amino acids.

### Production of Library

M13KBst RF DNA was produced for library construction in one liter of LB broth (2) containing kanamycin at 75  $\mu\text{g/ml}$ . The medium was divided among four two-liter flasks, and each flask was inoculated with 0.5 ml log phase M13KBst-infected K91 cells and incubated 16.5 hours at 37° C with strong aeration. Phage RF DNA was extracted from the cells and purified on CsCl gradients as described (2). Yield by this method was about 1.5 mg of purified RF DNA per liter of culture. Eight hundred  $\mu\text{g}$  of purified RF DNA was treated with 800 units of *Bst*XI restriction endonuclease for 20 hours at 55° C in 1.6 ml reaction volume to excise the 31 base pair *Bst*XI fragment (stuffer). Cleaved DNA was diluted in 10 mM TE (10 mM Tris base, 1 mM EDTA, pH 8.0) to give a DNA concentration of 0.25  $\mu\text{g}/\mu\text{l}$ . The 31 base stuffer was separated from the linear vector on a potassium acetate (KOAc) gradient as described (1), with the following modifications. Six, 5 ml linear 5-20% (w/v) KOAc gradients containing 2 mM EDTA were prepared (2). The top of each gradient was loaded with 532  $\mu\text{l}$  (133  $\mu\text{g}$ ) of the *Bst*XI cleaved RF DNA and the gradients were spun in a Beckman SW 50.1 rotor at 45,000 RPM for three hours at 20° C. The

gradients were then fractionated manually from the top by removing 500  $\mu$ l samples.  $OD_{260}$  measurements were performed on each fraction to identify the position of the linear 8.1 kBp phage DNA fragment in the gradient. Gradient fractions containing the large fragment were pooled and DNA was recovered by ethanol precipitation and centrifugation. The DNA was dried in a vacuum and resuspended in distilled water and the concentration of recovered DNA was determined photometrically at  $OD_{260}$ .

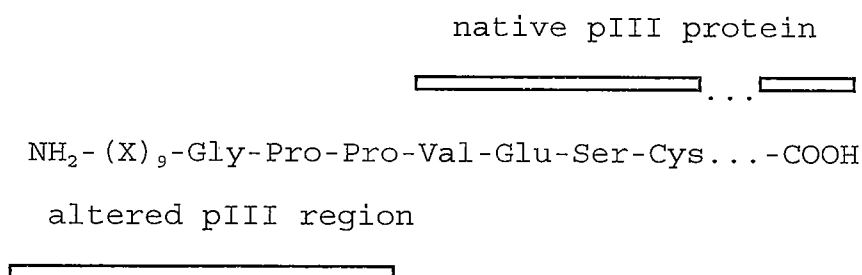
The synthetic DNA insert was produced by annealing three oligonucleotides (7) which had previously been phosphorylated using polynucleotide kinase and ATP. Sequences of the J364 oligonucleotides are listed below.

- A) 5'-c,tct,cac,tcc,(nnk)<sub>9</sub>,ggc,ccg,ccg,gtt,gaa,agt,tgt-3'
  - B) 5'-gga,gtg,aga,gta,ga-3'
  - C) 5'-ct,ttc,aac,cgg,cgg,gcc-3'
- n= a, t, g, or c, k= g or t

*Bst*XI-cleaved, KoAc gradient-purified M13KBst RF and phosphorylated oligonucleotide DNA samples were combined by heating to 70° C, and cooling slowly to room temperature. The molar ratio of DNA species during annealing was: vector, 1: oligo A, 2.5: oligo B, 2.5: and oligo C, 50. The inserts were ligated to the vector using T4 DNA ligase at an activity of 303 cohesive end units per picomole of vector DNA. The single-stranded region of the resulting circular molecules corresponding to the random 27 bases was filled in with a mixture of the four nucleoside triphosphates (275  $\mu$ M dNTP) and Sequenase® ver. 2.0 (0.325 U/ $\mu$ g vector DNA) at 37° C for 90 minutes.

The synthetic construct formed by annealing the oligonucleotides includes

oligonucleotide A which contains 27 random bases coding for a nine amino acid peptide of random sequence. Oligos B and C anneal to the 5' and 3' ends of oligo A, respectively, and produce the ligation-compatible ends necessary to recircularize the *Bst*XI-cleaved vector. Oligonucleotide A also contains codons for a glycine and two proline residues at the carboxyl flank of the random peptide region, resulting in the following configuration of the mature pIII protein:



The glycine residue adjacent to the random region of the pIII protein is intended to act as a flexible linker, and the proline residues are included to discourage association of the random peptide with the native pIII protein (12). Following ligation, the DNA was transfected into *E. coli* cells to allow production of recombinant phage bearing random peptides.

Electrocompetent MC1061 cells were prepared as described (13) and transfected in aliquots of 50  $\mu$ l, each with  $\sim$ 5  $\mu$ g of DNA suspended in 2  $\mu$ l of dH<sub>2</sub>O. Sixty-three separate transfections were used to introduce 320  $\mu$ g of recombinant DNA using an electroporation apparatus as described (37). Following transfection, each sample of cells was immediately collected in one ml of SOC medium (2) and allowed to incubate with strong aeration at 37° C for 40-60 minutes without antibiotic

selection. During this recovery period, small samples were removed to determine the titer of phage by appropriately diluting the SOC which was then plated on LB agar containing kanamycin at 75  $\mu\text{g/ml}$ . In this way, the library diversity and number of unique transfectants could be determined. The transfectants in the remaining SOC were inoculated into four liters of LB broth with kanamycin at 75  $\mu\text{g/ml}$ . The broth was incubated overnight at 37° C with strong aeration in 16 two-liter flasks. The phage library (J404) was then harvested from the culture supernatant as described (7).

## Results

### Vector Construction

The M13KBst phage was created using recombinant DNA technology for use as a phage-display vector. Agarose gel analysis was used to follow the DNA material through the steps of oligonucleotide-directed mutagenesis in which the *Bst*XI sites were produced in the PIII gene (Figure 4). This and subsequent analysis by agarose gel electrophoresis (except Figure 7) were performed as described in Methods. Linear DNA standards are shown in Lane A of Figure 4 to indicate relative migration during electrophoresis. Double-stranded M13mp18 RF DNA is shown in lane B, with supercoiled forms at ca. 4.7 kBp, relaxed circular DNA at ca. 12 kBp, and a faint linearized band at ca. 7.2 kBp. In lane C, single-stranded M13mp18 DNA templates containing uracil migrate at ca. 5 kBp. In lane D, *in vitro* synthesis of double-stranded DNA from single-stranded templates during oligonucleotide-directed priming and chain extension can be seen (arrowhead). Lane E represents the same conditions of lane D, except the oligonucleotide-primer was omitted, resulting in a diffuse smear of DNA caused by nonspecific priming and variable complimentary strand synthesis.

Transfected phage clones were produced from oligonucleotide-directed mutagenesis (lane D, Figure 4), and selected at random to be screened for *Bst*XI sites by miniprep extraction (2), *Bst*XI endonuclease digestion, and agarose gel analysis. Approximately 25% of all clones tested in this way were found to produce RF DNA which could be cleaved with *Bst*XI. Recombinant phage containing at least one *Bst*XI site were identified by the digestion of the RF DNA which ran on the agarose gel as a

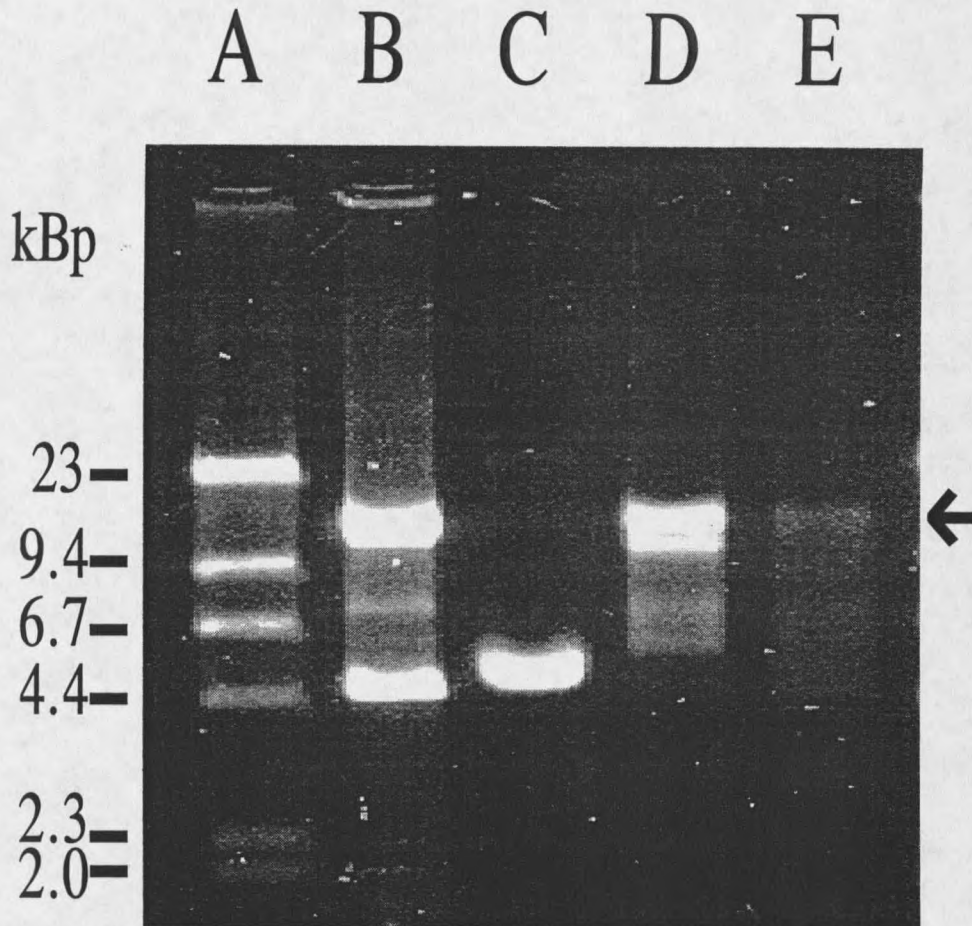


**Figure 4.** Agarose gel analysis of mutant bacteriophage DNA during oligonucleotide-directed mutagenesis. Linear  $\lambda$  *Hind*III fragments are shown in lane A to indicate relative mobilities of DNA species rather than actual fragment sizes. Uncleaved double-stranded M13mp18 RF DNA is shown in lane B, with supercoiled forms at ca. 4.7 kbp, relaxed circular DNA at ca. 12 kbp, and a faint linearized band is present at ca. 7.2 kbp. Lane C contains single-stranded M13mp18 DNA templates containing uracil which migrate as a single band at ca. 5 kbp. In lane D, *in vitro* synthesis of double-stranded DNA (arrowhead) from the single-stranded templates (lane C), during oligonucleotide-directed priming and chain extension is shown. Lane E represents the same conditions of lane D, except the mutagenic J97 oligonucleotide-primer was omitted, resulting in a diffuse smear caused by nonspecific priming and subsequent DNA synthesis. For conditions of electrophoresis for this and subsequent gels, see Methods.

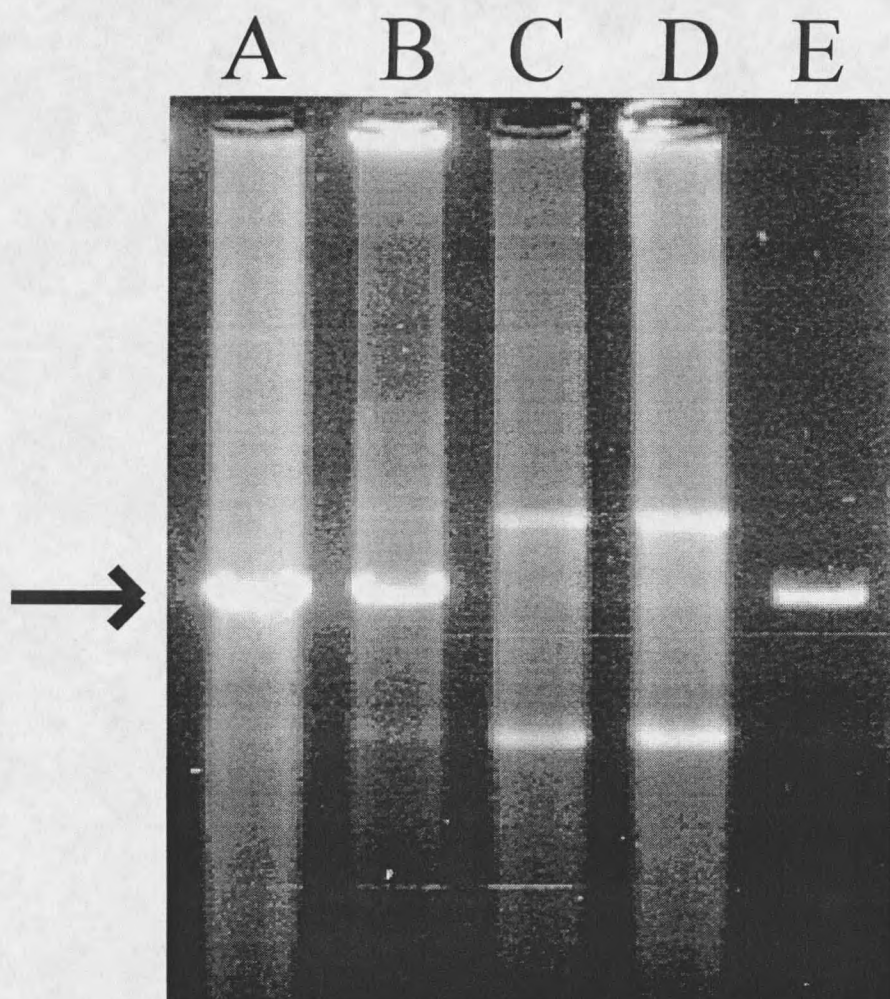


**Figure 5.** Transfected phage clones resulting from oligonucleotide-directed mutagenesis were selected at random and screened for *Bst*XI sites by miniprep extraction, *Bst*XI endonuclease digestion, and agarose gel analysis. Approximately 25% of all clones tested were found to produce RF DNA which could be linearized by digestion with *Bst*XI. Recombinant phage containing at least one cleaveable *Bst*XI site were identified by the digestion of both bands, resulting in a single band (arrowhead) of linearized RF (lanes A and B). Phage clones lacking a cleaveable *Bst*XI site were recognized by the supercoiled RF and nicked circular bands (lanes C and D). Lane E contained CsCl-purified M13mp18 DNA linearized with *Pst*I to serve as a linearized RF control.

single band (Figure 5, lanes A and B) corresponding to the position of the arrowhead. Phage clones lacking a cleaveable *Bst*XI site were recognized by the supercoiled RF and nicked circular bands (Figure 5, lane C and D). A *Hind*III cleaved sample of CsCl-purified M13mp18 RF DNA was included in Lane E to serve as a control of linearized RF DNA. Sixteen *Bst*XI-cleaveable clones were identified by this method, and were propagated for sequence analysis. Following sequencing of the 5' end of the PIII gene for each of these clones, it was determined that one clone contained both *Bst*XI sites and all intended point mutations. The mutated nucleotide sequence in the containing both intended *Bst*XI sites is shown in Figure 6B, and point mutations produced in the PIII gene which create the two *Bst*XI sites are boxed. This clone was propagated, resequenced to verify the *Bst*XI sites, and RF DNA was prepared for the cloning of the APT gene.

The APT gene was purified from *Pst*I-digested pUC119.K using a preparative agarose gel. A 1.0% low-melting agarose preparative gel was prepared using the same TAE buffer and electrophoresis as indicated above, and was used to resolve the 1.4 kBp *Pst*I fragment containing the APT gene. Figure 7 shows four adjacent lanes of the preparative gel used to purify the fragment. Each of the lanes was loaded with 2.5  $\mu$ g of the cleaved pUC119.K plasmid. Following electrophoresis, a *Pst*I fragment was found to migrate at ca. 1.4 kBp, and was presumed to contain the APT gene (arrowhead). The remaining DNA produced by the *Pst*I-digestion of pUC119.K plasmid can be seen as a band migrating at ca. 2.8 kBp, and represents the pUC119 plasmid vector from which the insert containing the APT gene was obtained. Each of

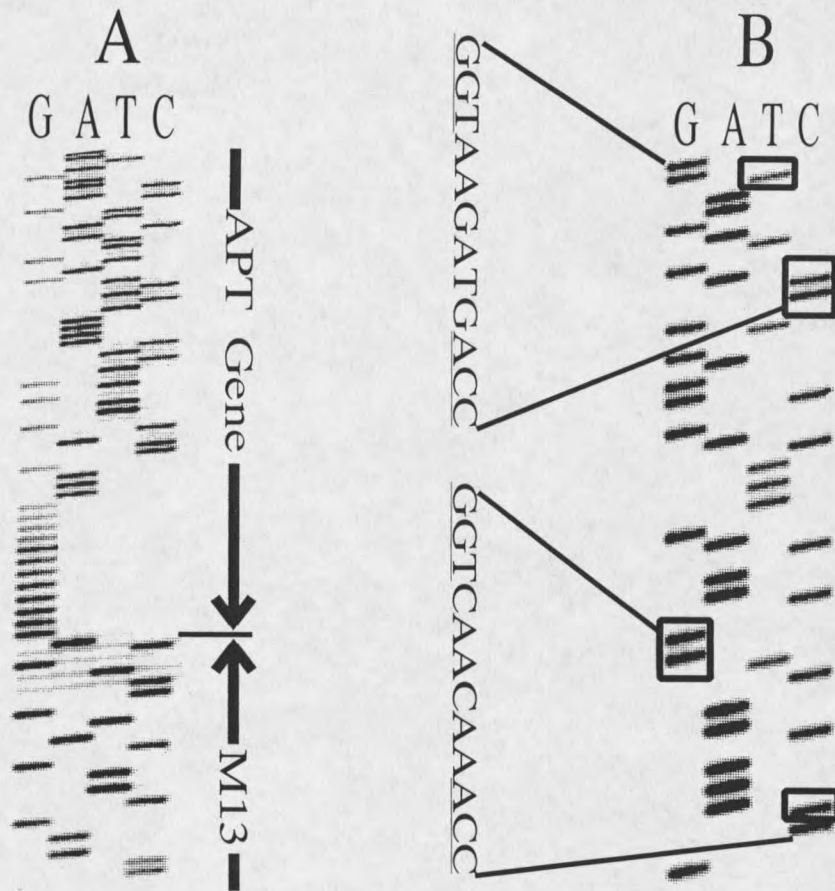


**Figure 6.** Nucleotide sequence analysis of mutations creating recombinant vector, M13KBst. The M13KBst virions were produced and regions of the genome showing mutations used to create the vector are shown. The nucleotide sequence shown in A was obtained by standard dideoxy sequencing techniques using a primer with the sequence, 5'-gtttccagtcacgac-3'; the sequence shown in B was determined on the same DNA material with the J140 primer sequence, 5'-gtttgtcgtcttccagac-3'. The juncture site between the M13 polycloning region at the cleaved *Pst*I site is shown joining the 3' end of the ligated APT gene (A). Point mutations required for the creation of two *Bst*XI sites near the 5' end of the PIII gene of M13 are boxed (B). The recognition sequence is shown to the left of Figure B, and nucleotide bases required for cleavage are underlined.

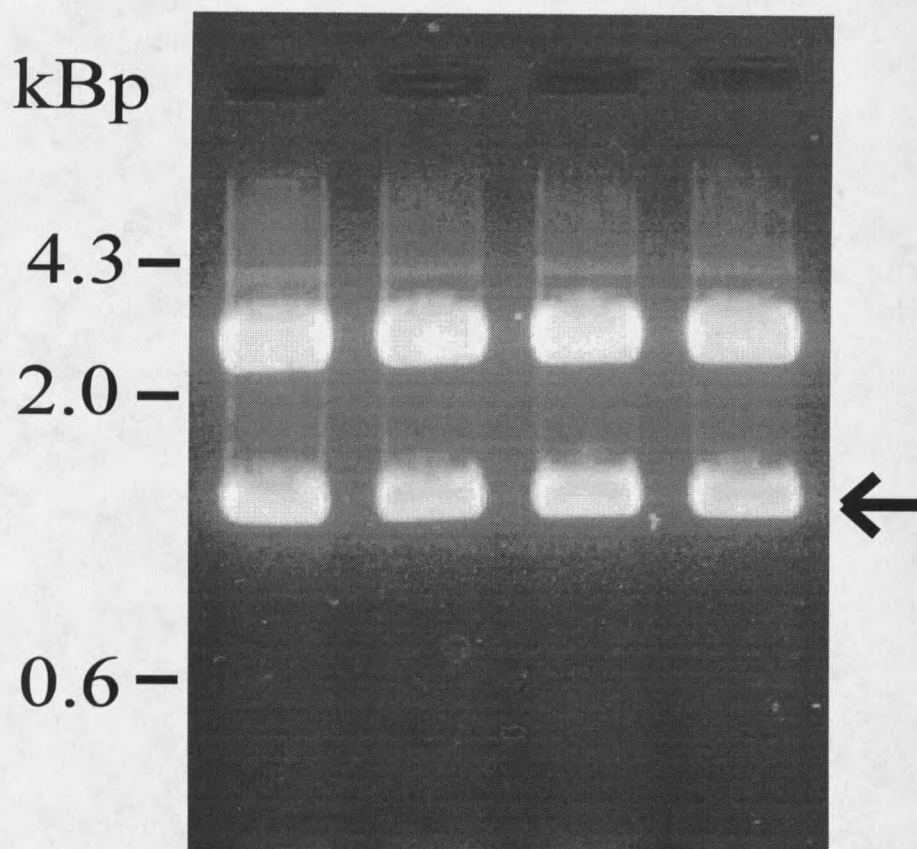


**Figure 7.** Agarose preparative gel of the 1.4 kbp *Pst*I fragment encoding the aminoglycoside-3'-phosphotransferase (APT) enzyme which imparts kanamycin resistance. The fragment was produced by complete digestion of 10  $\mu$ g CsCl-purified pUC119.K plasmid with *Pst*I restriction endonuclease and subsequent agarose gel electrophoresis as described in Chapter 2, except a 1.0% low melting point gel was used. Two plasmid fragments are produced from the digestion, due to the cleavage of the two *Pst*I sites which flank the APT gene. Following electrophoresis at two hours in the TAE gel and staining in ethidium bromide, the large fragment migrates at about 2.8 kbp and corresponds to the pUC119 plasmid vector. The other band (arrowhead) is comprised of the 1.4 kbp fragment which contains the APT gene. Each of the four bands containing the smaller fragment contained about 850 ng of the fragment containing the APT gene and were excised from the gel slab for DNA extraction by the Gelase<sup>®</sup> enzyme system. Once purified, the fragment was ligated into the *Pst*I site of the double-stranded replicative form of M13mp18 using standard techniques (2).

these bands comprised of the 1.4 kBp fragment contained about 850 ng of DNA and was excised for extraction of the APT gene as described in Methods. Following extraction of the 1.4 kBp fragment, this DNA was ligated into the *Pst*I-cleaved M13 vector and the resulting ligation product was transfected into MC1061 cells which were subsequently plated on LB plates with 75 µg/ml kanamycin. Following overnight incubation at 37° C, the kanamycin resistant colonies were found to produce the recombinant M13KBst phage-display vector. The phage produced by these colonies were sequenced and found to contain the 1.4 kBp fragment at the *Pst*I site of the vector. Figure 6A shows the nucleotide sequence data corresponding to bases complimentary to the coding strand near the 3' terminus of the APT gene in M13KBst. The insert containing the APT gene begins with the 12 base poly-C tract (lane G) (38) ligated to the cleaved *Pst* I site in the polycloning region (15) and extends for ca. 1.4 kB in the 5' direction. Alpha-complementation capability of the vector was found to be abolished (data not shown), presumably by insertional inactivation of the lac Z region by the cloned insert (15).

Expression of the kanamycin resistance gene is essential for the use of antimicrobial selection of infected host cells. Broth dilution determination of the minimum inhibitory concentration (MIC) of M13KBst-infected K91 cells challenged by specific concentrations of kanamycin was used to determine expression and activity of the APT protein. APT activity encoded by the phage confers kanamycin resistance to infected K91 cells to 2.5 mg/ml kanamycin, with an MIC value of 5 mg/ml. The APT protects sensitive cells to almost 50 times the concentration of kanamycin (75

ug/ml) used for antimicrobial selection of phage-infected K91 cells. This degree of APT expression is identical to levels expressed by the plasmid-borne gene in pUC119.kan when produced in JF805 cells (15) (Table 4).

**Table 4.** Activity of Aminoglycoside 3-Phosphotransferase Gene Expressed as the Minimum Inhibitory Concentration for M13KBst Phage-display Vector and pUC119.K in LB Broth<sup>a</sup> Containing Kanamycin.

	Concentration of Kanamycin in $\mu\text{g/ml}$				313
	5000	2500	1250	625	
M13KBst <sup>b</sup>	-	+	+	+	+
pUC119.K <sup>c</sup>	-	+	+	+	+

<sup>a</sup> Incubations were performed in 1.5 ml cultures for 18 hours at 37° C with strong aeration.

<sup>b</sup> APT activity of M13KBst was tested in K91 cells (36).

<sup>c</sup> APT activity of pUC119.K was test in JF805 cells (15).

### Library Production

M13KBst RF DNA was produced as described above, purified on CsCl gradients, cleaved with *Bst*XI, and the 31 base stuffer which was cleaved from between the two sites was removed on KOAc gradients. The synthetic insert construct was then ligated to the two *Bst*XI-cleaved restriction sites.

Figure 8 shows agarose gel analysis of M13KBst RF DNA during steps of preparing the vector and insert for transfection. All DNA samples shown were obtained from CsCl-purified RF DNA. Ligation reactions were performed on DNA samples shown in Lanes A, B, and C under identical conditions. Steps of DNA

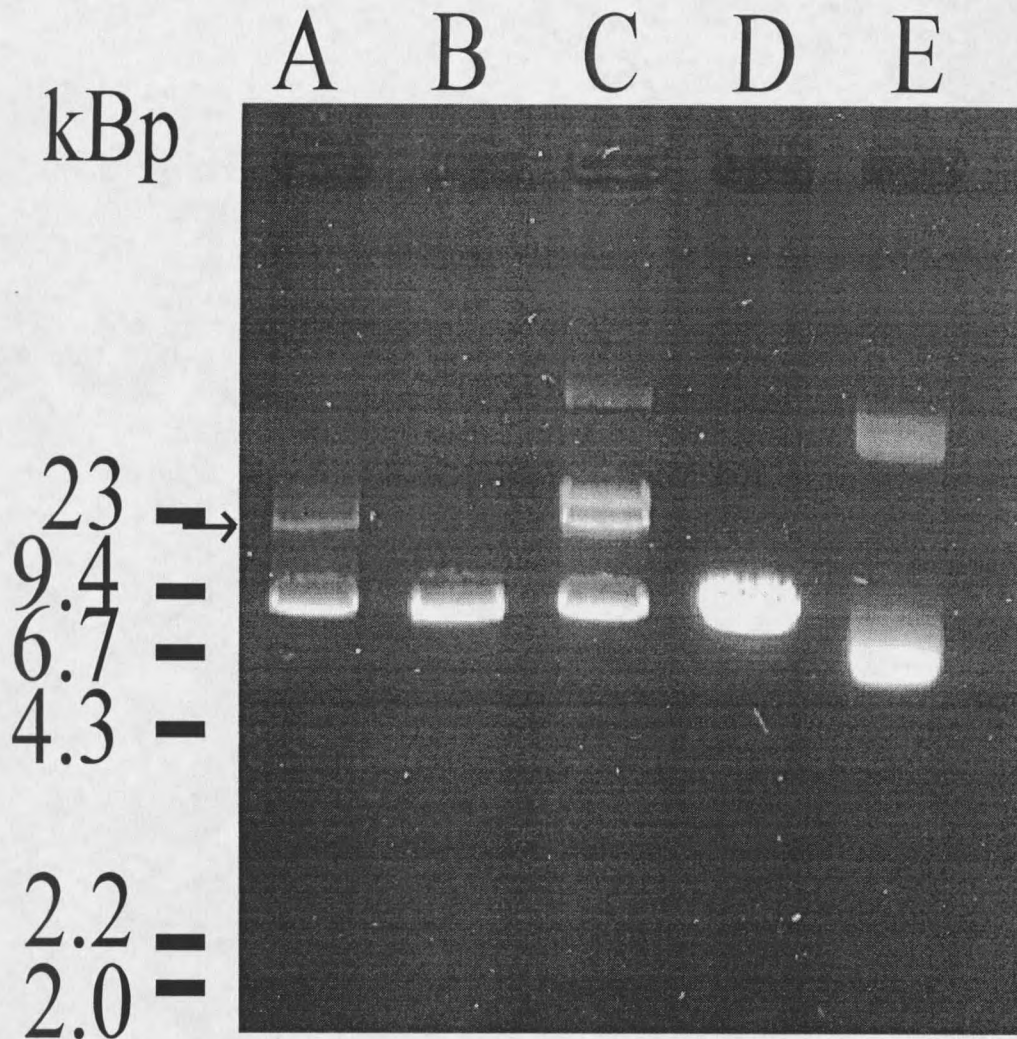


**Figure 8.** Agarose gel analysis of M13KBst DNA showing preparation for transfection of MC1061 cells. M13KBst RF DNA was produced and purified as described in Materials and Methods. Ethidium bromide staining was used following 1% (w/v) TAE-agarose electrophoresis gel analysis to determine DNA fragment mobilities shown for *Bst*XI-cleaved, KOAc gradient-purified M13KBst vector RF ligated with synthetic insert showing the band of recombinant RF containing the synthetic insert (arrowhead), (A); *Bst*XI-cleaved, KOAc gradient-purified vector ligated without insert, (B); *Bst*XI-cleaved vector ligated without synthetic insert, (C); unligated *Bst*XI-cleaved vector (D); and uncleaved circular M13KBst RF, (E). See results for interpretation of bands.

manipulation are: lane E, uncleaved circular M13KBst RF, showing lower supercoiled RF band and upper relaxed circular RF band; lane D, *Bst*XI-cleaved linear vector; lane C, *Bst*XI-cleaved vector (without KOAc purification as described in Methods) ligated without synthetic insert; lane B, *Bst*XI-cleaved, KOAc gradient-purified vector ligated without insert; lane A, *Bst*XI-cleaved, KOAc gradient-purified vector ligated with synthetic insert as described in Methods. In lane A, presence of a visible amount of recircularized RF DNA (arrowhead) following ligation in the presence of synthetic insert suggests the production of the intended ligation product. Absence of ligation product which migrates to this position in lane B suggests a reduced amount of null-insert RF following KOAc-gradient removal of the 31 base stuffer fragment. In lane C, at least three new bands are produced following ligation, suggesting several types of unintended multimers and circular forms are created when the 31-base fragment is not removed by KOAc gradient purification. This result suggests the importance of careful removal of the stuffer fragment. In lane D, a single band of linear DNA indicates the completion to which at least one of the two *Bst*XI sites is cleaved during endonuclease digestion. The degree to which both *Bst*XI sites are cleaved is suggested in lane B, by the absence of a visible band corresponding to the position of the arrowhead in lane A. This result suggests that both sites are cleaved and that stuffer removal by the KOAc gradient is effective. However, agarose-gel analysis is not adequately sensitive to detect all recircularized DNA capable of producing null-insert phage. The observation that as many as 20% of library clones lack inserts suggests some degree of recircularization without synthetic insert occurs before (or possibly

after) transfection. Nevertheless, the relative amounts of recircularized DNA in lanes A (arrowhead) compared to lane B suggest the numbers of phage containing inserts should be significantly greater than those without.

Transfection was used to introduce ligated vector DNA containing synthetic inserts into electrocompetent MC1061 cells (13,36). Samples of transfected cells were plated on LB agar (24) containing kanamycin at 75  $\mu\text{g/ml}$ . Resulting colonies were randomly selected and propagated in two ml cultures of 2xYT (24) containing kanamycin at 75  $\mu\text{g/ml}$  for phage DNA extraction and nucleotide sequence analysis. This information was obtained to determine the percentage of phage containing inserts and the distribution of codons in the variable insert region. The nucleotide sequences in the 5' end of 64 such clones were determined. Of these, 53 (83%) were found to contain inserts and five of these were found to contain truncated inserts. The deduced random nonapeptides of the 48 randomly selected library members displaying full length inserts are listed in Table 5. Duplicate occurrences of peptide sequences expressed on unfractionated library members were not found.

About 8% of all phage library members were found to contain truncated inserts. In these phage, the DNA inserts were found to contain random nucleotides in multiples of three, expressing codons for random peptides shorter than the intended nine residues. For this reason, the synthetic oligonucleotides A, B, and C were examined by UV shadowing (2) for the presence of DNA strands which were shorter than the expected length. However, truncated forms of the synthetic oligonucleotides were not observed by this method (data not shown). This observation, together with the low

occurrence (<1%) of unintended nucleotides (A or C) in the third position of codons in the random region suggest accurate oligonucleotide synthesis.

The amino acids of random nonapeptides deduced from the nucleotide sequence of 54 clones suggested the occurrence of codons in the inserts assumed a fairly random distribution (Figure 9).

**Table 5.** Deduced Amino Acid Sequences of Random Peptides Displayed on 48 Unfractionated J404 Library Members.

MDPAHATTM	GSWYNSTRF	TYFEAKTRP	AKSATTKAS
LANVLARGL	DFRGGRGLG	EKLRYPFL	SQGGTQAMG
VMGLGGRGD	GMANTSSQG	NRSMGTIQL	DYVAGGPSL
LSQSHILRG	QGYLTARQL	WVFGFGSTE	WGVAGMCRP
GLLSLRKYH	AETMDGLQL	HFGNDSAGA	QQQGNWLGA
SGLPAATRG	AERATDKLR	LKNRLRIEA	WGSCRFDWN
RLGQLGGSL	MYMLQEVPG	LHVNRLLOQY	EQFSLEMDM
EQMNTWQWS	ATGETGGKL	DTQSVMGRY	GGWQGNHVV
QLIGFEKVG	LIQPTSLMA	LWVQMENRI	HWMLDYCMP
EMVLMHNFR	HLDVMMIAV	ESYQGTRAA	GPWMYTRCG
QALGTRRAP	CHVPAYNRV	DIVWLKRL	LKGPARDPG
QGPKRDREV	QYRRAVSVV	RLADKTLKA	ELDGLGHVL

We examined randomly selected phage library members to determine if cleavage of the signal peptide is sensitive to the presence of particular amino acids on the carboxyl side of the cleavage site. Such a situation could potentially bias certain positions of the random peptides. Therefore, the first two amino acids of unique peptides expressed on the randomly selected phage clones listed in Table 5 were compared to expected frequencies and tabulated in Table 6.

The diversity of the library was calculated from the number of transfectants ( $6.9 \times 10^8$ ) and the percentage of phage containing inserts, and was thus found to represent  $5.7 \times 10^8$  unique phage-displayed sequences.

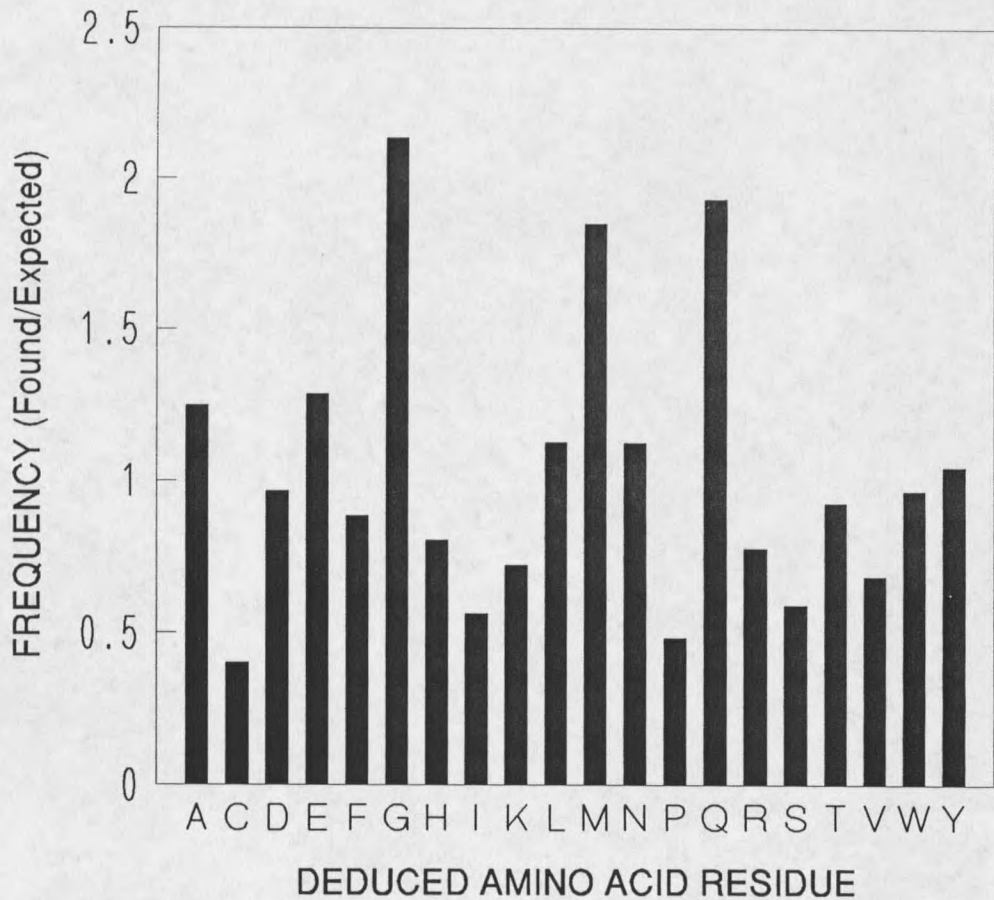


**Figure 9.** Distribution of codons within the random region of unfractionated phage library members. Unfractionated J404 library material was diluted and plated on a lawn of K91 cells to obtain isolated plaques. Fifty-four randomly selected plaques were selected to recover phage clones for nucleotide sequence analysis. The region of the phage genome coding for the displayed nonapeptide was sequenced to deduce the encoded amino acids. The observed codon frequency within the random region is plotted for each amino acid.

**Table 6.** Deduced Amino Acids in First Two Positions of Random Nonapeptides of 45 Unfractionated Library Members.

Amino Acid	Occurrences 1st Position	Occurrences 2nd Position	Total Occurrences	Predicted <sup>a</sup> Total Occurrences
A	4	2	6	6
C	1	0	1	3
D	4	1	5	3
E	3	3	6	3
F	0	2	2	3
G	5	7	12	6
H	5	1	6	3
I	0	2	2	3
K	0	3	3	3
L	7	5	12	8
M	2	3	5	3
N	1	0	1	3
P	0	1	1	6
Q	6	3	9	3
R	2	1	3	8
S	2	3	5	8
T	1	2	3	6
V	1	1	2	6
W	1	2	3	3
Y	0	3	3	3
Hydrophobic	14	16	30	35
Charged	9	8	17	17
Polar	17	14	31	32
Glycine	5	7	12	6

<sup>a</sup> Prediction were based on the number of amino acids examined and the percentage of possible codons which represent the amino acid.

Discussion

The M13KBst filamentous phage vector was constructed for the production of a random nonapeptide library. The amenities of the M13 series of vectors have been recognized for many years, and have gained wide popularity for use in site specific mutagenesis (20), and primed synthesis nucleotide sequence analysis (31). The additional advantages of filamentous phage vectors, based on the ability to express polypeptides encoded by foreign DNA inserts (34), has set the stage for phage-display technology. In our view, an advantage of the M13 vector over the fd-tet vector, on which many phage-display vectors is based, is that M13 does not contain a defect in the negative strand origin of synthesis. Because of this, a larger plaque size is produced by the M13 vector, and the amount of replicative form DNA in the cell is greater, making phage enumeration and preparation of DNA for library construction easier. For this reason, we have chosen to use the M13 filamentous phage vector as the parent for a new phage display vector to be used in the construction of a novel phage-display library.

Construction of the M13KBst vector involved two alterations of M13mp18. One set of mutations of the M13 genome involved the use of oligonucleotide-directed mutagenesis to produce two *Bst*XI restriction sites in the 5' end of the PIII gene so that foreign DNA could be inserted in a position allowing the expression of protein encoded by the DNA in an accessible location, fused to the pIII capsid protein. The other alteration of the phage genome was to insert a gene which codes for the resistance to kanamycin. The ability of a phage-borne antibiotic resistance gene is

required for the selection of bacterial hosts which are infected by the phage. This facilitates several steps of handling phage-display peptide library members, including the propagation of clones independently of the infection process, and because antibiotics can be used in most procedures where phage are replicated, bacterial contaminants can be avoided.

Alteration of the M13 genome in the 5' end of the pIII gene required six point mutations to produce two *Bst*XI sites. The *Bst*XI recognition sequence (ccaxxxxxtgg) contains six contiguous variable positions. Therefore, two sites can be created which contain different bases in each recognition sequence, yet when cleaved by *Bst*XI, will not be compatible for religation. In this way, a pair of orientation-specific restriction sites can be cleaved by a single enzyme. Because the two *Bst*XI recognition sites are located on either side of the site which corresponds to the signal peptidase cleavage site, the synthetic oligonucleotide construct can be designed to allow expression of the foreign peptide immediately adjacent to the amino terminus of the pIII protein. This arrangement avoids the possibility of confounding effects of possibly undesirable amino acid residues on the amino side of the displayed protein or peptide. A potential drawback of expressing libraries of random peptides at the amino terminus of the pIII protein, adjacent to the signal peptidase cleavage site, is that some residues may bias the cleavage of the bacterial signal peptidase I. However our data listed in Figure 9 and Table 6 suggests that an obvious bias does not exist in the random region of library members.

Expression of the APT protein imparts kanamycin resistance to cells infected

by J404 library members. The level of kanamycin resistance is at least 30-fold greater than necessary for normal antimicrobial selection, and suggests the gene contains all necessary regulatory elements for expression of the functional APT protein.

The M13KBst vector was used to produce nonapeptide library J404, which comprises over half a billion different nonapeptide sequences expressed as fusion proteins with the pIII capsid protein of the recombinant M13KBst phage. Approximately 83% of phage randomly selected from the library contained inserts. Five of 64 unfractionated library members expressed random peptides containing fewer than nine random residues. While phage library members expressing truncated peptides of random sequence were not intended, many fruitful reports have been generated by the use of phage-display libraries containing peptides as short as six residues. Therefore, many of the phage expressing fewer than nine random residues are probably useful in presenting potential interactive sequences.

Previous examination by others has suggested phage-displayed peptides of library members contain a random distribution of amino acids (9). However, randomness cannot be assumed in all such cases. Diversity of library peptides is probably dictated by the quality of the degenerate synthetic oligonucleotide insert, and to a lesser extent by potential selective pressures exerted by the vector during expression of the peptides. Our analysis of unfractionated library clones suggest fairly random occurrence of codons. Glycine and cysteine were found to be the most over- and under-represented codons in the random peptides, respectively. In our J404 library, glycine residues are found to occur about twice as frequently as expected

within the entire random region, and cysteine residues occur at about half the expected frequency (Figure 9). These results are similar to values determined for other phage-display libraries (3,7,16). One factor that may have contributed to the increased number of glycine residues in our unfractionated library members is the fact that guanine bases were found more frequently than expected (about 112% of the expected frequency) in the nucleotide sequence of the random DNA inserts (data not shown). Using the strategy we adopted for oligonucleotide degeneracy, codons with guanine in the first and second positions (GGG and GGT) code for glycine. Therefore, an increase of guanine bases would be reflected by an increased number of glycine residues in expressed peptides. An apparent biological selection against an uneven number of cysteine residues in the random region may account for their reduced representation in the library peptides (16).

The random region of J404 library members exist immediately adjacent (carboxyl) to the signal peptidase cleavage site of the pIII protein. Strong conservation for certain amino acids has been observed in positions -1, -3, and -6 on the amino side of the cleavage site (19,28). We predicted that if bias were observed for residues carboxyl to the signal peptidase cleavage site, the effect would probably be evident in either of the first two residue positions. Therefore, we examined the observed frequencies of codons in the first two positions of the random nonapeptides of phage listed in Table 5. Table 6 suggests an expected distribution in both positions for individual amino acids and categories of residues, except that the prevalence of glycine residues mentioned earlier also occurs in each of these two positions. Otherwise,

neither of the first two positions of the random regions (or any of the remaining seven, data not shown) were found to contain an obvious amino acid bias.

The decision for producing a library of random nonapeptides reflects our goal of epitope mapping. The library was produced to obtain information about the epitopes bound by monoclonal antibodies and to determine interactive regions of multisubunit protein systems. Libraries of six-residue sequences clearly contain a sufficient number of amino acids for identification of interactive peptide regions. The goal of utilizing a longer nine-residue library for the identification of epitopes bound by mAbs was the intention of revealing epitope regions of greater than six amino acids. In addition, libraries of longer peptides have a greater chemical diversity than libraries of shorter peptides containing the same number of unique phage clones. However, construction of libraries expressing peptides of increasing length can be compromised by the increasing number of unavoidable amber (stop) codons in the random region (32). A recombinant phage containing an amber codon at any position in the random region of the pIII protein presumably would not be infectious, and may not be capable of assembly (25). With nine random codons, the expected frequency of amber codons within the peptide is slightly less than 25%. A partial solution to this problem may be to include cytosine residues in the third position of the codon (16). This reduces the ratio of amber codons to the productive codons from one in 32 to one in 48, and may be useful in producing libraries of longer randomized regions.

This library was produced following the transfection of recombinant DNA into host *E. coli* cells. This type of phage-display library is referred to as a primary

library, and differs from many similar secondary (or subsequent) libraries in use, which were produced by infecting a sample of an earlier library into host cells, and amplifying the number of phage (but not the diversity) as much as five orders of magnitude. Thus, the production of subsequent libraries is a means of propagating the library. However, subsequent libraries presumably do not contain the diversity of the primary library, and therefore may offer fewer sequences which can interact with a chosen ligand. Currently, subsequent libraries have not produced from the J404 stock.

The J404 library has been used to identify a number of interactive peptide sequences. The identification of several of these interactive peptide sequences including eight amino acid residues has been possible with the use of the J404 library. For example, the epitopes of two mAbs which bind subunits of human neutrophil cytochrome  $b_{558}$  have mapped to the <sup>181</sup>GGPOVNPI<sup>188</sup> segment of p22-*phox* and the <sup>382</sup>PKIAVDGP<sup>389</sup> region on gp91-*phox* (5). In addition, the <sup>86</sup>STRVRRQL<sup>93</sup> region of the proposed first cytosolic loop of gp91-*phox* and a domain near the cytosolic carboxyl tail, which includes the sequence <sup>450</sup>FEWFADLLQLL<sup>460</sup> were identified as regions of these proteins which interact with other subunits of the NADPH oxidase (11). Amino acid residues which were identified by phage-display analysis to be critical in binding are underlined. At the time of this writing, the identification of interactive regions including this many binding residues has not been reported using any method of interactive sequence determination with preformed molecular libraries.

References Cited

1. **Aruffo, A. and B. Seed.** 1987. Molecular cloning of a CD28 cDNA by a high-efficiency COS cell expression system. *Proc. Natl. Acad. Sci. USA* **84**:8573-8577.
2. **Ausubel, F., R. Brent, R. Kingston, D. Moore, J. G. Seidman, J. Smith, and K. Struhl.** 1995. *Current Protocols in Molecular Biology*. Greene Publishing Assoc. and Wiley-Interscience, New York.
3. **Blond-Elguindi, S., S. E. Cwirla, W. J. Dower, R. J. Lipshutz, S. R. Sprang, J. F. Sambrook, and M. -J. H. Gething.** 1993. Affinity panning of a library of peptides displayed on bacteriophages reveals the binding specificity of BiP. *Cell* **75**:717-728.
4. **Böttger, V. and E. B. Lane.** 1994. A monoclonal antibody epitope on keratin 8 identified using a phage peptide library. *J. Mol. Biol.* **235**:61-67.
5. **Burritt, J. B., M. T. Quinn, M. A. Jutila, C. W. Bond, and A. J. Jesaitis.** 1995. Topological mapping of neutrophil cytochrome b epitopes with phage-display libraries. *J. Biol. Chem.* (In Press)
6. **Christian, R. B., R. N. Zuckermann, J. M. Kerr, L. Wang, and B. A. Malcolm.** 1992. Simplified methods for construction, assessment and rapid screening of peptide libraries in bacteriophage. *J. Mol. Biol.* **227**:711-718.
7. **Cwirla, S, E. Peters, R. Barrett, and W. Dower.** 1990. Peptides on phage: a vast library of peptides for identifying ligands. *Proc. Natl. Acad. Sci. USA* **87**:6378-6382.
8. **Dedman, J. R., M. A. Kaetzel, H. Chang Chan, D. J. Nelson, and G. A. Jamieson, Jr..** 1993. Selection of targeted biological modifiers from a bacteriophage library of random peptides. The identification of novel calmodulin regulatory peptides. *J. Biol. Chem.* **268**:23025-23030.
9. **DeGraaf, M. E., R. M. Miceli, J. E. Mott, and H. D. Fischer.** 1993. Biochemical diversity in a phage display library of random decapeptides. *Gene* **128**:13-17.
10. **DeLeo, F. R., J. B. Burritt, C. W. Bond, A. J. Jesaitis, and M. T. Quinn.** 1994. Inhibition of the association of p47-phox with neutrophil flavocytochrome b-558 by an novel flavocytochrome b peptide. *Mol. Biol. of the Cell* **5**:121a.(Abstract)
11. **DeLeo, F. R., L. Yu, J. B. Burritt, L. R. Loetterle, C. W. Bond, A. J. Jesaitis, and M. T. Quinn.** 1995. Mapping sites of interaction of p47-phox and flavocytochrome b with random sequence peptide phage display libraries. *Proc. Natl. Acad. Sci. USA* (In Press)

12. **Devlin, J., L. Panganiban, and P. Devlin.** 1990. Random peptide libraries: a source of specific protein binding molecules. *Science*. **249**:404-406.
13. **Dower, W. J., J. F. Miller, and C. W. Ragsdale.** 1988. High efficiency transformation of E.coli by high voltage electroporation. *Nucleic Acids Res.* **16**:6127-6145.
14. **Ebright, R., Q. Dong, and J. Messing.** 1992. Corrected nucleotide sequence of M13mp18 gene III. *Gene*. **114**:81-83.
15. **Hackett, P., J. Fuchs, and J. Messing.** 1992. An Introduction to Recombinant DNA Techniques. Benjamin Cummings, Melno Park, Reading, Don Mills, Wokingham, Amsterdam, Sydney.
16. **Kay, B. K., N. B. Adey, Y. -S. He, J. P. Manfredi, A. H. Mataragnon, and D. M. Fowlkes.** 1993. An M13 phage library displaying random 38-amino-acid peptides as a source of novel sequences with affinity to selected targets. *Gene* **128**:59-65.
17. **Keller, P. M., B. A. Arnold, A. R. Shaw, R. L. Tolman, F. Van Middlesworth, S. Bondy, V. K. Rusiecki, S. Koenig, S. Zolla-Pazner, P. Conard, E. A. Emini, and A. J. Conley.** 1993. Identification of HIV vaccine candidate peptides by screening random phage epitope libraries. *Virology* **193**:709-716.
18. **Koivunen, E., B. Wang, and E. Ruoslahti.** 1994. Isolation of a highly specific ligand for the alpha-5, beta-1 integrin from a phage display library. *J. Cell Biol.* **124**:373-380.
19. **Kuhn, A and W Wickner.** 1985. Conserved residues of the leader peptide are essential for cleavage by leader peptidase. *J. Biol. Chem.* **260**:15914-15918.
20. **Kunkel, T., J. Roberts, and R. Zakour.** 1987. Rapid and efficient site-specific mutagenesis without phenotypic selection, p. 367-382. In R Wu and L Grossman (eds.), *Methods in Enzymology Volume 154, Recombinany DNA*. Academic Press, Inc., San Diego, CA.
21. **Luzzago, A., F. Felici, A. Tramontano, A. Pessi, and R. Cortese.** 1993. Mimicking of discontinuous epitopes by phage-displayed peptides, I. Epitope mapping of human H ferritin using a phage library of constrained peptides. *Gene* **128**:51-57.
22. **McLafferty, M. A., R. B. Kent, R. C. Ladner, and W. Markland.** 1993. M13 bacteriophage displaying disulfide-constrained microproteins. *Gene* **128**:29-36.

23. **Miceli, R. M., M. E. DeGraaf, and H. D. Fischer.** 1994. Two-stage selection of sequences from a random phage display library delineates both core residues and permitted structural range within an epitope. *J. Immunol. Methods* **167**:279-287.
24. **Miller, J. H.** 1972. *Experiments in Molecular Genetics*. Cold Spring Harbor Laboratory, Cold Spring Harbor.
25. **Model, P and M Russel.** 1988. Filamentous bacteriophages, p. 375-456. In R Calender (ed.), *The Bacteriophages* vol. 2. Plenum Press, New York.
26. **O'Neil, K. T., R. H. Hoess, S. A. Jackson, N. S. Ramachandran, S. A. Mousa, and W. F. DeGrado.** 1992. Identification of novel peptide antagonists for GPIIb/IIIa from a conformationally constrained phage peptide library. *Proteins* **14**:509-515.
27. **Oka, A., H Sugisaki, and M Takanami.** 1981. Nucleotide sequence of the kanamycin resistance transposon Tn903. *J. Mol. Biol.* **147**:217-226.
28. **Palzkill, T., Q. -Q. Le, A. Wong, and D. Botstein.** 1994. Selection of functional signal peptide cleavage sites from a library of random sequences. *J. Bacteriol.* **176**:563-568.
29. **Roberts, D., K. Guegler, and J. Winter.** 1993. Antibody as a surrogate receptor in the screening of a phage display library. *Gene* **128**:67-69.
30. **Saggio, I. and R. Laufer.** 1993. Biotin binders selected from a random peptide library expressed on phage. *Biochem. J.* **293**:613-616.
31. **Sanger, F., S. Nicklen, and A. R. Coulson.** 1977. DNA sequencing with chain-terminating inhibitors. *Proc. Natl. Acad. Sci. USA* **74**:5463-5467.
32. **Scott, J. and G. Smith.** 1990. Searching for peptide ligands with an epitope library. *Science*. **249**:386-390.
33. **Scott, J. K., D. Loganathan, R. B. Easley, and W. Gong.** 1993. A family of concanavalin A-binding peptides from a hexapeptide epitope library. *Proc. Natl. Acad. Sci. USA* **89**:5398-5402.
34. **Smith, G. P.** 1985. Filamentous fusion phage. Novel expression vectors that display cloned antigens on the virion surface. *Science* **228**:1315-1317.
35. **Smith, G. P., D. A. Schultz, and J. E. Ladbury.** 1993. A ribonuclease S-peptide antagonist discovered with a bacteriophage display library. *Gene* **128**:37-42.

36. **Smith, G. P. and J. K. Scott.** 1993. Libraries of peptides and proteins displayed on filamentous phage. *Methods Enzymol.* **217**:228-257.
37. **Speyer, J. F.** 1990. A simple and effective electroporation apparatus. *BioTechniques* **8**:28-30.
38. **Taylor, L. A. and R. E. Rose.** 1988. A correction in the nucleotide sequence of the Tn903 kanamycin resistance determinant in pUC4K. *Nucleic Acids Res.* **16**:358.

## CHAPTER THREE

TOPOLOGICAL MAPPING OF NEUTROPHIL  
CYTOCHROME B EPITOPES WITH  
PHAGE-DISPLAY LIBRARIESAbstract

Cytochrome *b* (Cyt *b*) of human neutrophils is the central component of the microbicidal NADPH-oxidase system. However, the folding topology of this integral membrane protein remains undetermined. Two random-sequence bacteriophage peptide libraries were used to map structural features of Cyt *b* by determining the epitopes of monoclonal antibodies (mAbs) 44.1 and 54.1, specific for the p22-*phox* and gp91-*phox* Cyt *b* chains, respectively. The unique peptides of phage selected by mAb affinity purification were deduced from the phage DNA sequences. Phage selected by mAb 44.1 displayed the consensus peptide sequence, GGPQVXPI, which is nearly identical to <sup>181</sup>GGPQVNPI<sup>188</sup> of p22-*phox*. Phage selected by mAb 54.1 displayed the consensus sequence, PKXAVDGP, which resembles <sup>382</sup>PKIAVDGP<sup>389</sup> of gp91-*phox*. Western blotting demonstrated specific binding of each mAb to the respective Cyt *b* subunit and selected phage peptides. In flow cytometric analysis, mAb 44.1 bound only permeabilized neutrophils, while 54.1 did not bind intact or permeabilized cells.

However, mAb 54.1 immunosedimented detergent solubilized Cyt *b* in sucrose gradients. These results suggest the <sup>181</sup>GGPQVNPI<sup>188</sup> segment of p22-*phox* is accessible on its intracellular surface, but the <sup>382</sup>PKIAVDGP<sup>389</sup> region on gp91-*phox* is not accessible to antibody, and probably not on the protein surface.

### Introduction

The NADPH-oxidase system of neutrophils is a host-defensive plasma membrane redox system that produces superoxide anion ( $O_2^-$ ) (1,31), which subsequently is converted to a variety of other toxic oxygen species that kill invading microbes and cause damage to tissue (45). Humans lacking this enzyme system are unable to produce neutrophil-generated superoxide and suffer recurrent bacterial infections, granulomatous lesions of multiple organs, and early death (10). This condition was first reported in 1957 (2,28), and is known as chronic granulomatous disease (CGD) (10,15,45).

Cytochrome *b* (Cyt *b*) (a.k.a., flavocytochrome *b*, cytochrome  $b_{558}$ , cytochrome  $b_{559}$ , cytochrome  $b_{245}$ ) is the central redox component of the phagocyte NADPH-oxidase system of human neutrophils. This component is a heterodimeric integral membrane protein composed of 91 kDa (gp91-*phox*) and 22 kDa (p22-*phox*) subunits (32,35). At least two heme groups are coordinated by these subunits (37), and FAD and NADPH binding activities have been demonstrated (27,40,43). The primary structure of gp91-*phox* includes two asparagine-linked glycosylation sites (35) and contains five possible transmembrane regions suggested by hydropathy analysis (34,41). p22-*phox* contains three possible transmembrane regions, one of which includes a His 94 residue, conserved between species, that probably coordinates one of the Cyt *b* heme irons.

A number of studies have provided information about Cyt *b* native structure. Electron microscopy and immunochemical analysis were used to localize Cyt *b* in the

neutrophil and eosinophil (18,25), and we have found that the epitopes of Cyt *b* containing the amino acid residues <sup>547</sup>KQSI<sup>559</sup>NSSESGPRG of gp91-*phox* and <sup>162</sup>EARKK<sup>174</sup>PSEEEAAA of p22-*phox* are surface accessible epitopes of native Cyt *b* (25). Rotrosen *et al.* found that synthetic peptides corresponding to the carboxyl terminus of gp91-*phox* inhibited NADPH-oxidase activation in electrically permeabilized cells, and antipeptide antibodies directed against this region prevented superoxide formation in a cell-free system (39). These data suggest functional roles for the carboxyl termini of both subunits, which are presumed to occupy cytosolic locations. In addition, p22-*phox* contains a proline-rich region in the carboxyl-terminal tail which may provide Src homology, (SH3) domain binding sites, for p47-*phox* or p47-*phox*/p67-*phox* complexes (12). Initial analysis of the folding topology of Cyt *b* has been reported by Imajoh-Ohmi *et al.*, who determined accessibility of the subunits to anti-peptide antibodies and proteolytic enzymes (23). Two regions of gp91-*phox* were exposed to proteolytic enzymes on the outer surface of the cell, while p22-*phox* was not found to be sensitive to such external proteolysis (37). The carboxyl termini of both subunits were accessible to antibody on the internal surface of the plasma membrane (23).

The protein sequence of the carboxyl terminal half of gp91-*phox* shows some similarity to other NAD(P)H-oxidoreductases (40,46) such as ferredoxin NADP reductase, a flavoprotein for which the crystal structure is known. Studies by Pick and coworkers (26) have shown that Cyt *b* binds FAD and can function as a superoxide generating NAD(P)H-oxidase, even without added cytosolic constituents normally

required for superoxide production in other cell free systems (6,9). These results have prompted speculation that Cyt b is the only electron transporting component of the NADPH oxidase and that its nucleotide binding domains may resemble ferredoxin reductase (46) or other redox proteins. However, the structural studies by Imajoh-Ohmi *et al.* suggest that major portions of the putative nucleotide binding domains are extracellular. This contention is also supported by the evidence of Umei *et al.* suggesting that the putative NAD(P)H binding component of the oxidase is present in neutrophils of normal and CGD patients and is thus not part of Cyt b.

These ambiguities in structure indicate that additional approaches for determining the topology of this protein are required. In this study, we have identified the epitopes bound by two monoclonal antibodies that recognize a specific subunit of Cyt *b* using random peptide phage-display libraries. In addition, we present data relating the accessibility of these epitopes on native Cyt *b* to their respective antibodies.

## Materials and Methods

### Reagents

Diisopropylfluorophosphate (DFP), Tween 20, SDS, acrylamide, bis-acrylamide, ammonium persulfate, TEMED, Hank's solution, FITC-labeled goat anti-mouse IgG, bovine serum albumin (BSA), and Histopaque were purchased from Sigma Chemical Co. (St. Louis, MO). Prestained protein molecular weight standards were purchased from Life Technologies BRL (Gaithersburg, MD). Western blots were developed with anti-mouse or anti-rabbit immunoglobulin purchased from BioRad (Hercules, CA) and BCIP/NBT chromogen was purchased from Kirkegaard and Perry Laboratories, Inc. (Gaithersburg, MD). Cyanogen bromide activated sepharose CL-4B was purchased from Pharmacia (Piscataway, NJ). Sequencing data was obtained using a Sequenase version 2.0 sequencing kit purchased from United States Biochemical (Arlington, Heights, IL).

### Epitope library and bacterial strains

Two random phage-display libraries were used in this study. A hexapeptide phage-display library and *E. coli* strains K91 and MC1061 were kindly provided by Dr. George P. Smith (42) (University of Missouri, Columbia) and a nonapeptide phage-display library was produced in our lab (8).

### Affinity purification

Affinity purification of phage bearing epitopes bound by mAbs was performed

as follows:  $5 \times 10^{11}$  phage (5  $\mu$ l) from the hexapeptide phage peptide-display library (42) or  $1 \times 10^{12}$  phage (75  $\mu$ l) from the nonapeptide library were combined with 1.0 ml of Sepharose beads conjugated with 4 mg of either mAb 44.1 or 54.1. The beads were mixed with the phage at 4° C for 16 hours by gentle inversion. The mixture was then loaded into a 5 ml plastic column barrel (Evergreen) and unbound phage were removed by washing with 50 ml phage buffer (50 mM Tris-Cl pH 7.5, 150 mM NaCl, 0.5% Tween 20 (v/v), 1 mg/ml BSA). Bound phage were eluted from the column with 2.0 ml of eluting buffer (0.1 M glycine, pH 2.2), and the pH of the eluate was neutralized immediately with four drops of 2 M Trizma base (44). The titer of phage (nonapeptide library) was determined for each column eluate by plaque assay according to standard procedures (21). The column matrices were preserved for reuse in second and third round affinity purifications by washing with 10 ml PBS pH 7.0, followed by 3.0 ml PBS containing 0.02% sodium azide. The column was stored at 4° C until the next affinity purification, and was prepared for reuse by rinsing with 20 ml of phage buffer prior to mixing with amplified phage. As a control for antibody-specific selection, one column was prepared without antibody bound to the beads; all steps of affinity purification of phage were carried out on this control column and a sample of the resulting phage was sequenced.

#### Phage amplification

Eluate phage were amplified in host K91 "starved" *E. coli* cells which were prepared as previously described (44,47) to maximize phage attachment and infection.

The entire volume of the first eluate, minus a small amount used for titering, was added to 200  $\mu$ l starved K91 cells and incubated 15 minutes at room temperature without shaking. Two ml LB broth (30) with tetracycline at 0.2  $\mu$ g/ml (for the hexapeptide library) or kanamycin at 0.75  $\mu$ g/ml (for the nonapeptide library) was added to the cells which were then incubated with aeration at 37° C for 45 minutes. The infected cells were spread with a sterile glass rod on the surface of LB agar containing tetracycline (40  $\mu$ g/ml) or kanamycin (75  $\mu$ g/ml) in a sterile 9 x 24 inch glass baking dish. After 24-48 hours of incubation at 37° C, the antibiotic resistant colonies were suspended in 25 ml of TBS (50 mM Tris.HCl pH 7.5, 150 mM NaCl) by gentle scraping with a bent glass rod. Phage were harvested from the culture as described (44), and diluted in 1.0 ml phage buffer and allowed to mix with the column matrix, which was also resuspended in one ml phage buffer. These steps were repeated so that a total of three purifications and two amplifications were used to select and amplify adherent phage from the library.

#### Sequencing phage

One hundred  $\mu$ l phage from the final column eluate were used to infect starved K91 cells as described above. Serial 100-fold dilutions of infected cells were used to inoculate LB agar plates containing the appropriate dilution which were then incubated overnight at 37° C. Isolated colonies were used to inoculate 2 ml 2xYT (30) containing the appropriate antibiotic and the minipreps were incubated overnight at 37° C in a shaking water bath. DNA from the isolated phage was prepared and sequenced

according to the directions of the USB Sequenase version 2.0 kit. An oligonucleotide primer (J140) with the sequence, 5'-gttttgctgtctttccagacg-3', was used to determine the nucleotide sequence of the unique region of the phage, and autoradiographs were viewed using a Molecular Dynamics Model 400E Phosphorimager.

#### Large scale purification of selected phage

Some phage bearing hexapeptides of interest (Figure 11, sequences #3, #27-29) were propagated by infecting 750  $\mu$ l of mid log phase K91 cells with 20  $\mu$ l of phage supernatant saved from sequencing minipreps. The phage were produced in a method similar to amplifications described above, except the infected cells were grown in 100 ml 2xYT with 40  $\mu$ g/ml tetracycline, and the purified phage were resuspended in 400  $\mu$ l TBS.

#### Neutrophil preparation and FACS analysis

Human neutrophils were purified from citrated blood using Histopaque gradients as described by Boyum (5). Purified cells were incubated on ice for 15 minutes with 2 mM DFP to inhibit serine proteases.  $5 \times 10^5$  cells were used for each sample to determine antibody binding by FACS analysis. Some cell samples were permeabilized on ice for 10 minutes by adding 500  $\mu$ l of saponin solution (0.01% saponin, 0.1% gelatin in Dulbecco's PBS) and pelleted by centrifugation as before. Permeabilized cells were incubated on ice for 30 minutes with 80  $\mu$ l of the primary antibody (usually 50  $\mu$ g/ml in saponin solution), then washed one time with 3.0 ml

saponin solution, centrifuged to collect, and resuspended in 80  $\mu$ l of the FITC conjugated goat anti-mouse antibody diluted 1:150 in saponin solution, and incubated on ice for 30 minutes. Permeabilized cells were washed one time with 3.0 ml saponin solution containing propidium iodide at 10  $\mu$ g/ml, pelleted as before, and resuspended in 500  $\mu$ l of FACS buffer (Dulbecco's PBS containing 10% rabbit serum). In separate experiments, 100  $\mu$ l of mAb 44.1 at 10  $\mu$ g/ml was incubated at 37° C for 30 minutes with ca.  $2 \times 10^{10}$  TU (44) phage expressing phage sequence #3 or #27 (Figure 11) prior to incubation with the saponin-permeabilized cells to determine if the phage-expressed peptide could compete with the natural epitope for binding by the mAb. Control samples in all experiments consisted of cells not incubated with either primary or secondary mAb, cells not incubated with primary mAb, and cells incubated with both an isotype matched primary mAb and the labeled secondary mAb. Staining of some samples of intact cells was performed as above without treatment with saponin solution. Fluorescence intensity of the FITC-labeled cells was determined on a Becton Dickinson *FACScan* model FACS analyzer with a 15 milliwatt argon-ion laser using CONSORT 30 and LYSYS software according to the manufacturer's directions.

#### Western blotting

Immunoaffinity purified phage bearing peptides resembling a region of Cyt *b* were isolated and grown as indicated above. Approximately  $5 \times 10^{11}$  purified phage in 20  $\mu$ l TBS were heated in a boiling water bath for five minutes with an equal volume of SDS sample buffer (3.3% (w/v) SDS, 167 mM Tris-Cl pH 6.8, 33% (v/v) glycerol,

0.03% (w/v) bromphenol blue, 0.035% (v/v) 2-mercaptoethanol). Heparin Ultrogel-purified Cyt *b* prepared as described (32), was combined with an equal volume of SDS sample buffer without heating. Protein samples were separated by SDS-PAGE at room temperature on 12% (w/v) polyacrylamide gels as described (32,37) and electrophoretic mobility of sample proteins were compared to prestained protein standards.

Following electrophoresis, protein samples were transferred to nitrocellulose as previously described (32). Monoclonal antibodies 44.1 and 54.1 were diluted to 2 µg/ml in diluting buffer (3% (v/v) goat serum, 1% (w/v) BSA, 0.2% (v/v) Tween 20, 0.1% (w/v) thimerosal in PBS) and incubated with separate regions of the blot for one hour at room temperature with continuous rocking. The blot was developed using alkaline phosphatase-conjugated goat anti-mouse IgG and BCIP/NBT phosphatase substrate system.

#### Cyt *b* Immunosedimentation

Purified Cyt *b* (10 µg) was diluted in 100 µl of relax buffer (32) containing 50 µg of mAb (44.1, 54.1, irrelevant, or none) and then incubated overnight at 4° C. The pretreated Cyt *b* was then loaded onto a 1.36 ml continuous 5-20% sucrose gradient in relax buffer and centrifuged at 53,000 RPM in a Beckman TLS-55 rotor for seven hours at 4° C. The gradient was manually fractionated into twelve 120 µl samples from the top. A 20 µl sample of each fraction was separated by SDS-PAGE and transferred to nitrocellulose membranes as described above. Cyt *b* was detected by Western Blot using a rabbit anti-p22-*phox* polyclonal primary antibody. Western blots

were digitized and quantitated using an image analysis system as described (36).

## Results

To determine the structure of immunogenic surface regions of Cyt *b* and acquire additional information about its membrane topology, monoclonal antibodies were produced against the Triton X-100-solubilized wheat germ agglutinin and heparin-Ultrogel-purified Cyt *b* protein (32). Hybridoma supernatants were screened for neutrophil specific IgG producing clones that recognized intact or saponin-permeabilized neutrophils and either subunit of heparin-purified Cyt *b*. Numerous clones were identified, and two were chosen that recognized either the light or heavy chain of Cyt *b*. Epitope mapping of Cyt *b* was carried out using these Cyt *b* specific antibodies and phage random peptide-display library technology (11,14,42,44). FACS and immunosedimentation analysis were then used to confirm accessibility of the epitope on native Cyt *b* to antibody, and placement of the epitope relative to the plasma membrane. Finally, confirmation of the specificity of the mAb for both the Cyt *b* subunit and the phage peptide-bearing pIII protein selected by the mAb was demonstrated by Western blot analysis.

### Identification of Monoclonal Antibody Epitopes

To identify the amino acid sequence of the epitopes of Cyt *b* recognized by the reactive mAbs, a nonapeptide phage-display library capable of binding to the mAbs was created. Using this library, mAb-binding epitopes were selected from a collection of  $5 \times 10^8$  unique nine residue sequences of all 20 amino acids. The epitopes thus mimic the original immunogenic Cyt *b* epitope. By sequencing the relevant region of

the phage genome, the original Cyt *b* epitope was deduced (7). Confirmation of the epitope selection was achieved using a second epitope library kindly provided by George P. Smith at the University of Missouri, Columbia (44). Three cycles of immunoaffinity purification and amplification were used to select phage expressing peptides bound by either mAb 44.1 or 54.1. Figure 10 shows selection and amplification of phage bound by mAb columns. An increase of about five logs was observed for the population of binding phage for each mAb, and about three logs for phage which interacted with the control column without mAb.

The random insert region was sequenced in 34 phage selected from the nonapeptide library and 27 from the hexapeptide library as described in Materials and Methods. Figure 11 shows 30 of the 34 sequences (88%) from the nonapeptide library which exhibited an obvious consensus pattern matching a region of Cyt *b* shown in Figure 12. This consensus peptide sequence, GGPQVXPI, closely resembles <sup>181</sup>GGPQVNPI<sup>188</sup> of p22-phox (Figure 12). The remaining four sequences did not resemble any region of Cyt *b* or each other (data not shown). Nineteen of the 27 sequences (70%) from the hexapeptide library showed similarity to the same Cyt *b* epitope, and the same nucleotide sequence coding for the PQVRPI peptide was recovered in 17 of the 19 cases. The remaining eight hexapeptide sequences showed no consensus (data not shown). Phage expressing the hexapeptide sequences PQVRPI, FKRGVD, LRRGID, and PKGAYD (Figure 11; sequences #3, #27-29, respectively) were isolated and propagated for further study by Western blot and FACS analysis.

Phage selected by mAb 54.1 expressed the consensus amino acid sequence,

PKXAVDGP, (the GP is adjacent in the constant pIII region in all phage except phage sequence #34) which is similar to  $^{382}\text{PKIAVDGP}^{389}$  of gp91-*phox* (Figure 12). All phage sequenced which were selected from each library by mAb 54.1 suggested a match to this putative gp91-*phox* epitope. Peptides of phage selected on the column without antibody suggested no match to Cyt *b*, or to each other (data not shown).

### Immunological Analysis

Western blotting analysis was used to show specificity of the mAb for both the Cyt *b* subunit and the unique hexapeptide expressed on the phage. As shown in Figure 13, mAb 54.1 specifically recognized gp91-*phox* (lane A), which migrates between the 68 and 97 kDa molecular weight markers, and a 20 kDa proteolytic fragment. The appearance of this 20 kDa immunoreactive fragment can be enhanced in Cyt *b* samples treated with V8 protease (37). This mAb also bound to the phage pIII protein expressing the FKRGVD peptide (Figure 11, sequence #27) which migrates at about 64 kDa (lane C). MAAb 54.1 also recognized pIII proteins of phage expressing the LRRGID and PKGAYD peptides (Figure 11, sequences #28 and #29, respectively) by Western blot with equal intensity (data not shown). Phage expressing the PQVRPI peptide (Figure 11, sequence #3) was not recognized by mAb 54.1 (lane B), confirming the specificity of mAb 54.1 for the former sequences.

As seen in Figure 13, mAb 44.1 bound to a band migrating at 22 kDa in lane D (p22-*phox*) and a less intense band at 44 kDa (subunit dimer). The pIII protein of phage containing the PQVRPI peptide (Figure 11; sequence #3) was also recognized

by mAb 44.1 (lane F), but not the pIII protein of phage expressing the FKRGVD peptide (Figure 11, sequence #27) in lane E. The pIII protein migrates at an apparent molecular weight of 64 kDa. This mobility appears slow, considering the size of the protein is 406 amino acids (16); however, our migration rate compares favorably with other reported PAGE mobilities for this protein (19,22,24,51).

Binding of mAb 44.1 and 54.1 to both the specific Cyt *b* subunit and phage pIII protein confirmed the presence of a similar epitope on each. In addition, mAbs did not bind the pIII protein on phage displaying irrelevant peptides in the random region. Therefore, the sequence of the peptide alone, expressed in the variable region simulates the natural epitope recognized by the mAb. Although, the variable peptide of the selected phage may not represent the complete and exact epitope, it clearly contains the residues sufficient for recognition by the mAb.

In order to determine the accessibility of the identified epitopes to mAb on native Cyt *b* in the cell, FACS analysis was performed on purified leukocytes. While saponin-permeabilized cells stained strongly with mAb 44.1 at 50  $\mu\text{g/ml}$  (Figure 14, trace B), intact cells show background staining when incubated with either mAb 44.1 (Figure 14, trace A), or an irrelevant mAb (data not shown). A similar background level of staining intensity was noted when cells were permeabilized and stained with FITC-conjugated secondary antibody only (Figure 14, trace C). Histogram A of figure 5 shows a sample of cells which were incubated with mAb 44.1 but not previously saponin-permeabilized. The majority of the cells of this histogram show background fluorescence, but a small population stains as strongly as the saponin-permeabilized

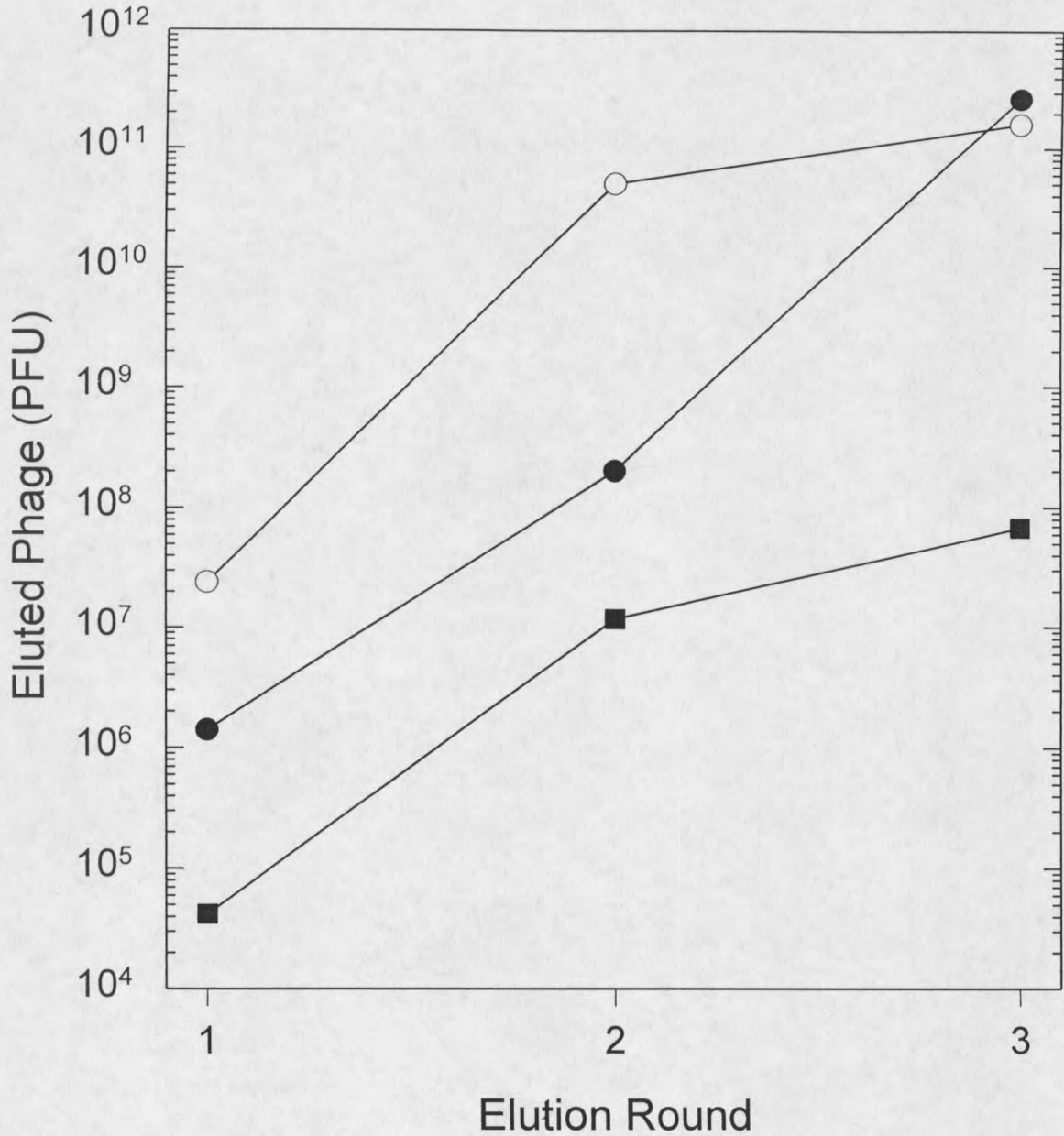


**Figure 10.** Selection of Phage from a Phage-Display Library by Affinity Chromatography. M13 phage expressing random nonapeptides were incubated with Sepharose beads conjugated with mAb 44.1 (●), 54.1 (×), or a sham matrix containing no antibody (○). Adherent phage numbers (plaque forming units) were determined in samples of each column eluate by plating appropriate dilutions on a lawn of late log phase K91 cells and determining phage number as described under Methods.

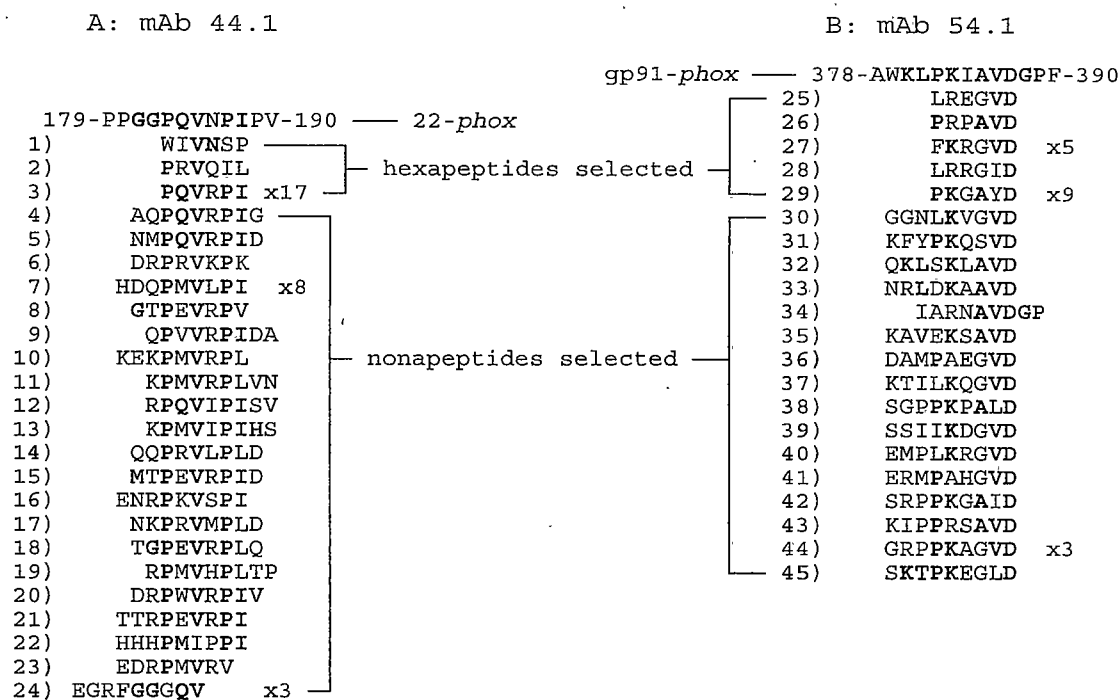


**Figure 11.** Hexapeptide and Nonapeptide Sequences Selected on mAb Affinity Matrices. Plaques of phage isolated from mAb 44.1 Sepharose (A) and mAb 54.1 Sepharose (B) were used to inoculate individual cultures and phage DNA samples prepared from the cultures were sequenced as described under Methods. Both hexapeptide and nonapeptide sequences are shown, and the region of Cyt *b* matching the consensus phage peptide sequence is indicated. Phage amino acid residues demonstrating exact matches to the Cyt *b* amino acid sequence are indicated by bold lettering. Some phage peptide sequences (#3, #7, #24, #27, #29, #44) were multiply recovered. These phage sequences represent results of two separate experiments.

p22-phox				
10	20	30	40	50
NH2-MGQIEWAMWA	<u>NEQALASGLI</u>	LITGGIVATA	GRFTQWYFGA	<u>YSIVAGVFVC</u>
60	70	80	90	100
<u>LLEYPRGKRK</u>	KGSTMERWGO	KHMTAVVKLF	GPFTRNYYVR	<u>AVLHLLLSVP</u>
110	120	130	140	150
<u>AGFLLATILG</u>	TACLAIASGI	YLLAAVRGEQ	WTPIEPKPRE	RPQIGGTIKQ
160	170	180	190	
PPSNPPPRPP	AEARKKPSEE	EAAAAAGGPP	<b>GGPQVNP</b> IPV	TDEVV-COOH
gp91-phox				
10	20	30	40	50
NH2-GNWAVNEGLS	<u>IFAILVWLGL</u>	NVFLFVWYYR	VYDIPPKFFY	TRKLLGSALA
60	70	80	90	100
LARAPAACLN	FNCMLLILPV	CRNLLSFLRG	SSACCSTRVR	<u>RQLDRNLTFH</u>
110	120	130	140	150
<u>KMVAWMIALH</u>	<u>SAIHTIAHLF</u>	NVEWCVNARV	NNSDPYSVAL	SELGDRQNES
160	170	180	190	200
YLNFAKRIK	<u>NPEGGLYLAV</u>	<u>TLLAGITGVV</u>	<u>ITLCLILIIIT</u>	SSTKTIRRSY
210	220	230	240	250
<u>FEVFWYTHHL</u>	<u>FVIFFIGLAI</u>	<u>HGAERIVRGQ</u>	TAESLAVHNI	TVCEQKISEW
260	270	280	290	300
GKIKECPIPQ	FAGNPPMTWK	WIVGPMFLYL	CERLVRFWRS	QQKVVITKVV
310	320	330	340	350
THPFKTIELQ	MKKKGFKMEV	GQYIFVKCPK	VSKLEWHPFT	LTSAPPEEDFF
360	370	380	390	400
SIHIRIVGDW	TEGLFNACGC	DKQEFQDAWK	<b>LPKIAVDGPF</b>	GTASEDVFSY
410	420	430	440	450
<u>EVVMLVGAGI</u>	<u>GVTPFASILK</u>	<u>SVWYKYCNA</u>	TNLKLLKIYF	YWLCRDTHAF
460	470	480	490	500
EFWADLLQLL	ESQMQRNNA	GFLSYNIYLT	GWDESQANHF	AVHHDEEKDV
510	520	530	540	550
ITGLKQKTLY	GRPNWDNEFK	TIASQHPNTR	IGVFLCGPEA	LAETLSKQSI
560	569			
SNSESGPRGV	HFIFNKENF			-COOH

**Figure 12.** Location of Similarity Between Antibody-selected Phage Sequences and Primary Structure of Cyt *b*. The deduced amino acid sequence of the Cyt *b* subunits, p22-phox and gp91-phox are shown with the identified epitopes boxed, and putative transmembrane regions underlined.

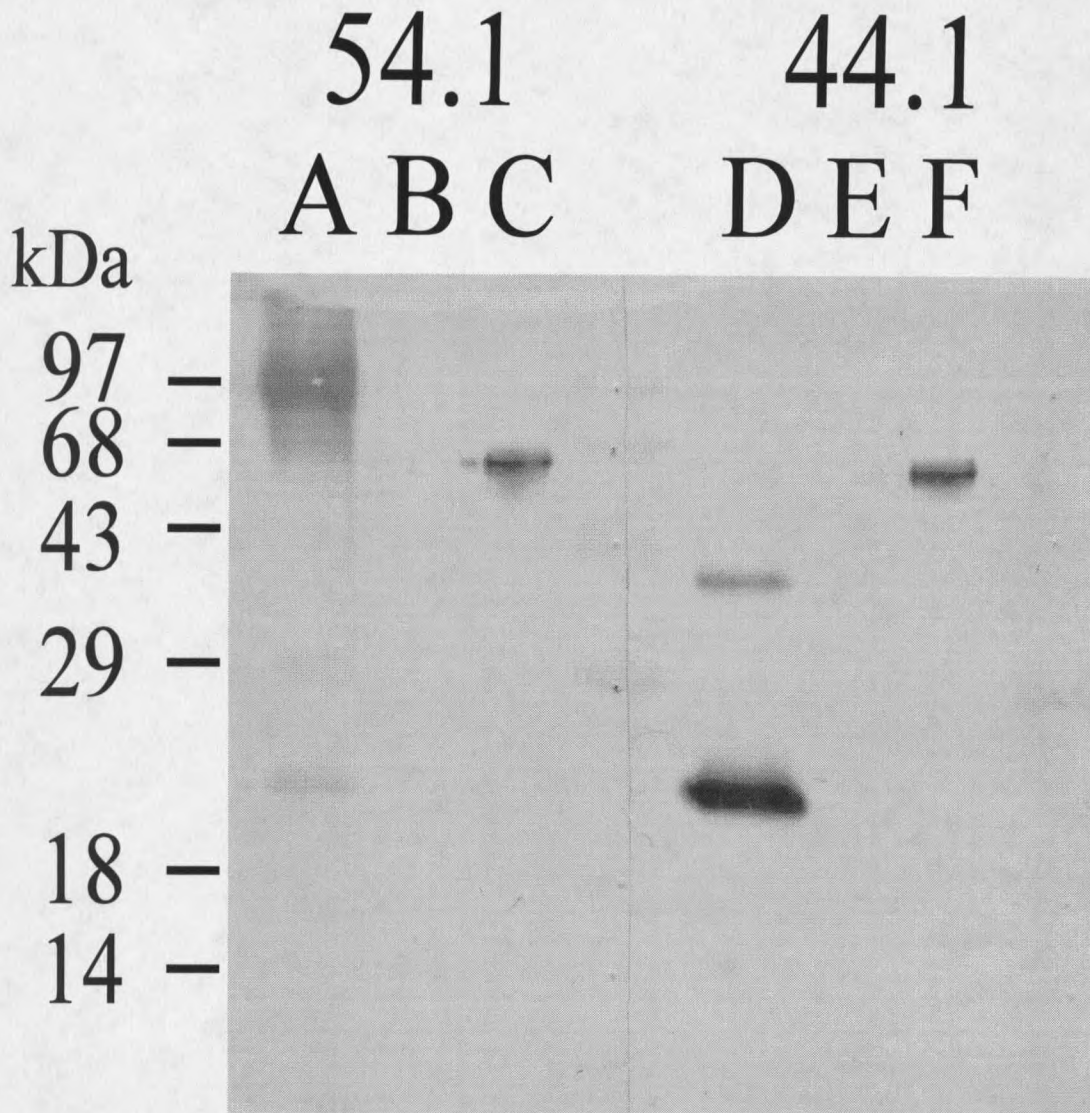


**Figure 13.** Specificity of mAb for Cyt *b* and Phage pIII Proteins. Intact phage expressing known amino acid sequences (lanes B, C, E, and F) and partially purified Cyt *b* (lanes A and D) were separated on SDS-PAGE polyacrylamide gels and transferred to nitrocellulose as described under Methods. Samples were Western blotted with mAb 54.1 (lanes A-C) or mAb 44.1 (lanes D-F). Lanes B and F contain proteins of phage sequence #3 (PQVRPI), and lanes C and E contain proteins of phage sequence #27 (FKRGVD). Results were confirmed by four separate experiments.

cells shown in histogram B. This small population of highly fluorescent cells in histogram A probably represents cells with membranes inadvertently damaged and permeabilized during preparation, as this small group was also found to stain strongly with propidium iodide (data not shown). Propidium iodide stains cellular DNA, and was used in the final wash of all cells to indicate cells with permeabilized membranes.

To demonstrate that this binding was competed by a phage-expressed epitope, intact phage expressing the PQVRPI peptide (Figure 11, sequence #3) were used to pretreat mAb 44.1 and block binding of the mAb to the  $^{181}\text{GGPQVNPI}^{188}$  epitope of p22-*phox*. Cells incubated with 10  $\mu\text{g/ml}$  mAb 44.1 pretreated with phage (Figure 15, trace A) showed a 10 fold reduction in staining intensity compared to cells incubated with the same concentration of untreated mAb (Figure 15, trace B). No inhibition occurred if mAb 44.1 was pretreated with the same concentration of phage expressing the irrelevant peptide, FKRGVD (Figure 11, sequence #27), (data not shown). In contrast, intact and permeabilized cells displayed background staining when incubated with mAb 54.1 (Figure 16, trace A and B, respectively), as did permeabilized cells stained with the secondary FITC-labeled antibody only (Figure 16, trace C). Although a small shift in staining intensity was seen if the cells stained by mAb 54.1 were first permeabilized (Figure 16, trace B), this shift was also seen in permeabilized cells incubated with an irrelevant primary mAb (data not shown), or with labeled secondary mAb only (Figure 14 and 16, trace C). This population of cells staining at a low intensity probably represents residual fluorescent label present within the cells following washing.

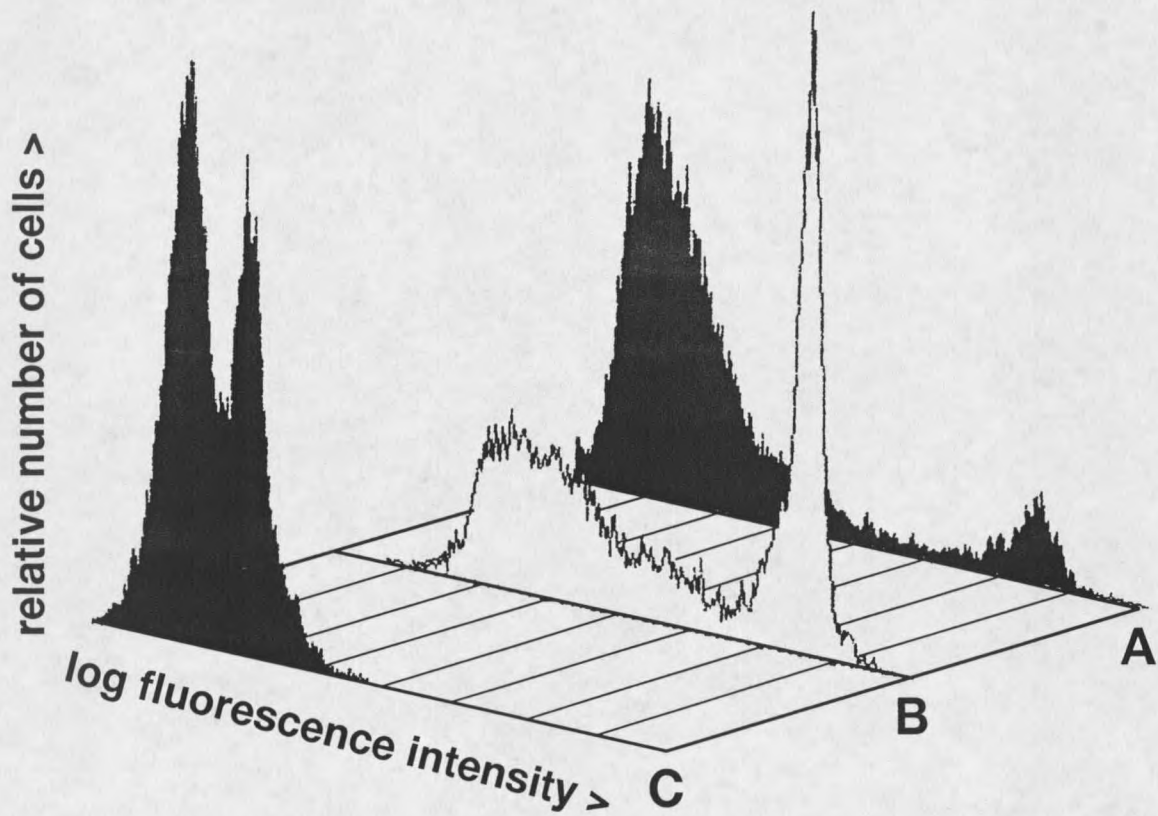


**Figure 14.** FACS Analysis of Neutrophils Stained with mAb 44.1. Intact (A), or saponin-permeabilized human neutrophils (B and C) were incubated with either 50  $\mu\text{g/ml}$  primary antibody 44.1 and a secondary FITC-conjugated antibody (A and B), or the secondary antibody only (C). Cells were then analyzed for fluorescence intensity using a Becton Dickinson *FACScan* model FACS analyzer as described under Methods. The results were reproducible in four separate experiments using neutrophils from different donors.

Because a mAb generally recognizes the cognate epitope on native antigen, the inability to detect staining with mAb 54.1 by FACS analysis was surprising. However, since the original immunogen was detergent solubilized and partially purified Cyt *b*, the mAb may have been generated in response to an epitope accessible only in this form of the protein. To determine whether mAb 54.1 binds to heparin-purified, spectrally active Cyt *b*, a rate-zonal immunosedimentation analysis in detergent-containing sucrose gradients (33) was performed. Purified Cyt *b* (10  $\mu$ g) was pretreated overnight at 4°C with either mAb 54.1, 44.1, an irrelevant mAb, or no mAb, as described in Materials and Methods. Following centrifugation on a 5-20% Triton-X-100-containing sucrose gradient and fractionation, Western blots were performed on samples from each fraction using a rabbit polyclonal antibody specific for p22-*phox* (25). Densitometry was used to measure relative amounts of Cyt *b* in each fraction, which was then plotted as a function of fraction number (Figure 17). Untreated Cyt *b* and a sample exposed to an irrelevant mAb sedimented to a position in the gradient compatible with its 5.6 S sedimentation coefficient (33). When treated with mAb 44.1, the entire sedimentation profile was shifted from fraction 4-5 to fraction 8. Cyt *b* treated with mAb 54.1 displayed a bimodal distribution with a new peak with a sedimentation coefficient of 10 S or greater, suggesting that a majority (>50%) of detergent soluble Cyt *b* is recognized by the mAb. Since approximately 27% of the Cyt *b* remains unaffected when pretreated with mAb 54.1 over a range of 50  $\mu$ g/ml to 500  $\mu$ g/ml (data not shown), the result suggests that part of the population of Cyt *b* has a sequestered epitope, inaccessible to mAb 54.1. Immunoprecipitation of Cyt *b*

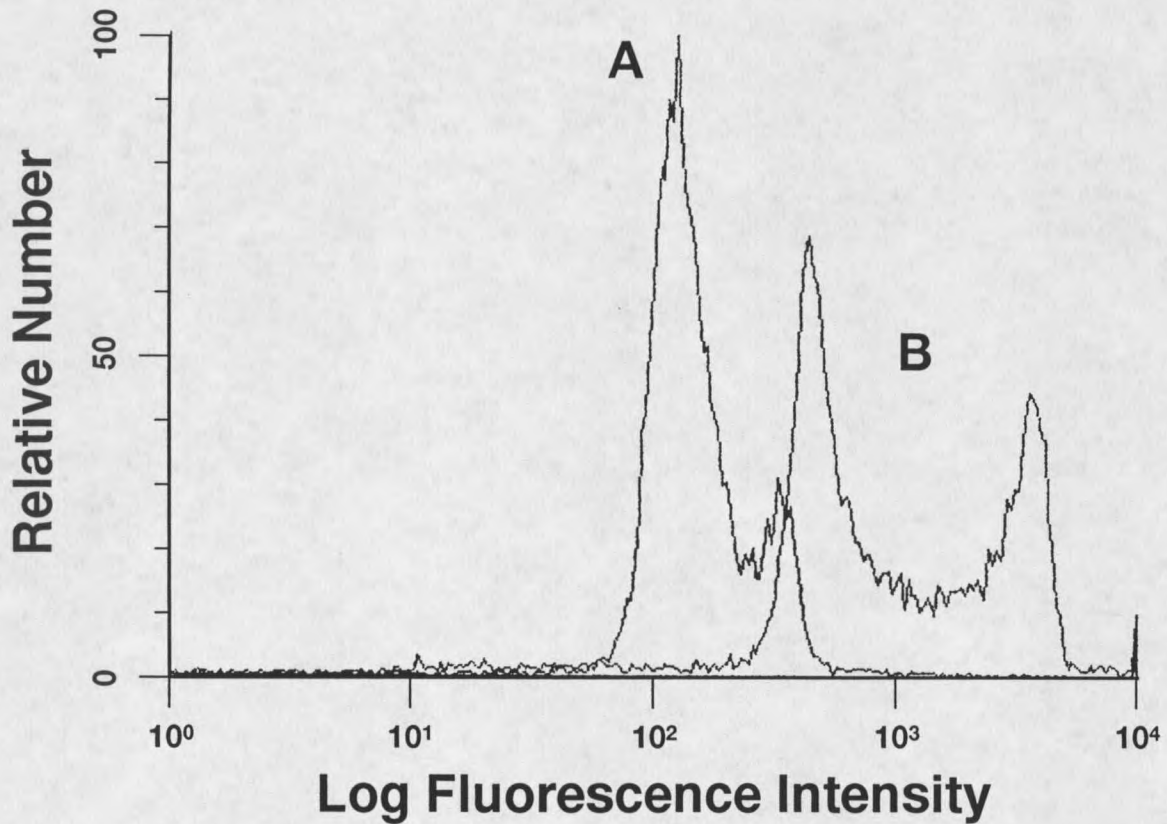


**Figure 15.** Specific Phage Block mAb 44.1 Binding to Permeabilized Neutrophils. Neutrophils were incubated with mAb 44.1 following pretreatment of the antibody with  $\sim 2 \times 10^{11}$  phage expressing the peptide PQVRPI (A), or with mAb 44.1 not pretreated with phage (B). Cells were then exposed to FITC-conjugated secondary antibody as described under Methods, and the effect of the phage-displayed PQVRPI peptide on mAb 44.1 staining was determined as a function of reduction in cell fluorescence intensity. Results were confirmed in two separate experiments.

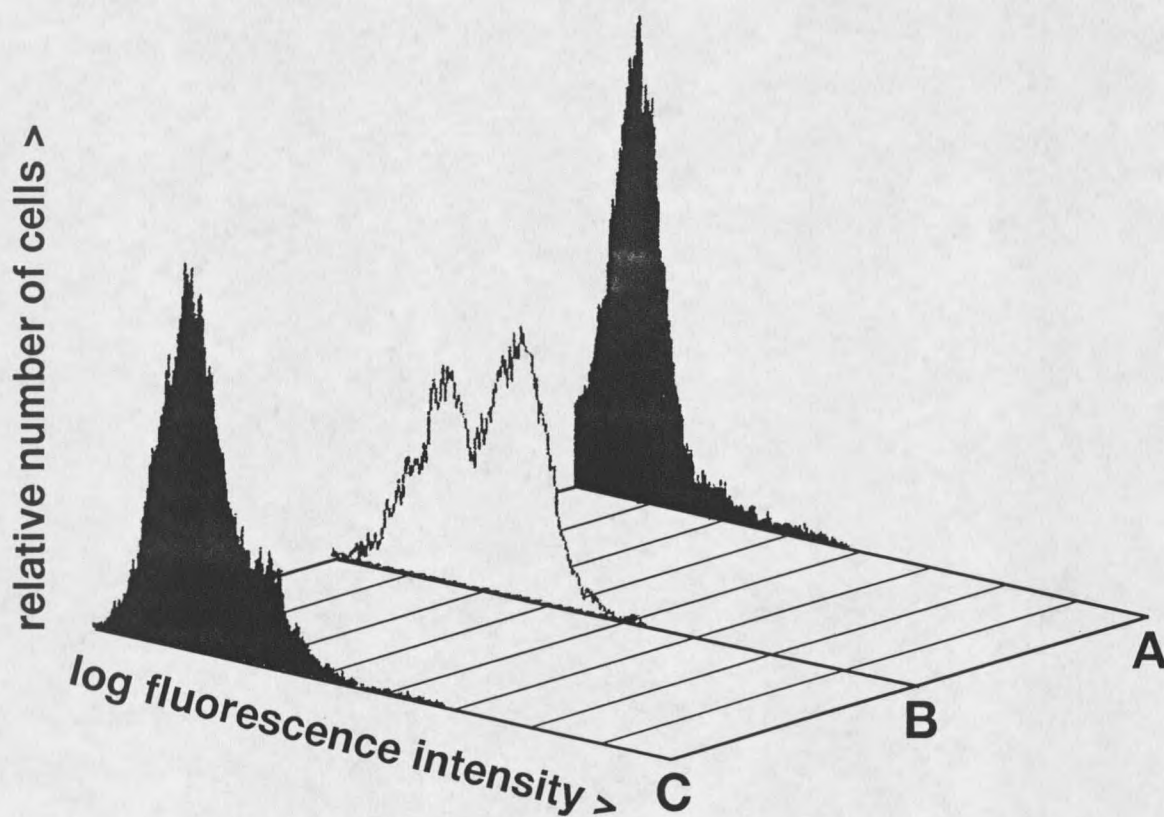


**Figure 16.** FACS Analysis of Neutrophils Stained with mAb 54.1. Intact (A) or saponin-permeabilized human neutrophils (B and C) were incubated with either 50  $\mu\text{g/ml}$  primary antibody 54.1 and a secondary FITC-conjugated antibody (A and B), or the secondary antibody only (C). Cells were then analyzed for fluorescence intensity using a Becton Dickinson *FACScan* model FACS analyzer as described under Methods. The results were reproducible in four separate experiments using neutrophils from different normal human donors.

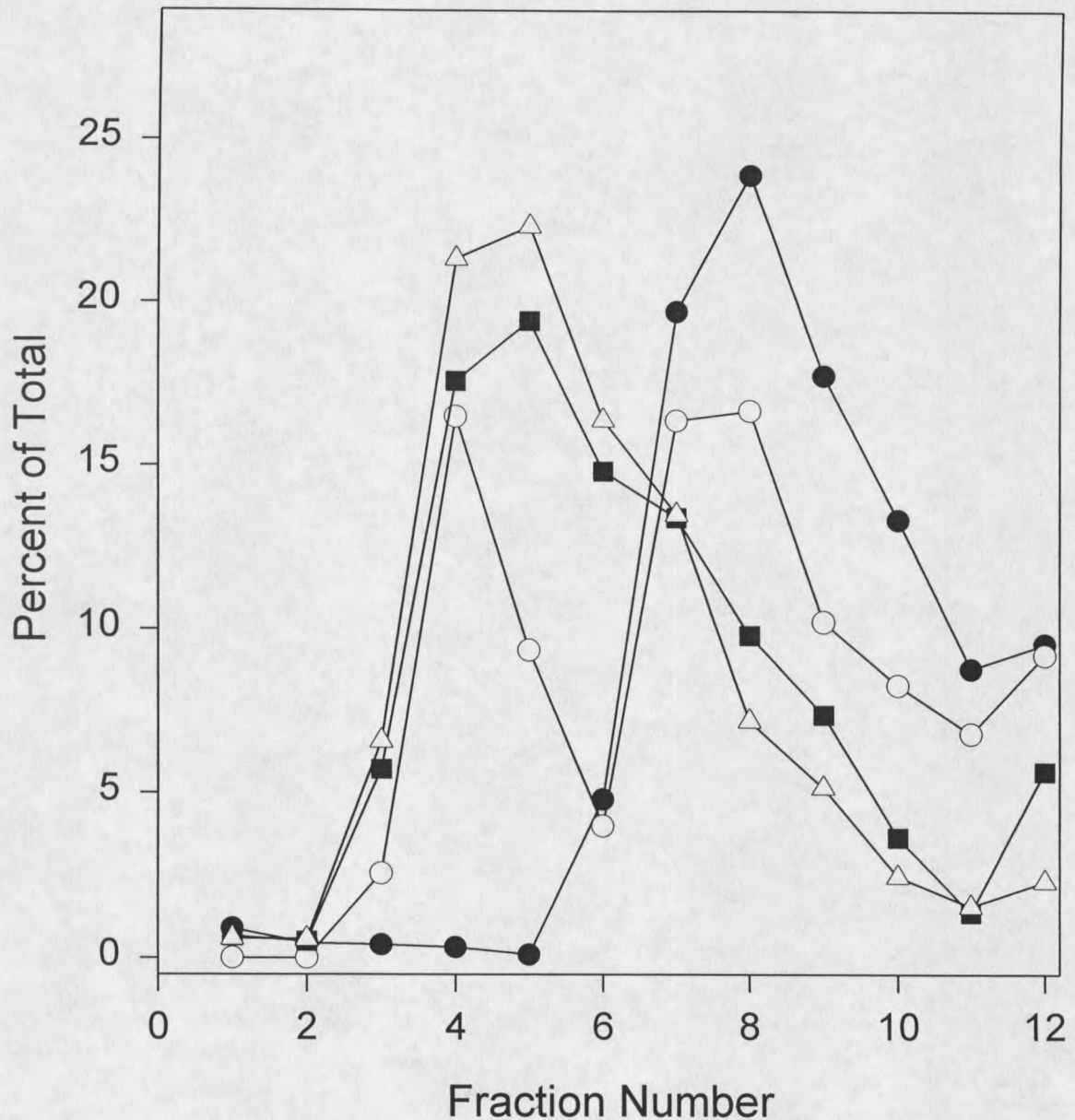


**Figure 17.** Immunosedimentation of mAbs Detergent-solubilized Cyt *b*. Heparin Ultrogel-purified human Cyt *b* was incubated with mAb 44.1 (●), 54.1 (○), irrelevant (■), or no mAb (x) overnight at 4° C and sedimented in a 5-20% sucrose gradient as described under Methods. The relative amount of Cyt *b* in each fraction of the gradient was detected with a rabbit anti-p22-*phox* polyclonal antibody by Western blot analysis. Signal intensities were measured as previously described (36) and plotted for each fraction number. Results were confirmed by three separate experiments.

using mAbs 44.1 and 54.1 confirmed the above immunosedimentation data, as immunoprecipitation of Cyt *b* from 2% octyl glucoside extracts of neutrophil membranes by mAb 54.1 was only half as effective as immunoprecipitation by mAb 44.1 (data not shown). In addition, Rap1A was found to be associated with the Cyt *b* complexes (38) immunoprecipitated by both mAbs 44.1 and 54.1 (data not shown).

Discussion

Because prospects for X-ray crystal or NMR solution structures of Cyt *b* are currently limited, modeling of protein structures must be carried out within constraints imposed by identification of surface domains and functional and structural features. Epitope mapping using random phage-display libraries offers another tool to aid in determining surface features of proteins. We have used two such libraries to identify the epitopes recognized by each of two Cyt *b* specific mAbs and characterized the accessibility of these epitopes to mAb binding on the native protein (8). The unique peptides expressed on phage obtained following the third round of selection were compared to the Cyt *b* amino acid sequences, and regions of remarkable similarity were identified. Each mAb was then characterized according to its ability to bind either denatured, spectrally active, but detergent-solubilized Cyt *b*, or native Cyt *b* in intact and saponin-permeabilized neutrophils. This information was then used to help predict if a particular region of Cyt *b* is exposed to antibody on the cytosolic or external surface of the neutrophil. Our epitope mapping data suggests the epitope recognized by mAb 44.1 includes the amino acids #181-188 of p22-*phox* (<sup>181</sup>GGPQVNPI<sup>188</sup>) and mAb 54.1 binds amino acids #382-389 of gp91-*phox* (<sup>382</sup>PKIAVDGP<sup>389</sup>). The data includes a number of unique phage sequences from each library to support the identification of the epitope for each mAb. Moreover, data obtained from the two libraries is complimentary. An excellent example which shows agreement between the libraries is the similarity of hexapeptide #3 to nonapeptides #4 and #5 (Figure 11). The three phage-displayed peptides were selected by mAb 44.1

from two different libraries, and express the sequence, PQVRPI. The chance recovery of two identical six residue peptides is  $1/32^6$ , or about one in one billion (42).

Bacteriophage epitope mapping exploits the specificity of the monoclonal antibody and the unique sequence of the peptide expressed on selected phage. When mAbs which recognize linear epitopes are used, this technique allows identification of protein epitopes with little ambiguity. Clearly, not all mAbs recognize linear epitopes, thus the approach may not be universally applicable. However, it is conceivable the information might be obtained in those cases which support epitopes corresponding to different regions in the same molecule, split by a fold or invagination of the peptide backbone (17,29).

Phage selected by mAb 44.1 suggest this mAb may be able to recognize some sequences without regard to the orientation of the peptide backbone. Phage #2 of Figure 11, selected by mAb 44.1, expresses the sequence PRVQIL, which contains five of the residues found in PQVRPI, four of which are in reverse order. The ability of this mAb to recognize an epitope may involve recognition of exposed amino acid side chains and charge placement (20) rather than the stereospecific alignment of side chains on the peptide backbone. This result supports our recent finding that the reverse sequence of certain synthetic peptides mimicking the structure of the N-formyl peptide chemoattractant receptor (FPR) retain a diminished, but clearly measurable inhibitory activity in reconstitution of FPR-G-protein complexes in detergent solution (4).

To gain information about the accessibility of the mAb to the native epitope,

FACS analysis was used with saponin-permeabilized and intact neutrophils. This analysis strongly suggests the  $^{181}\text{GGPQVNPI}^{188}$  epitope of p22-*phox* is accessible on the cytosolic but not external aspect of the plasma membrane in neutrophils. The possibility that the epitope is resident, but masked on the external surface of the cell and subsequently made accessible during permeabilization is unlikely. Neighboring regions have been shown to be accessible to mAb in slam-frozen molecular distillation dried cells (25) and freeze-thaw permeabilized cells (23). These regions overlap a p22-*phox* domain clearly shown to be involved in interaction with cytosolic p47-*phox* of the NADPH-oxidase system. Together, these data suggest that the epitope bound by mAb 44.1 is made accessible because of membrane permeabilization, and not because of disruption and subsequent exposure of the Cyt *b* epitope by the action of saponin on the molecule itself. In addition, they strongly support the conclusion that this region of Cyt *b* must be on the surface of the molecule.

Our results repeatedly showed that mAb 54.1 failed to bind Cyt *b* on intact or saponin-permeabilized cells. Hydropathy predictions suggest the  $^{382}\text{PKIAVDGP}^{389}$  region of gp91-*phox* may exist on an external loop between the fourth and fifth putative transmembrane regions, assuming a five membrane-spanning domain model of Cyt *b* (35). The work of Imijoh-Ohmi supports this notion, and identified an extracellular papain cleavage site in the region of the epitope (23). Their results, however, are incompatible with the proposed structure of the gp91-*phox* NADPH and flavin-binding regions (27,40,43,48-50). Because mAb 54.1 binds denatured gp91-*phox* on Western blots, but does not bind native Cyt *b* in either intact or permeabilized

neutrophils, the intracellular or extracellular location of  $^{382}\text{PKIAVDGP}^{389}$  still remains to be confirmed. The epitope, however, must retain a conformation that is either not recognized by the mAb or is in a sterically unfavorable environment. This region has a charge and lies in the middle of a relatively hydrophilic sequence, and is thus not likely to be integrated in the plasma membrane. Since solubilized, partially purified Cyt *b* is immunosedimented by mAb 54.1, it is a greater possibility that accessibility to this area of the protein is blocked by unknown inter- or intra-molecular associations. Possible candidates are other NADPH-oxidase components, including Rap1A since it is known to dissociate from Cyt *b* in sucrose gradient separations (3).

The epitope recognized by mAb 54.1 appears to be less accessible than the epitope recognized by mAb 44.1, as determined by immunoprecipitation (data not shown). This information supports our immunosedimentation data (Figure 17), further suggesting that the  $^{382}\text{PKIAVDGP}^{389}$  region of gp91-*phox* may be sensitive to the association with another cytosolic component. According to this view of the assembled complex, another NADPH-oxidase subunit or accessory group could sterically block or disrupt the conformation of the epitope on native Cyt *b* in permeabilized and intact neutrophils. Varying dissociation of the component from Cyt *b* during purification would explain accessibility of the epitope on some, but not all of the detergent solubilized or heparin Ultrogel-purified Cyt *b* molecules (Figure 17). Complete separation of the component from Cyt *b* under denaturing conditions could account for strong staining of gp91-*phox* by mAb 54.1 on Western blot, which is similar to the level of staining of p22-*phox* by mAb 44.1 (Figure 13).

Rap1A was found to be present in immunoprecipitates of both mAbs 44.1 and 54.1. This result suggests the epitopes recognized by the respective mAbs are probably not blocked by the interaction with Rap1A. The <sup>382</sup>PKIAVDGP<sup>389</sup> epitope of mAb 54.1 might, however, be affected by the presence of accessory nucleotides. This epitope region lies between, and close to (<45 amino acids) proposed binding sites for both FAD and NADPH, as suggested by sequence similarities with other nucleotide-binding proteins (40,43). Further studies by this method of epitope mapping, with activated Cyt *b* or additional mAbs specific for other regions of Cyt *b* may provide sufficient structural evidence to design a more accurate model for neutrophil Cyt *b*. Additionally, screening phage libraries with protein components of the NADPH-oxidase system may identify protein regions involved in forming the active NADPH-oxidase (13), and suggest a molecular architecture for the phagocyte oxidase system.

References Cited

1. **Badwey, J. A. and M. L. Karnovsky.** 1980. Active oxygen species and the functions of phagocytic leukocytes. *Ann. Rev. Biochem.* **49**:695-726.
2. **Berendes, H., R. A. Bridges, and R. A. Good.** 1957. Fatal granulomatosis of childhood: clinical study of a new syndrome. *Minn. Med.* **40**:309-312.
3. **Bokoch, G. M., L. A. Quilliam, B. P. Bohl, A. J. Jesaitis, and M. T. Quinn.** 1991. Inhibition of Rap1A binding to cytochrome b-558 of NADPH oxidase by phosphorylation of Rap1A. *Science* **254**:1794-1796.
4. **Bommakanti, R. K., K. Klotz, E. A. Dratz, and A. J. Jesaitis.** 1993. A carboxyl-terminal tail peptide of neutrophil chemotactic receptor disrupts its physical complex with G protein. *J. of Leukoc. Biol.* **54**:572-577.
5. **Boyum, A.** 1968. Isolation of mononuclear cells and granulocytes from human blood. *J. Clin. Invest.* **21**:77-89.
6. **Bromberg, Y. and E. Pick.** 1985. Activation of NADPH-dependent superoxide production in a cell-free system by sodium dodecyl sulfate. *J. Biol. Chem.* **260**:13539-13545.
7. **Burritt, J. B., M. T. Quinn, M. A. Jutila, C. W. Bond, K. W. Doss, and A. J. Jesaitis.** 1994. Random sequence peptide library analysis of neutrophil flavocytochrome b structure. *Mol. Biol. of the Cell* **5**:121a.(Abstract)
8. **Burritt, J. B., M. T. Quinn, M. A. Jutila, C. W. Bond, and A. J. Jesaitis.** 1995. Topological mapping of neutrophil cytochrome b epitopes with phage-display libraries. *J. Biol. Chem.* (In Press)
9. **Curnutte, J. T.** 1985. Activation of human neutrophil nicotinamide adenine dinucleotide phosphate reduced (triphosphopyridine nucleotide, reduced) oxidase by arachidonic acid in a cell-free system. *J. Clin. Invest.* **75**:1740-1743.
10. **Curnutte, J. T.** 1993. Chronic granulomatous disease: the solving of a clinical riddle at the molecular level. *Clin. Immun. and Immunopath.* **67**:S2-S15.
11. **Cwirla, S, E. Peters, R. Barrett, and W. Dower.** 1990. Peptides on phage: a vast library of peptides for identifying ligands. *Proc. Natl. Acad. Sci. USA* **87**:6378-6382.
12. **De Mendez, I., M. C. Garrett, A. G. Adams, and T. L. Leto.** 1994. Role of p67-*phox* SH3 domains in assembly of the NADPH oxidase system. *J. Biol. Chem.* **269**:16326-16332.

13. **DeLeo, F. R., L. Yu, J. B. Burritt, L. R. Loetterle, C. W. Bond, A. J. Jesaitis, and M. T. Quinn.** 1995. Mapping sites of interaction of p47-phox and flavocytochrome b with random sequence peptide phage display libraries. Proc. Natl. Acad. Sci. USA (In Press)
14. **Devlin, J., L. Panganiban, and P. Devlin.** 1990. Random peptide libraries: a source of specific protein binding molecules. Science. **249**:404-406.
15. **Dinauer, M. C., S. H. Orkin, R. Brown, A. J. Jesaitis, and C. A. Parkos.** 1987. The glycoprotein encoded by the X-linked chronic granulomatous disease locus is a component of the neutrophil cytochrome b complex. Nature **327**:717-720.
16. **Ebright, R., Q. Dong, and J. Messing.** 1992. Corrected nucleotide sequence of M13mp18 gene III. Gene. **114**:81-83.
17. **Felici, F., A. Luzzago, A. Folgori, and R. Cortese.** 1993. Mimicking of discontinuous epitopes by phage-displayed peptides, II. Selection of clones recognized by a protective monoclonal antibody against the *Bordetella pertussis* toxin from phage peptide libraries. Gene **128**:21-27.
18. **Ginsel, L. A., J. J. M. Onderwater, J. M. Fransen, A. J. Verhoeven, and D. Roos.** 1990. Localization of the low-Mr subunit of cytochrome b-558 in human blood phagocytes by immunoelectron microscopy. Blood **76**:2105-2116.
19. **Goldsmith, M. E. and W. H. Koingsberg.** 1977. Adsorption protein of the bacteriophage fd: isolation, molecular properties, and location in the virus. Biochemistry **16**:2686-2694.
20. **Guillet, V., A. Laphorn, R. W. Hartley, and Y. Mauguen.** 1993. Recognition between a bacterial ribonuclease barnase, and its natural inhibitor, borston. Struct. **1**:165-176.
21. **Hackett, P., J. Fuchs, and J. Messing.** 1992. An Introduction to Recombinant DNA Techniques. Benjamin Cummings, Mélno Park, Reading, Don Mills, Wokingham, Amsterdam, Sydney.
22. **Henry, T. J. and D. Pratt.** 1968. The proteins of bacteriophage M13. Proc. Natl. Acad. Sci. USA **62**:800-807.
23. **Imajoh-Ohmi, S., K. Tokita, H. Ochiai, M. Nakamura, and S. Kanegasaki.** 1992. Topology of cytochrome b558 in neutrophil membrane analyzed by anti-peptide antibodies and proteolysis. J. Biol. Chem. **267**:180-184.

24. **Jazwinski, M., R. Marco, and A. Kornberg.** 1973. A coat roptein of the bacteriophage M13 virion participates in membrane-oriented synthesis of DNA. Proc. Natl. Acad. Sci. USA **70**:205-209.
25. **Jesaitis, A. J., E. S. Buescher, D. Harrison, M. T. Quinn, C. A. Parkos, S. Livesey, and J. Linner.** 1990. Ultrastructural localization of cytochrome b in the membranes of resting and phagocytosing human granulocytes. J. Clin. Invest. **85**:821-835.
26. **Koshkin, V. and E. Pick.** 1994. Superoxide production by cytochrome  $b_{559}$ : Mechanism of cytosol-independent activation. FEBS Lett. **338**:285-289.
27. **Koshkin, V. and E. Pick.** 1994. Superoxide production of cytochrome b-559: mechanism of cytosol-independent activation. FEBS Lett. **338**:285-289.
28. **Landing, B. H. and H. S. Shirkey.** 1957. A syndrome of recurrent infection and infiltration of viscera by pigmented lipid histiocytes. Pediatr, **20**:431-438.
29. **Miceli, R. M., M. E. DeGraaf, and H. D. Fischer.** 1994. Two-stage selection of sequences from a random phage display library delineates both core residues and permitted structural range within an epitope. J. Immunol. Methods **167**:279-287.
30. **Miller, J. H.** 1972. Experiments in Molecular Genetics. Cold Spring Harbor Laboratory, Cold Spring Harbor.
31. **Morel, F., J. Doussiere, and P. V. Vagnais.** 1991. The superoxide-generating oxidase of phagocytic cells. Eur. J. Biochem. **201**:523-546.
32. **Parkos, C. A., R. A. Allen, C. G. Cochrane, and A. J. Jesaitis.** 1987. Purified cytochrome b from human granulocyte plasma membrane is comprised of two polypeptides with relative molecular weights of 91,000 and 22,000. J. Clin. Invest. **80**:732-742.
33. **Parkos, C. A., R. A. Allen, C. G. Cochrane, and A. J. Jesaitis.** 1988. The quaternary structure of the plasma memembrane b-type cytochrome of human granulocytes. Biochim. Biophys. Acta **932**:71-83.
34. **Parkos, C. A., M. C. Dinauer, L. E. Walker, R. A. Allen, A. J. Jesaitis, and S. H. Orkin.** 1988. Primary structure and unique expression of the 22-kilodalton light chain of human neutrophil cytochrome b. Proc. Natl. Acad. Sci. USA **85**:3319-3323.
35. **Parkos, C. A., M. T. Quinn, S. Sheets, and A. J. Jesaitis.** 1992. Molecular Basis of Oxidative Damage by Leukocytes. p.45-55. CRC Press Inc., Boca Raton, Ann Arbor, London, Tokyo.

36. **Quinn, M. T., T. Evans, L. R. Loetterle, A. J. Jesaitis, and G. M. Bokoch.** 1993. Translocation of rac correlates with NADPH oxidase activation. *J. Biol. Chem.* **268**:20983-20987.
37. **Quinn, M. T., M. L. Mullen, and A. J. Jesaitis.** 1992. Human neutrophil cytochrome b contains multiple hemes. *J. Biol. Chem.* **267**:7303-7309.
38. **Quinn, M. T., C. A. Parkos, L. Walker, S. H. Orkin, M. C. Dinauer, and A. J. Jesaitis.** 1989. Association of a ras-related protein with cytochrome b of human neutrophils. *Nature* **342**:198-200.
39. **Rotrosen, D., M. E. Kleinberg, H. Nuno, T. Leto, J. I. Gallin, and H. L. Malech.** 1990. Evidence for a functional cytoplasmic domain of phagocyte oxidase cytochrome b558. *J. Biol. Chem.* **265**:8745-8750.
40. **Rotrosen, D., C. L. Yeung, T. L. Leto, H. L. Malech, and C. H. Kwong.** 1992. Cytochrome b-558: the flavin-binding component of the phagocyte NADPH oxidase. *Science* **256**:1459-1462.
41. **Royer-Pokora, B., L. M. Kunkel, A. P. Monaco, S. C. Goff, R. L. Newburger, R. L. Baehner, F. S. Cole, J. T. Curnutte, and S. H. Orkin.** 1986. Cloning the gene for an inherited human disorder-chronic granulomatous disease-on the basis of its chromosomal location. *Nature* **322**:32-38.
42. **Scott, J. and G. Smith.** 1990. Searching for peptide ligands with an epitope library. *Science.* **249**:386-390.
43. **Segal, A. W., I. West, F. Wientjes, J. H. A. Nugent, A. J. Chavan, B. Haley, R. C. Garcia, H. Rosen, and G. Scrase.** 1992. Cytochrome b-245 is a flavocytochrome containing FAD and the NADPH-binding site of the microbicidal oxidase of phagocytes. *Biochem. J.* **284**:781-788.
44. **Smith, G. P. and J. K. Scott.** 1993. Libraries of peptides and proteins displayed on filamentous phage. *Methods Enzymol.* **217**:228-257.
45. **Smith, R. M. and J. T. Curnutte.** 1991. Molecular basis of chronic granulomatous disease. *Blood* **77**:673-686.
46. **Taylor, W. R., D. T. Jones, and A. W. Segal.** 1993. A structural model for the nucleotide binding domains of flavocytochrome b-245 beta-chain. *Prot. Science* **2**:1675-1685.
47. **Tzagloff, H. and D. Pratt.** 1964. The initial steps in infection with Coliphage M13. *Virology* **24**:372-380.

48. **Umei, T., B. M. Babior, J. T. Curnutte, and R. M. Smith.** 1991. Identification of the NADPH-binding subunit of the respiratory burst oxidase. *J. Biol. Chem.* **266**:6019-6022.
49. **Umei, T., K. Takeshige, and S. Minakami.** 1986. NADPH binding component of neutrophil superoxide-generating oxidase. *J. Biol. Chem.* **261**:5229-5232.
50. **Umei, T., K. Takeshige, and S. Minakami.** 1987. NADPH-binding component of the superoxide-generating oxidase in unstimulated neutrophils and the neutrophils from the patients with chronic granulomatous disease. *Biochem. J.* **243**:467-472.
51. **Woolford, J. L. Jr., H. M. Steinman, and R. E. Webster.** 1977. Adsorption protein of bacteriophage f1: solubilization in deoxycholate and localization in the f1 virion. *Biochemistry* **12**:2694-2700.

## CHAPTER FOUR

### IDENTIFICATION OF A DISCONTINUOUS CYTOCHROME B EPITOPE WITH A NONAPEPTIDE PHAGE-DISPLAY LIBRARY

#### Abstract

Random sequence phage peptide libraries were used to identify the epitopes recognized by two Cytochrome *b* (Cyt *b*)-specific monoclonal antibodies (mAbs) (Chapter 3). In the absence of X-ray crystal and NMR structural methods for determination of Cyt *b* structure, alternative methods are necessary to come to an understanding of the three-dimensional structure of this protein. Application of a second method of antibody-mediated selection to obtain phage clones allowing better resolution of the epitope recognized by the anti-p22-*phox* mAb, 44.1 was achieved. This method involved colony-lift immunological screening to probe a population of *E. coli* colonies infected by phage-display library members previously selected by an immunoaffinity column using mAb 44.1. Two different phage-expressed peptides identified by colony-lift screening displayed the hexapeptide, PQVRPI, which matched five of six residues in the  $^{183}\text{PQVNPI}^{188}$  region of p22-*phox*. Nineteen other phage identified by this method displayed the sequences supporting a consensus match of the peptide sequence, TAGRFGGGQVGPP. This sequence contained segments similar to

the  $^{181}\text{GGPQVNPI}^{188}$  and  $^{29}\text{TAGRF}^{33}$  regions of p22-*phox*, suggesting a more complete epitope recognized by this mAb may include both regions of the protein. A mutant phage was produced which expressed the ATAGRFGGG peptide alone, and was bound by mAb 44.1 by Western blot analysis. The ability of mAb 44.1 to recognize both p22-*phox* regions was supported by synergistic binding of the mAb to the phage-expressed PQVRPI epitope in the presence of either the synthetic peptide which matches the  $^{29}\text{TAGRFTQW}^{36}$  region of p22-*phox*, or the phage-expressed ATAGRFGGG peptide. Thus, this report suggests a means by which phage-display library analysis was used to identify two segments of Cyt b which may be juxtaposed by tertiary structure.

### Introduction

Flavocytochrome b (Cyt b) (a.k.a., flavocytochrome *b*, cytochrome *b*<sub>558</sub>, cytochrome *b*<sub>559</sub>, cytochrome *b*<sub>245</sub>) is the central redox component of the NADPH-oxidase system of human neutrophils (3,15). Cyt b is a heterodimeric integral membrane protein comprised of two subunits, gp91-*phox* and p22-*phox* (7). This protein acts as the electron transferase that directs metabolic electrons across the plasma membrane to the external surface of the cell where molecular oxygen is reduced to form microbicidal O<sub>2</sub><sup>-</sup>, a precursor for other reactive oxygen compounds (9,10,12). Patients with an impaired NADPH-oxidase suffer a heterogeneous group of symptoms referred to as chronic granulomatous disease (CGD). These symptoms result from an abnormal inflammatory and anti-microbial response when challenged by bacterial and fungal pathogens. The phenotype of these diseases is defective respiratory burst of neutrophils and other phagocytes, predisposing the affected individual to repeated life-threatening infections and granulomatous lesions (1,3,14).

The molecular basis of CGD and the architecture of the oxidase complex is not well understood because of insufficient knowledge about the interaction of protein subunits. Examination of the assembled complex outside the cell is difficult, owing to the instability of interactions between subunits and accessory groups during purification. Because of the absence of X-ray crystallography and only recent nuclear magnetic resonance (NMR) structural data for this protein, little is known about the surface-accessible regions of the molecule.

We previously reported epitope mapping of Cyt b using monoclonal antibodies

specific for each subunit and random sequence phage peptide display libraries (Chapter 3). A portion of this earlier report described the selection of phage from the J404 library which contained information to implicate the cytosolic  $^{181}\text{GGPQVNPI}^{188}$  region of p22-*phox* as the epitope bound by mAb 44.1. Our recent evidence obtained using a colony-lift method of immunological selection of phage, suggests that this antibody may recognize the  $^{29}\text{TAGRF}^{33}$  region of p22-*phox* in addition to the previously identified  $^{181}\text{GGPQVNPI}^{188}$  region. These interactive regions, in which the continuity of the peptide backbone may not be as important as residue placement, specificity, and charge, can still be mimicked by linear peptide sequences, and thus identified by phage-display library analysis.

The identification of such a discontinuous epitope with a phage-display library strengthens the contention that phage-expressed peptides resemble interactive regions of proteins, and can resemble complex epitopes or interactive sequences.

## Materials and Methods

### Reagents

Tween 20, yeast extract, tryptone, agar, kanamycin, Trizma base, PBS, EDTA, SDS, acrylamide, bis-acrylamide, ammonium persulfate, TEMED, and bovine serum albumin (BSA) were purchased from Sigma Chemical Co. (St. Louis, MO).

Sequencing data was obtained using a Sequenase version 2.0 sequencing kit purchased from United States Biochemical (Arlington, Heights, IL) and autoradiography images were obtained using a Molecular Dynamics Model 400E Phosphorimager.

Oligonucleotides were synthesized at Integrated DNA technologies (Coralville, IA) or at Montana State University. The J140 oligonucleotide sequencing primer (5'-gtttgtcgtctttccagacg-3'), was used to determine the nucleotide sequence of the unique region of the phage. *E. coli* strains K91 and MC1061 were kindly provided by Dr. George P. Smith at University of Missouri, Columbia. Unless indicated otherwise, when kanamycin was used in media to grow cultures of cells infected by the phage, the concentration of kanamycin used was 75 µg/ml.

### Colony-lift Immunological Screening

We previously reported the selection of J404 library clones on mAb 44.1 sepharose columns (Chapter 3). Phage selected by this method were subjected to a second method of immunological selection. A three µl sample of mAb 44.1-selected phage containing ca.  $3 \times 10^8$  virions was mixed with one ml of mid-log phase K91 cells and phage were allowed to infect cells at room temperature for 15 minutes. The

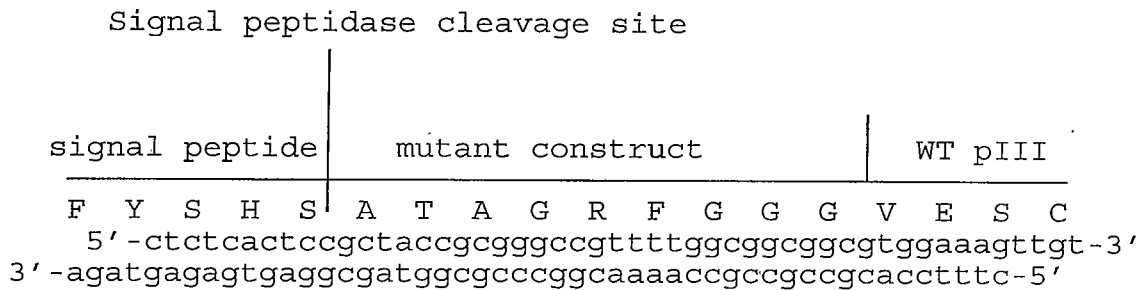
kanamycin concentration was then adjusted to 0.75  $\mu\text{g/ml}$ , and the cells were incubated at 37° C in a shaking water bath for 20 minutes to stimulate the production of aminoglycoside-3'-phosphotransferase protein which imparts kanamycin resistance. The infected cells were diluted and plated on LB/kan agar to produce ca. 100 colonies per plate following overnight incubation at 37° C. Resulting colonies were blotted to nitrocellulose for five minutes, residual colonies were rinsed from the blot in PBS (pH 7.4), and blots were probed with 2  $\mu\text{g/ml}$  mAb 44.1 for 2 hours at room temperature. After colonies were blotted from the surface of the agar, the plates were returned to 37° C incubation overnight to allow regrowth of the colonies. Blots were washed and probed with a goat anti-mouse IgG tagged with alkaline phosphatase for one hour at room temperature. The blots were developed using alkaline phosphatase-conjugated goat anti-mouse IgG and BCIP/NBT phosphatase substrate system. Darkly staining signals on the blots were used to locate the corresponding colonies which were then used to inoculate individual two ml cultures of 2XYT/kan for the production of phage DNA for nucleotide sequence analysis as previously described (13). The nucleotide sequences of the unique regions of the phage clones were determined and the phage-expressed peptides were deduced.

#### Mutant Phage Construction

Phage selected by colony-lift screening displayed a consensus TAGRFGGGQVGPP peptide sequence (see below). Most phage clones selected in this way suggested the <sup>29</sup>TAGR<sup>F33</sup> region of p22-*phox* might participate with the

previously identified  $^{181}\text{GGPQVNPI}^{188}$  regions of the protein to form a more complete epitope for mAb 44.1. To establish if the TAGRF sequence could be bound alone by this mAb, a phage was constructed using recombinant DNA techniques which displayed the ATAGRFGGG peptide sequence. This sequence was chosen because ATAGRF represents the first six residues of this putative cytosolic loop region of the transmembrane protein, p22-*phox*, which is predicted to have three potential transmembrane domains by hydropathy analysis (8). In addition, three glycine residues were included at the carboxyl end of the ATAGRF region because of the consensus sequence of peptides on phage selected by colony-lift screening. It is not known if the glycine residues of the GGG segment contribute to the antibody recognition sequence or if they merely function as a flexible linker for the two regions of the protein. Thus, the pIII protein of this mutant is designed to display the ATAGRFGGG peptide which is intended to represent the putative second portion of the mAb 44.1 epitope. In order to construct such a phage, two complimentary oligonucleotides were synthesized to form a segment of DNA coding for the amino acid sequence ATAGRFGGG when cloned into the *Bst*XI sites of the M13KBst vector (Chapter 2). The sequence of the oligonucleotides used for this construct are shown below with the overlapping 3' ends compatible for ligation into the *Bst*XI-cleaved vector. In addition, the encoded pIII fusion product is shown, which includes regions of mutant and wild-type (WT) pIII protein, the carboxyl end of the signal peptide, and signal peptidase cleavage site. The two oligonucleotides were phosphorylated on the 5' termini and allowed to anneal under conditions previously described (2). The insert

was then ligated to the vector in a molar ratio of 1:2.5 for vector: insert, respectively.



The ligation product was precipitated in ethanol, lyophilized, resuspended in water, and transfected into electrocompetent MC1061 cells which were then allowed to recover as described (4,13). The transfected cells were then plated on a lawn of K91 cells to produce isolated plaques. Phage clones from isolated plaques were propagated and the recombinant region of the PIII gene was sequenced to verify the correct placement and sequence of the oligonucleotides.

#### Western Blot of Mutant

To determine the extent to which mAb 44.1 was able to recognize the putative regions of its cognate epitope, phage expressing the ATAGRFGGG, EGRFGGGQVGPP, and AQPQVRPIG peptides were produced and the capsid proteins were probed with mAb 44.1 by Western blot analysis as previously described (Chapter 3). A negative control for this experiment consisted of the M13KBst vector (Chapter 2), which expresses no unique peptide.

Western Blot to Show Effect of TAGRF Sequence

Western blotting was used to determine if the synthetic ATAGRFTWQ peptide or the phage-expressed ATAGRFGGG or PQVRPI sequences could affect binding of mAb 44.1 to the PQVRPI peptide segment expressed on the pIII protein of phage. The proteins of approximately  $10^{10}$  phage expressing the PQVRPI sequence were resolved in each lane on PAGE gels and transferred to nitrocellulose as described (Chapter 3). The blots were probed in 2  $\mu\text{g/ml}$  mAb 44.1 overnight at 4° C. During incubation of the blots with mAb 44.1, the following conditions were used to test the perturbing effect of the phage-expressed or synthetic peptides: a) 230  $\mu\text{M}$  TAGRFTQW synthetic peptide, b) 2.8 nM phage-expressed PQVRPI sequence, c) 2.8 nM phage-expressed ATAGRFGGG sequence, and d) mock treatment controls. The blots were then developed and quantitated by densitometry as described in Chapter 3.

## Results

Using the J404 phage-display library, we have previously shown the identification of the  $^{181}\text{GGPQVNPI}^{188}$  epitope of p22-*phox* for mAb 44.1 (Chapter 3). Immunological screening was performed on a sample of phage previously selected by mAb 44.1, to identify clones expressing peptides most similar to the natural Cyt b epitope. K91 cells were infected with affinity purified phage and grown as isolated colonies on LB/kan agar. The colonies were blotted to nitrocellulose, and probed with mAb 44.1 by a method similar to Western blot analysis. Signals corresponding to individual colonies were produced on the blot, and the intensities of the signals showed significant variation (Figure 18). Figure 18 shows two populations of colonies; those which demonstrate weak but positive staining are represented by colonies labeled A (about 95% of the clones), and the remaining minority which stain strongly are represented by colonies labeled B. In order to determine if the variation of the signals in Figure 18 was due to qualitative differences of the expressed peptide regions, nucleotide sequence analysis was used to deduce the unique nonapeptides of phage produced by the two groups of colonies represented by A and B. The peptides expressed by phage recovered from weakly staining (A-type) colonies were found to belong to the previously identified PxVxP sequence, such as the phage expressed peptides, MTPEVRPID, KPMV $\underline{\text{V}}$ PIHS, and TGPEVRPLQ (Figure 11). When the pIII proteins of phage produced by strongly staining (B-type) colonies were sequenced, a new consensus sequence was observed. These phage expressed the consensus peptide sequence, TAGRFGGGQVGPP (the three invariant residues, GPP, of all library

members adjacent to the unique peptide is included because they may be involved in binding by mAb 44.1). Phage expressing this type of peptide were not observed without colony-lift immunological screening. Some phage sequences obtained by this method were previously reported (Chapter 3) because they supported the identification of the  $^{183}\text{PQVNPIP}^{189}$  region of *p22-phox* as the mAb 44.1 epitope (Figure 11A, sequences #4, 5, and 24). This consensus sequence included the GGGQVXPP residues similar to the  $^{181}\text{GGPQVNPIP}^{189}$  region of *p22-phox*, but also contained a group of residues on the amino side of the GGGQVXPP sequence, suggesting these phage contained additional residues resembling the  $^{29}\text{TAGR}^{\text{F33}}$  segment of *p22-phox*, which may also be recognized by mAb 44.1. The two regions of *p22-phox* which resemble the consensus sequence of phage selected by colony-lift screening are compared to the sequences of phage identified by colony lift in Table 7.

**Table 7.** Comparison of *p22-phox* Discontinuous Regions and Deduced Peptides on Phage Detected by Colony-lift Immunological Screening with mAb 44.1<sup>a</sup>.

Juxtaposed Segments of <i>p22-phox</i>	Unique Regions <sup>b</sup> of Phage Detected by Colony-lift Immunological Screening <sup>c</sup>
.. 175-AAGGPP <b>GGPQVNPIP</b> V-190...	<u>EGR<b>F</b>GGG<b>Q</b>VGPP</u> (X14)
....27- <b>ATAGR</b> F <sup>T</sup> QW-36.....	<u>IS<b>R</b>FGGG<b>Q</b>VGPP</u>
	<u>TRRHRGG<b>Q</b>VGPP</u>
	<u>TAAHAGG<b>Q</b>VGPP</u> (X3)
	AQPQVRPIG
	NMPQVRPID

<sup>a</sup> Identical amino acid match between phage sequence and *p22-phox* are shown in bold.

<sup>b</sup> The constant region of the pIII protein suspected of being involved in binding by mAb 44.1 is underlined.

<sup>c</sup> Multiple recoveries of identical clones are indicated parenthetically.

Because mAb 44.1 readily demonstrates the pIII protein of phage expressing the PQVRPI peptide in Western blot (Chapter 3), this method was used to determine if the pIII protein of phage expressing only the TAGRFGGG sequence was recognized by this mAb in a similar manner. Using oligonucleotides which code for this sequence, we created a mutant which expressed the ATAGRFGGG peptide at the amino terminus of the pIII protein. We then probed the phage pIII fusion protein of this mutant with mAb 44.1 by Western blot analysis (Figure 19).

All lanes in Figure 19 contain the same amount of phage pIII protein and each protein differed only by the sequence of the unique peptide expressed at the amino terminus. In each case, the pIII protein migrates to a position in the gel equivalent to a 64 kDa protein. The sequence of the peptide expressed on the pIII protein in Lane A is ATAGRFGGG, Lane B is EGRFGGGQVGPP, Lane C is AQPQVRPIG, and Lane D contains pIII protein from the phage vector which expresses no unique peptide. A weak, but detectable amount of staining which corresponds to the position of the pIII protein is evident in Lane A, suggesting at least part of the ATAGRFGGG sequence contributes to the binding by mAb 44.1. In lane B, a strong signal corresponds to the complex epitope, EGRFGGGQVGPP, on the pIII protein. In lane C, a strong but less intense band represents the pIII protein of phage expressing the PQVRPI peptide. The bands in Lanes A-C were measured by densitometry (data not shown) and the intensity of bands in Lanes A and B were found to be 4% and 130% of the signal of the band in Lane C, respectively. Lane D contains no detectable signal, suggesting it is the unique regions of the pIII proteins, and not the constant

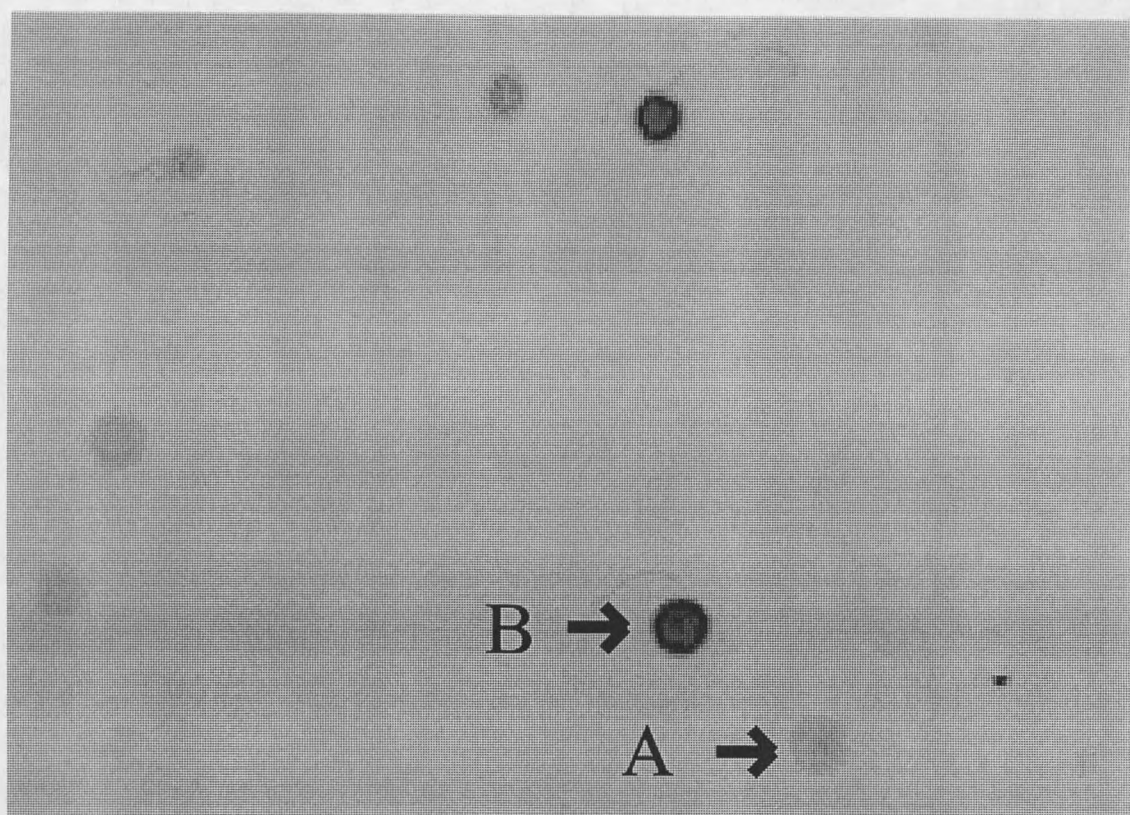


**Figure 18.** Colony-lift immunological screening. Approximately  $3 \times 10^8$  phage selected as described (Chapter 3) using mAb 44.1 were used to infect one ml of mid-log phase K91 cells for 15 minutes at room temperature. The kanamycin concentration was then adjusted to  $0.75 \mu\text{g/ml}$ , and the cells were incubated at  $37^\circ \text{C}$  in a shaking water bath for 20 minutes to stimulate the production of aminoglycoside-3'-phosphotransferase (APT). APT imparts kanamycin resistance so that the infected cells can be grown individually as colonies on solid medium. Limiting dilutions of the cells were performed to obtain isolated colonies when plated on LB agar containing kanamycin at  $75 \mu\text{g/ml}$  following overnight incubation at  $37^\circ \text{C}$ . Resulting colonies were blotted to nitrocellulose for five minutes, visible colonies were rinsed from the blot in PBS (pH 7.4), and blots were probed with  $2 \mu\text{g/ml}$  mAb 44.1 for 2 hours at room temperature. The blots were then developed as described in Methods. Darkly staining signals on the blots were used to locate the corresponding colonies which were then used to inoculate individual two ml cultures of 2XYT/kan for the production of phage DNA for nucleotide sequence analysis as previously described (13).

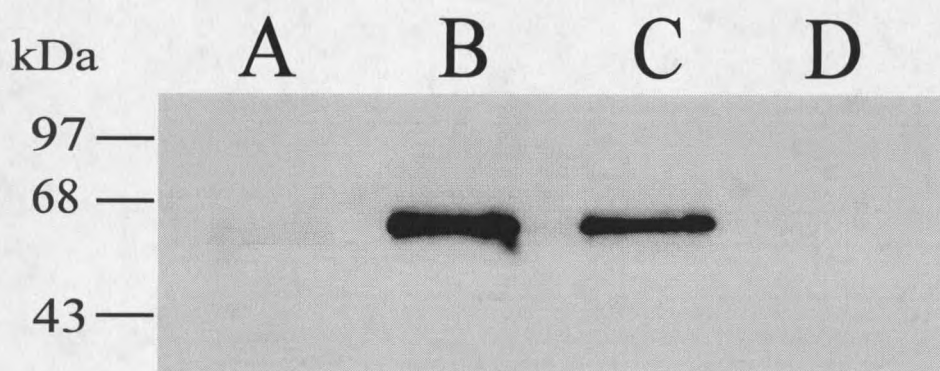


**Figure 19.** Western blotting of putative epitope regions recognized by mAb 44.1. To determine relative extent to which mAb 44.1 was able to recognize the putative epitope regions expressed on the pIII protein of phage, 100 mls of LB broth/kan was inoculated with K91 cells infected with the phage expressing the different peptide sequences listed below. Resulting phage were harvested from this culture and the phage proteins were separated by PAGE and probed with mAb 44.1 by Western blot analysis as described (Chapter 3). The unique regions expressed on the pIII proteins expressed on the phage were: Lane A, ATAGRFGGG; Lane B, EGRFGGGQVGPP; Lane C, AQPQVRPIG; and Lane D contained phage proteins from the M13KBst vector (Chapter 2), which expresses no unique peptide.

region of the pIII molecule which is recognized by mAb 44.1. These results suggest that: a) the ATAGRFGGG sequence expressed alone on the pIII protein is recognized by mAb 44.1 to a small extent, b) the PQVRPI phage-expressed peptide is demonstrated with greater staining intensity than the ATAGRFGGG peptide, and c) the combination of both regions constitutes the highest (synergistic) binding affinity by the mAb.

We previously showed the pretreatment of mAb 44.1 with phage expressing the PQVRPI peptide results in the ability to partially block binding of the mAb to the native Cyt b epitope in saponin-permeabilized neutrophils by flow cytometric analysis (Chapter 3). We tested whether the binding of mAb 44.1 to the phage-expressed PQVRPI sequence could be affected by the presence of either the PQVRPI or TAGRF sequences by Western blot. During the incubation of mAb 44.1 with the immunoblots of the phage-expressed PQVRPI sequence, the PQVRPI phage-expressed and TAGRFTQW synthetic peptide (resembling the <sup>29</sup>TAGRFTQW<sup>36</sup> region of p22-*phox*) were included independently. Blots were probed by mAb 44.1 at 2 µg/ml overnight at 4° C, developed, and quantitated by densitometry as described in Chapter 3. The blots and graph shown in Figure 20 indicate the relative staining intensities of the phage-expressed PQVRPI sequence when probed by mAb 44.1 in the following conditions: a) 230 µM TAGRFTQW synthetic peptide, b) 2.8 nM phage-expressed PQVRPI sequence, c) 2.8 nM phage-expressed ATAGRFGGG sequence, and d) mock treatment controls. The results suggest the synthetic TAGRFTQW and phage-expressed ATAGRFGGG peptide (sequence in common is underlined) increase binding of mAb

44.1 to the phage-expressed PQVRPI peptide 135% and 126%, respectively; and the phage-expressed PQVRPI peptide reduced the staining of the same phage-expressed sequence to 40% of control.

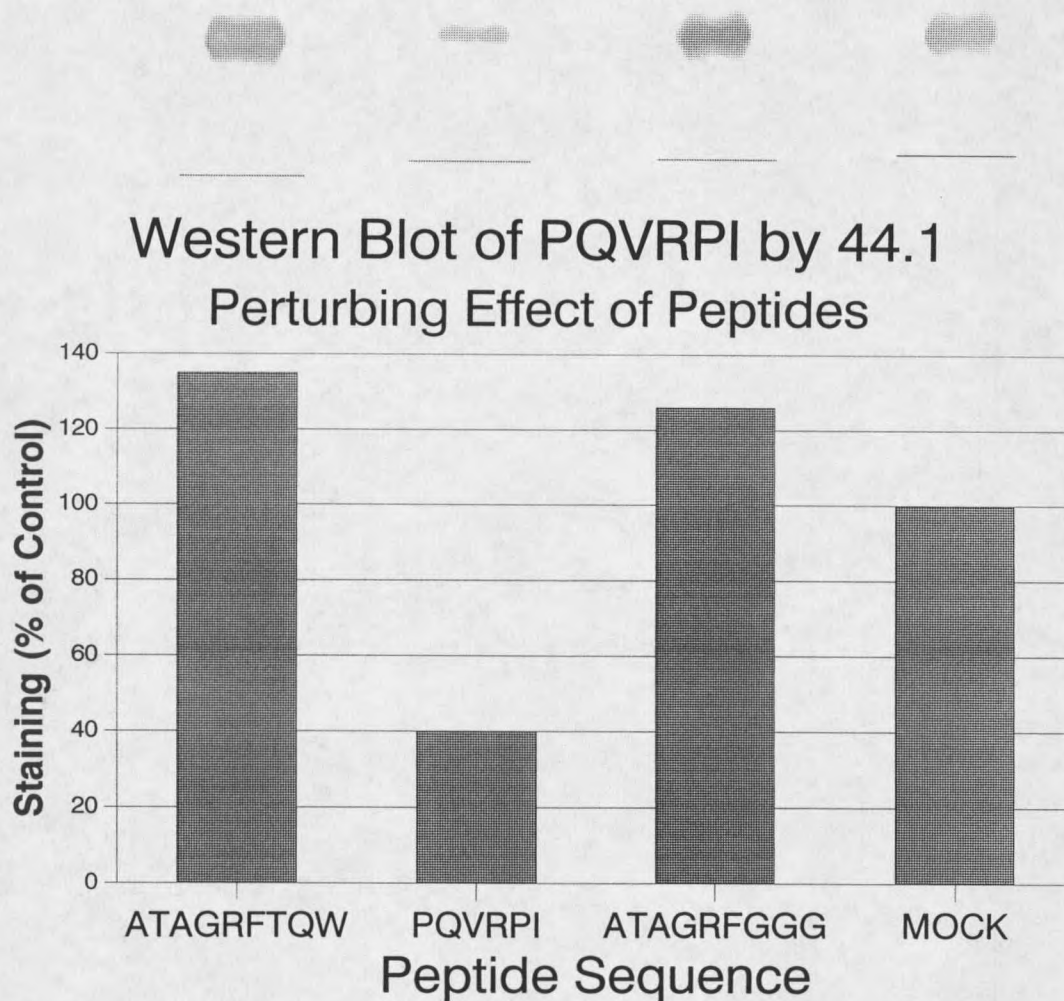


**Figure 20.** Western blot analysis showing influence of specific peptide sequences on the binding of the PQVRPI phage-expressed epitope by mAb 44.1. For each sample, phage proteins from ca.  $2 \times 10^{10}$  virions expressing five copies each of the PQVRPI peptide were separated by PAGE and blotted to nitrocellulose as described in Chapter 3. Each lane was probed in  $1 \mu\text{g/ml}$  of mAb 44.1 overnight at  $4^\circ \text{C}$  in the presence of synthetic or phage-expressed peptides listed below. The signal intensities of bands shown were quantitated by densitometry and plotted against the percent total staining dictated by mock control samples. Staining intensities of blots represented by each bar were produced following the probing of the phage-expressed PQVRPI sequence with mAb 44.1 in the presence of: A)  $230 \mu\text{M}$  TAGRFTQW synthetic peptide, B)  $2.8 \text{ nM}$  phage-expressed PQVRPI sequence, C)  $2.8 \text{ nM}$  phage-expressed ATAGRFGGG sequence, and D) mock treatment controls.

Discussion

Colony-lift immunological screening was used to identify phage clones displaying a unique group of peptides which contain information about the binding specificity of mAb 44.1. The phage probed by this method were previously selected from the J404 library on a Sepharose immunoaffinity column, and were thus biased to express sequences bound by mAb 44.1. The colony-lift screening was used to provide an additional means of immunological selection of phage peptides which may most closely resemble the natural epitope bound by mAb 44.1.

Twenty-one phage clones demonstrated unusually dark staining by colony-lift screening. The unique regions of the pIII proteins of these phage were deduced from the nucleotide sequences of the expressing phage, and found to segregate into two groups. The first type of sequence consisted of two different clones, both of which expressed the PQVRPI sequence. This peptide region contained five of six contiguous residues of the  $^{183}\text{PQVNPI}^{188}$  segment of p22-*phox*, which probably serves as the dominant region of the epitope for this mAb. These two phage sequences strongly represented the  $^{183}\text{PQVNPI}^{188}$  segment of p22-*phox*, suggesting the other group of peptides identified by this method may also provide information about the epitope bound by mAb 44.1.

The unique peptides of the second group of nineteen phage showed strong similarity and suggested the consensus sequence, TAGRFGGGQVGPP. Two of these phage sequences, ISRFGGGQV and EGRFGGGQV, contained exact matches in seven of the nine random residues. In theory, a phage-display library capable of producing

any two phage with seven identical residues would contain at least  $32^7$  ( $3 \times 10^{10}$ ) unique clones (11). Because a phage-display library of this complexity has not been produced, this result indicates the strong selective pressure by which these phage were recovered.

The carboxyl half of the TAGRFGGGQVGPP sequence is similar to the  $^{181}$ GGPQVNPIP $^{189}$  region of p22-*phox*, indicating these peptides were selected specifically by mAb 44.1. To support the notion that mAb 44.1 specifically recognizes the amino half of the TAGRFGGGQVGPP segment, Western blot analysis was used to demonstrate the specific binding of mAb 44.1 to the TAGRFGGG peptide sequence. A recombinant phage was specifically prepared which displayed this sequence, and was probed with mAb 44.1 by Western blot analysis. The pIII protein of the mutant phage which displays the ATAGRFGGG sequence consistently demonstrated weak but positive staining (Figure 19, Lane A), supporting specific recognition by the mAb.

The significance of the TAGRFGGGQVGPP sequence has not been proven, but our data suggests two regions of Cyt b may be represented in this sequence. Because the  $^{29}$ TAGR $^{33}$  sequence is separated from the  $^{183}$ PQVNPI $^{188}$  region of p22-*phox* by 150 residues and two putative membrane-spanning domains, it is possible that the consensus sequence mimics an area on the three-dimensional surface of p22-*phox*, where two discontinuous regions of Cyt b are in close proximity and form a more complete epitope for the mAb. The  $^{29}$ TAGR $^{33}$  region of p22-*phox* appears to be involved because this sequence is included in the consensus sequence of phage identified by colony-lift analysis. This region is also a possibility because it is

believed to occupy the same (cytosolic) compartment of the neutrophil as  $^{183}\text{PQVNPI}^{188}$ , based on hydropathy analysis of the protein (8). Two hypothetical models of p22-*phox*, based on relative positions of the membrane-spanning domains are shown in Figure 21. The three contiguous glycine residues in the consensus sequence may represent the two glycines adjacent to the amino end of the  $^{183}\text{PQVNPI}^{188}$  region of p22-*phox* (see Table 7). In this case, the glycine residues may be recognized specifically by the mAb, and contribute to the binding affinity. However, our previous results suggest these glycines are poorly represented by phage clones which strongly implicate the  $^{183}\text{PQVNPI}^{188}$  region as the dominant region of the epitope (Figure 11). A more plausible role for the contiguous glycines in the consensus sequence is the linkage of the QVGPP and TAGRF regions of the phage-expressed peptide, into a conformation which mAb 44.1 can recognize. According to this view, the TAGRFGGGQVGPP phage-expressed peptides could have been selected because of their ability to assume either of two conformations which mimic the two regions of the native p22-*phox*. A simplified model of these conformations, along with the speculative arrangements of p22-*phox* are shown in Figure 21. In Figure 21A, the consensus TAGRFGGGQVGPP phage-displayed sequence assumes an extended configuration, as does the combination of the similar regions of p22-*phox*. In Figure 21B, the TAGRFGGGQVGPP phage sequence is folded back upon itself, resembling the two p22-*phox* segments which are now positioned with antiparallel orientation of the peptide backbone in this location. In the model shown in Figure 21B, the three contiguous glycine residues in the TAGRFGGGQVGPP sequence may

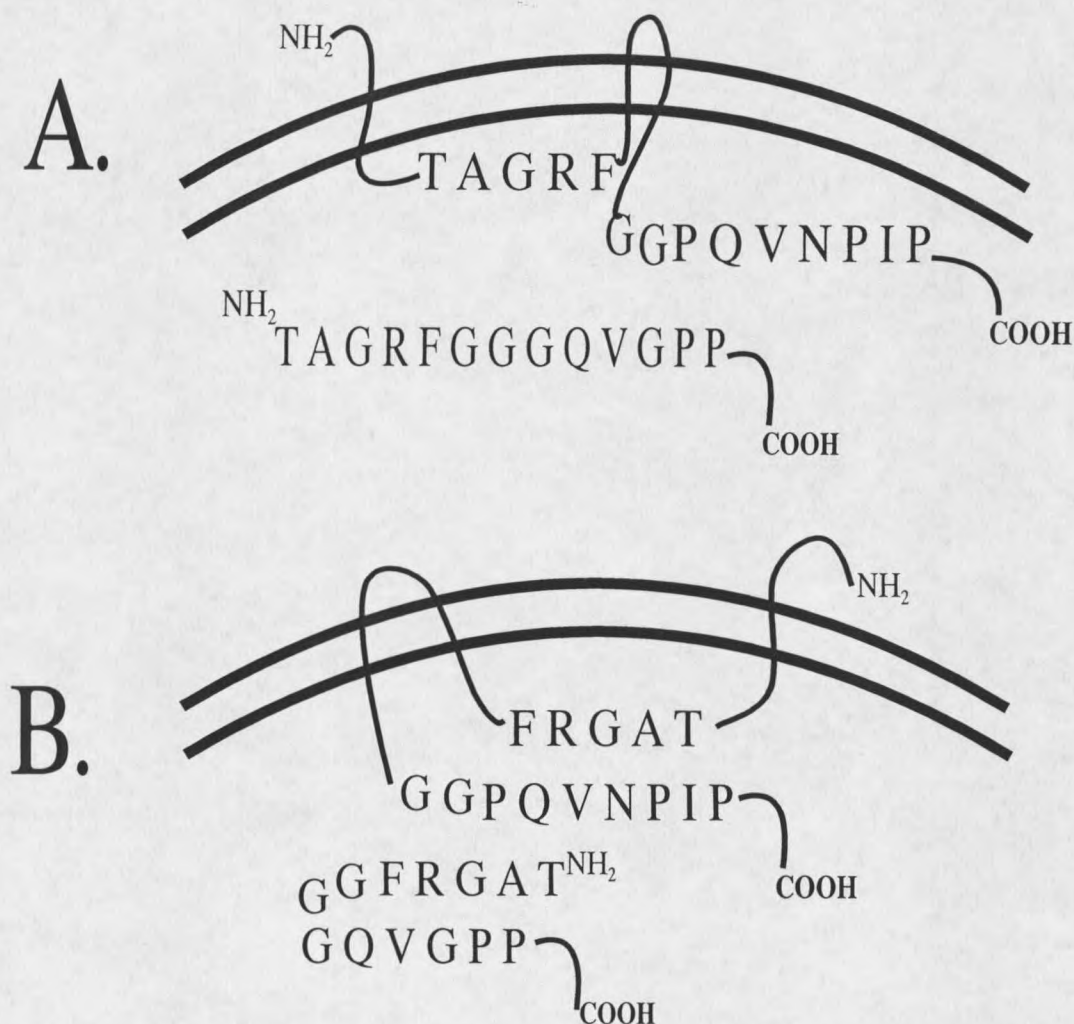


**Figure 21.** Putative models of p22-*phox*. Two different hypothetical models can be proposed to reflect possible tertiary structural constraints of the TAGRF and PQVNPI regions of p22-*phox*, suggested by the consensus phage-displayed peptide obtained by colony-lift immunological screening. (A) The TAGRFGGGQVGPP region of the phage-displayed sequence may assume an extended configuration, as does the combination of the similar regions of p22-*phox*. (B) The TAGRFGGGQVGPP phage sequence may fold back upon itself, resembling the two p22-*phox* segments which are positioned with antiparallel orientation of the peptide backbones in this location. Consistent with view B, the three contiguous glycine residues in the TAGRFGGGQVGPP sequence may allow a hairpin formation in the peptide backbone, and may not contribute to binding by the mAb in a sequence-specific manner, supporting the lack of recovery of glycines in this position as previously suggested.

allow hairpin formation in the peptide backbone, and may not contribute to binding by the mAb in a sequence-specific manner. This possibility supports the lack of glycines in this position in the majority of phage shown in Figure 11A. Our previous results (Figure 11A) also indicate the first proline residue in the phage-expressed PQVRPI sequence, corresponding to P-183 of *p22-phox*, is strongly selected for, and presumed to be critical for recognition by mAb 44.1. Therefore, the position underlined in the sequence, TAGRFGGGQVGPP, would be expected to contain a proline rather than a glycine residue. However, a glycine in this position may be part of the flexible hairpin structure as illustrated in Figure 21B, and without a bulky side chain, may be able to present a kinked peptide backbone and resemble a proline residue.

Our results suggest the phage belonging to the TAGRFGGGQVGPP group may be significant in their representation of the native three-dimensional mAb 44.1 epitope. The alternative explanation, that mAb 44.1 may include two distinct populations of antibody, one specific for each region of the protein is unlikely. Phage expressing peptides resembling only the TAGRF sequence were not recovered by affinity-selection or colony-lift screening with mAb 44.1 and thus it appears more likely that the <sup>29</sup>TAGRF<sup>33</sup> sequence of *p22-phox* is bound most strongly by the mAb when presented in combination with the <sup>183</sup>PQVNPI<sup>188</sup> segment.

It is possible that binding of the <sup>183</sup>PQVNPI<sup>188</sup> region in the native conformation of *p22-phox* by the mAb induces a conformational change in the binding region of the mAb which potentiates recognition of the <sup>29</sup>TAGRF<sup>33</sup> sequence. This hypothesis could explain why phage expressing the TAGRF sequence alone were not identified by this

mAb, and the apparent synergistic binding of the mAb to the putative complex epitope. This characteristic was observed by Western blot analysis in three different situations: 1) the presence of the minimal GRF sequence in the complex epitope, EGRFGGGQVGPP (Figure 19, Lane B), increased staining over the single PQVRPI segment (Figure 19, Lane C) 130%, 2 and 3) after coincubation of the phage-expressed ATAGRFGGG sequence or the synthetic TAGRFTQW peptide increases the staining of the phage-expressed PQVRPI peptide 126% and 135%, respectively. In order to confirm this speculation, a quantitative analysis of this "synergy" should be undertaken to determine the coefficients of binding of the PQVNPI segment in varying ATAGRF peptide concentration.

Folding the TAGRF segment of the TAGRFGGGQVGPP sequence back upon the GQVGPP region (Figure 21B) may bring the positively charged arginine residue in close proximity to the center of the GQVGPP region. This geometry may create a particular positive charge placement in the consensus phage-expressed peptide important for antibody recognition. The preference for an arginine in this vicinity might explain the recovery of many selected phage sequences containing an arginine residue in the consensus PQVRPI sequence as previously reported (Figure 11A). The lack of a positively charged residue in a phage-expressed PQVNPI sequence may explain why this sequence (an exact match to the p22-*phox*) was not selected from the phage library.

The ability to determine the placement of amino acids which exist in close proximity to the surface of folded proteins but not in the primary structure has

previously been reported by the use of a phage-display library (5,6). Our data extends this type of observation to suggest the  $^{183}\text{PQVNPI}^{188}$  and  $^{29}\text{TAGRF}^{33}$  regions of p22-*phox* may be juxtaposed by tertiary structure of the protein and comprise a more complete epitope for mAb 44.1. The inclusion of this number of residues in each region reduces the ambiguity regarding the exact residues involved, even in the absence of X-ray or NMR solution structure data of the protein. This application illustrates a potential use of phage-display library analysis and epitope mapping in revealing regions of tertiary structure in proteins.

References Cited

1. **Curnutte, J. T.** 1993. Chronic granulomatous disease: the solving of a clinical riddle at the molecular level. *Clin. Immun. and Immunopath.* **67**:S2-S15.
2. **Cwirla, S, E. Peters, R. Barrett, and W. Dower.** 1990. Peptides on phage: a vast library of peptides for identifying ligands. *Proc. Natl. Acad. Sci. USA* **87**:6378-6382.
3. **Dinauer, M. C., S. H. Orkin, R. Brown, A. J. Jesaitis, and C. A. Parkos.** 1987. The glycoprotein encoded by the X-linked chronic granulomatous disease locus is a component of the neutrophil cytochrome b complex. *Nature* **327**:717-720.
4. **Dower, W. and S. Cwirla.** 1992. Creating vast peptide expression libraries: electroporation as a tool to construct plasmid libraries of greater than 10exp9 recombinants, p. 291-301. In D. Chang, B. Chassy, J. Saunders, and A. Sowers (eds.), *Guide to Electroporation and Electrofusion*. Academic Press, Inc., San Diego, California.
5. **Felici, F., A. Luzzago, A. Folgori, and R. Cortese.** 1993. Mimicking of discontinuous epitopes by phage-displayed peptides, II. Selection of clones recognized by a protective monoclonal antibody against the *Bordetella pertussis* toxin from phage peptide libraries. *Gene* **128**:21-27.
6. **Luzzago, A., F. Felici, A. Tramontano, A. Pessi, and R. Cortese.** 1993. Mimicking of discontinuous epitopes by phage-displayed peptides, I. Epitope mapping of human H ferritin using a phage library of constrained peptides. *Gene* **128**:51-57.
7. **Parkos, C. A., R. A. Allen, C. G. Cochrane, and A. J. Jesaitis.** 1988. The quaternary structure of the plasma membrane b-type cytochrome of human granulocytes. *Biochim. Biophys. Acta* **932**:71-83.
8. **Parkos, C. A., M. T. Quinn, S. Sheets, and A. J. Jesaitis.** 1992. *Molecular Basis of Oxidative Damage by Leukocytes*. p.45-55. CRC Press Inc., Boca Raton, Ann Arbor, London, Tokyo.
9. **Quinn, M. T., M. L. Mullen, and A. J. Jesaitis.** 1992. Human neutrophil cytochrome b contains multiple hemes. *J. Biol. Chem.* **267**:7303-7309.
10. **Rotrosen, D., M. E. Kleinberg, H. Nuno, T. Leto, J. I. Gallin, and H. L. Malech.** 1990. Evidence for a functional cytoplasmic domain of phagocyte oxidase cytochrome b558. *J. Biol. Chem.* **265**:8745-8750.
11. **Scott, J. and G. Smith.** 1990. Searching for peptide ligands with an epitope library. *Science.* **249**:386-390.

12. **Segal, A. W.** 1993. The electron transport chain of the microbicidal oxidase of phagocytic cells and its involvement in the molecular pathology of chronic granulomatous disease. *J. Clin. Invest.* **83**:1785-1793.
13. **Smith, G. P. and J. K. Scott.** 1993. Libraries of peptides and proteins displayed on filamentous phage. *Methods Enzymol.* **217**:228-257.
14. **Smith, R. M. and J. T. Curnutte.** 1991. Molecular basis of chronic granulomatous disease. *Blood* **77**:673-686.
15. **Teahan, C., P. Rowe, P. Parker, N. Totty, and A. W. Segal.** 1987. The X-linked chronic granulomatous disease gene codes for the b-chain of cytochrome b-245. *Nature* **327**:720-721.

## CHAPTER FIVE

### CONCLUSION

The work included in this dissertation contributes to a new approach in studying the interactive surfaces of proteins; that is to mimic regions critical in binding with linear peptide sequences. These sequences can be affinity selected from preprepared molecular libraries on the basis of their binding to an immobilized molecular ligand. A unique advantage offered by this method is that interactive sequences can be identified without having to make any presumed judgements about the specific regions of proteins involved in binding. This advantage allows research to be performed without preexisting bias which may cause important results to be overlooked or missed entirely. Therefore, this method presents an opportunity to identify critical binding motifs in the absence of any previous information about their nature.

The experimental approach in this work involves the production and use of the J404 random sequence peptide phage-display library. The library is a collection of  $5 \times 10^8$  unique nonapeptides fused to the pIII capsid protein of individual phage virions. The library was used as a source of interactive peptide sequences for the identification

of regions of Cyt b which interact with mAbs or other proteins. Once the interactive peptide regions of Cyt b or other proteins were identified, the specific effect of synthetic or phage-expressed peptide sequence which mimicked the interactive sequence could usually be examined on the system in question. The sequence-specific perturbation of the system by a consensus peptide would thus confirm the specificity of the identified interactive sequence.

The J404 nonapeptide library was used for the identification of consensus peptide sequences critical for over a half dozen systems associated with the human NADPH-oxidase of neutrophils. This number translates to a success in more than half of the experiments in which this method was used. Because the method resolved a number of unrelated sequence specific for different systems, the randomness of the expressed peptides suggested in Chapter 2 corresponds to the utility of the library in varied biological applications.

The library expresses peptides of completely random sequence and thus its use is not limited to systems of the neutrophil. For any purified synthetic or naturally produced ligand, a set of phage-display library clones bearing peptide sequences bound by the ligand probably exists in the library. This suggests sequences of interest for almost any system are present in the library, and once selected, their identification involves relatively predictable nucleotide sequence analysis. Consequently, the most critical and difficult aspects of identifying interactive peptides by this method is the immobilization and presentation of the intended ligand in a biologically relevant manner. In systems in which we failed to identify a predominant binding peptide

sequence, the failure probably was a result of the inability to appropriately present the intended ligand. This inability probably resulted in the loss of clones bearing relevant peptides during selection to the larger pool of clones expressing irrelevant sequences.

Identifying the protein component of a system which contains a peptide region resembling the consensus peptide sequence bound by a particular ligand may be difficult. The ability to search large databases of protein sequences may be helpful in deciphering the relevance of the consensus. However, databases contain only linear sequences of proteins, and interactive peptide segments may be more likely to be produced by discontinuous residues of a protein, presented in the correct form only by the correct three-dimensional configuration of the protein. For this reason, a consensus linear peptide sequence which represents an interactive region may not be included in a database, and its absence does not in itself pale its importance.

An interesting facet of identifying interactive peptides by this method is the opportunity to determine the biological relevance of the some sequences obtained. The result of probing random peptide libraries with a ligand is generally not influenced by preconceived notions about what the outcome should be. In light of this, we have shown results may present interesting questions. Such was the case with the strong consensus KSDXR motif which was found to be involved in the binding of F-actin (Table 8).

Establishing the relevance of this sequence has involved an interesting set of investigations, and is beyond the scope of this discussion. These efforts have led into some pioneering areas of protein modeling based on the three-dimensional X-ray

crystallography of related proteins. The identification of such a three-dimensional conformer requires structural information provided by X-ray crystallography or NMR analysis.

**Table 8.** Deduced Unique Peptide Sequences of Phage Recovered by F-actin Affinity Purification<sup>a</sup>.

Consensus sequence of 128 individual clones <sup>b</sup> :		
<b>GKSDGRDS</b>		
HKSDGRTND	MKTDTREQS	GRKGDDRNS
KSDMRDRQS	EKSDQRNSV	MKTDDRFRND
DTGKQDNRD	KDDSRHGET	QKSDSRGYG
WAVKGDSDR	STFLKSDHR	TQKSDSRTQ
KEDGRVKYN	KSDHRGSLT	SHIVKSDDR
GPKSDDRWS	NKSDARDRW	AKSDLRSNG
NAIKNDSRG	GPAGKRDDR	GLKSDTRIG
SKSDQRDDR	GKSDERSA	ELGKSDDRM
NAGKSDSRH	KLSKGDDRG	EVTKADMED
ATSKSDKRD	AGFTKSDMR	KRDGRHGPP
SFAKDDSRG	AWKTDSRRD	TIKSDSRSG
NIKGDNRVS	TTSRSDKRD	KSDGRAYAA

<sup>a</sup> The above list includes 36 actual sequences which were typical of the 128 clones containing the motif.

<sup>b</sup> Sequence represents the consensus GKSDGRDS motif expressed by 128 of 190 individual clones examined.

The certainty of match between a consensus phage-displayed peptide sequence and the matching sequence in a biological system depends directly on the number of residues resolved. Reports which indicate identification of interactive sequences using other peptide libraries, including synthetic peptide libraries reported to contain three orders of magnitude greater complexity, have failed to resolve interactive peptide regions beyond six amino acid positions. Our data describes the identification of

several interactive sequences containing seven residues when using the J404 phage-display library. One example is the phage clone which expressed the amino acid sequence, QKLSKLAVD, suggests the dipeptide, KL corresponds to the first two positions of <sup>380</sup>KLPKIAVDGP<sup>389</sup> of gp91-*phox* (1). The probability of obtaining a six amino acid match from our library is approximately one in one million. If the KL region of this phage peptide was selected specifically by mAb 54.1 (few other clones contained these residues in these positions), then all residues except isoleucine in the <sup>380</sup>KLPKIAVDGP<sup>389</sup> segment of this protein are represented by residues in affinity-selected phage peptides (Figure 11). Currently, no precedent exists for a match of this degree from a random peptide library. For this reason, it is suggestive that the J404 library may have greater effective diversity than previously reported synthetic (4-6,10-12,14) and polysome libraries (9) of much greater theoretical chemical diversity. The effective diversity of these large synthetic libraries have so far not demonstrated the large potential which they theoretically possess.

The work described in Chapters 3 and 4 involves the identification of regions of Cyt b which are recognized by a mAb. Once the phage-display epitope mapping data is complete, the characterization of the way in which the mAb interacts with the system provides clues to the structure of the system. An advantage of such epitope mapping is that if the manner in which the mAb interacts with or affects the system is useful, the mAb itself may be used as an important reagent for subsequent preparative or analytical methods. One problem with mapping mAb epitopes to provide structural information about a system is that the immunodominant regions of a protein may not

be those most critical to the function. A more direct means of identifying interactive sequences is to probe the phage-display library with a purified system component.

Using both biopanning (13) and column affinity chromatography, recombinant p47-*phox* was used to probe the J404 PDL to identify regions of interaction with Cyt b (2). In this way, the novel <sup>86</sup>STRVRRQL<sup>93</sup> region of the proposed first cytosolic loop of gp91-*phox* and a domain near the cytosolic carboxyl tail, which includes the sequence <sup>450</sup>FEWFADLLQLL<sup>460</sup> were identified. The method was also used to confirm three previously identified regions of interaction between Cyt b and p47-*phox*. These regions of interaction are tabulated in Table 9. The biological relevance of these interactive regions identified by this method was confirmed by synthetic peptide inhibition studies in cell-free superoxide and component translocation assays.

**Table 9.** Deduced Amino Acid Sequences of p47-*phox*-binding Phage Displaying Sequences of Similarity with Cytochrome b.

<u>gp91-<i>phox</i> Cytochrome b Segments</u>		
<sup>85</sup> STRVRRQL <sup>93</sup>	<sup>450</sup> FEWFADLLQLL <sup>460</sup>	<sup>554</sup> ESGPRGVHFIF <sup>564</sup>
<u>Consensus Phage Sequences</u>		
STRVRRQL	FDLL	SGPXXVHFXIF
<u>p22-<i>phox</i> Cytochrome b Segment</u>		
<sup>177</sup> GGPPGGP <sup>183</sup>		
<u>Consensus Phage Sequence</u>		
GGPP		

The ability to mimic a discontinuous epitope with the PDL strengthens the contention that phage-displayed peptides resemble bioactive regions of proteins. This view implies the continuity of the peptide backbone may not be necessary in the interactive region. Alternatively, the presentation of amino acid residues or short regions of linear sequence separated by regions of intervening sequence may be common elements of interactive sequences. Therefore, the specificity of the interactive region may be provided by such variables as the placement, specificity, and perhaps the charges of residues involved. In this context, no general reason exists why these regions cannot be represented by short linear peptides, as long as they can assume the same conformation as the residues involved in the interactive region. The contention that the tertiary structure of a protein can be reproduced by a linear peptide expressed on a phage surface, presents the possibility that this method can be used to predict the three-dimensional structure. This may be especially useful for proteins for which structural data obtained by more conventional methods is not available.

Recently, a report by Luzzago *et al.* (7) illustrated this potential whereby phage-expressed peptides can mimic discontinuous regions of recombinant human ferritin. The phage peptides recovered by affinity selection with an anti-ferritin antibody, resembled an epitope encompassing three amino acids which exist on the native form of this protein. Two populations of phage were selected by this mAb, and found to express either of the consensus sequences motifs, YDxxxxW or GSxF. Support for these sequences as the epitopes of the mAb, which do not resemble any linear amino acid sequences of the protein, was provided by the crystal structure of the

protein. The X-ray crystallography indicated that all of these residues were present in a confined region on the surface of the protein. In a similar report, a discontinuous epitope recognized by a pertussis toxin (PTX) mAb was suspected after the recovery of phage expressing the consensus sequence, GRxPNP which did not resemble the primary structure of PTX (3). Because no three-dimensional structural data exists for PTX, confirmation that such a region exists on the surface of the protein is incomplete.

Prudent future strategies for producing phage-display peptide libraries for the identification of interactive regions of proteins should address: 1) the investigation of other capsid proteins for the expression of peptide sequences with consideration given to structural constraints of the proteins (8); and 2), possible alternatives for structurally unique tether sequences which link the random peptide to the expressing capsid protein.

The chemical diversity of large phage-display libraries reported has become sufficient to allow the inclusion of all five-residue (and probably any six-residue) interactive sequence. Our results indicated that specific binding between an immobilized ligand and a peptide sequence containing as few as three critically placed amino acids often occurs. This result further suggests that parameters affecting affinity selection of phage sequences, and not library diversity, dictates successful results by this method. Therefore, future strategies to produce more productive phage display libraries should address the parameters of affinity selection. Points to consider include the following:

- 1) high recovery of background phage which often interact non-specifically with the selection system,

- 2) the manner in which adherent phage are amplified without introducing any biological bias due to differences in the growth rate of certain phage clones,
- 3) quantities of protein which are used as ligands during selection and avoiding methods of immobilization which may introduce the binding of anomalous phage peptides.

The determination of interactive regions in biological systems by phage-display technology has presented an alternative avenue by which structural information can be determined. The prospect of blocking natural component interactions that take place during infectious and disease processes with novel components identified by this method has already prompted intense research in this area. Furthermore, the structural information gleaned by identifying interactive regions of multisubunit systems provides a better understanding of the interactions of proteins, and may be appropriate for many areas of biological research. Finally, the contention that aspects of tertiary structure of a protein can be mimicked by phage-displayed peptides, suggests that some aspects of the three-dimensional structure of many proteins may be learned in this way. This may be especially useful for determining topological information about proteins for which structural data obtained by more conventional methods is not available.

References Cited

1. **Burritt, J. B., M. T. Quinn, M. A. Jutila, C. W. Bond, and A. J. Jesaitis.** 1995. Topological mapping of neutrophil cytochrome b epitopes with phage-display libraries. *J. Biol. Chem.* (In Press)
2. **DeLeo, F. R., L. Yu, J. B. Burritt, L. R. Loetterle, C. W. Bond, A. J. Jesaitis, and M. T. Quinn.** 1995. Mapping sites of interaction of p47-phox and flavocytochrome b with random sequence peptide phage display libraries. *Proc. Natl. Acad. Sci. USA* (In Press)
3. **Felici, F., A. Luzzago, A. Folgori, and R. Cortese.** 1993. Mimicking of discontinuous epitopes by phage-displayed peptides, II. Selection of clones recognized by a protective monoclonal antibody against the *Bordetella pertussis* toxin from phage peptide libraries. *Gene* **128**:21-27.
4. **Houghten, R. A., C. Pinilla, S. E. Blondelle, J. R. Appel, C. T. Dooley, and J. H. Cuervo.** 1991. Generation and use of synthetic peptide combinatorial libraries for basic research and drug discovery. *Nature* **354**:84-86.
5. **Lam, K. S., M. Lebl, V. Krchnak, S. Wade, F. Abdul-Latif, R. Ferguson, C. Cuzzocrea, and K. Wertman.** 1993. Discovery of D-amino-acid-containing ligands with selectide technology. *Gene* **137**:13-16.
6. **Lam, K. S., S. E. Salmon, E. M. Hersh, V. J. Hruby, W. M. Kazmierski, and R. J. Knapp.** 1993. A new type of synthetic peptide library for identifying ligand-binding activity. *Nature* **354**:82-84.
7. **Luzzago, A., F. Felici, A. Tramontano, A. Pessi, and R. Cortese.** 1993. Mimicking of discontinuous epitopes by phage-displayed peptides, I. Epitope mapping of human H ferritin using a phage library of constrained peptides. *Gene* **128**:51-57.
8. **Makowski, L.** 1993. Structural constraints on the display of foreign peptides on filamentous bacteriophages. *Gene* **128**:5-11.
9. **Mattheakis, L. C., R. R. Bhatt, and W. J. Dower.** 1994. An in vitro polysome display system for identifying ligands from very large peptide libraries. *Proc. Natl. Acad. Sci. USA* **91**:9022-9026.
10. **Pinilla, C., J. R. Appel, and R. A. Houghten.** 1993. Synthetic peptide combinatorial libraries (SPCLs): identification of the antigenic determinant of beta-endorphin recognized by monoclonal antibody 3E7. *Gene* **128**:71-76.

11. **Pinilla, C., J. R. Appel, and R. A. Houghten.** 1994. Investigation of antigen-antibody interactions using a soluble, non-support-bound synthetic decapeptide library composed of four trillion ( $4 \times 10^{12}$ ) sequences. *Biochem. J.* **301**:847-853.
12. **Salmon, S. E., K. S. Lam, M. Lebl, A. Kandola, P. S. Khattri, S. Wade, M. Pátek, P. Kocis, V. Krchnák, D. Thorpe, and S. Felder.** 1993. Discovery of biologically active peptides in random libraries: Solution-phase testing after staged orthogonal release from resin beads. *Proc. Natl. Acad. Sci. USA* **90**:11708-11712.
13. **Smith, G. P. and J. K. Scott.** 1993. Libraries of peptides and proteins displayed on filamentous phage. *Methods Enzymol.* **217**:228-257.
14. **Wu, J., Q. N. Ma, and K. S. Lam.** 1994. Identifying substrate motifs of protein kinases by a random library approach. *Biochemistry* **33**:14825-14833.

APPENDIX

**Table 10.** One Letter Abbreviations for the Amino Acids.

Amino Acid	One-letter Symbol
Alanine	A
Arginine	R
Asparagine	N
Aspartic Acid	D
Cysteine	C
Glutamine	Q
Glutamic Acid	E
Glycine	G
Histidine	H
Isoleucine	I
Leucine	L
Lysine	K
Methionine	M
Phenylalanine	F
Proline	P
Serine	S
Threonine	T
Tryptophan	W
Tyrosine	Y
Valine	V
Undetermined	X

**Table 11.** One Letter Abbreviations for Nucleoside Triphosphates.

Nucleoside	One-letter Symbol
Adenine	a
Thymine	t
Guanine	g
Cytosine	c
Thymine and Guanine (equimolar).	k
Adenine, Thymine, Guanine, and Cytosine (equimolar)	n
Any base	x

**Table 12.** Synthetic Oligodeoxynucleotides.

Oligonucleotide Number	Sequence	Source*
J97 .	5'-ggtttgccaaacaactggcaacagtttcagcggagtgccagtagaatggaac-3'	<i>a</i>
J140 .	5'-gttttgctgtctttccagacg-3'	<i>b</i>
J352 .	5'-ggagattttcaacgtg-3'	<i>c</i>
J364A .	5'-ctctcactcc(nnk) <sub>9</sub> ggcccgcggttgaaagttgt-3'	<i>c</i>
J364B .	5'-ggagtgagagtaga-3'	<i>c</i>
J364C .	5'-ctttcaaccggcgggcc-3'	<i>c</i>
J431A .	5'-ctctcactccgctaccgcgggcccgtttggcggcggcgtggaaagttgt-3'	<i>d</i>
J431B .	5'-ctttccacgccgccccaaaacggcccgcggtagcggagtgagagtaga-3'	<i>d</i>
Universal -40	5'-gttttgctgtctttccagacg-3'	<i>e</i>

## \*Sources

*a* Dr. Tom Blake, Division of Plant and Soil Sciences, Montana State University, Bozeman, MT.

*b* Dr. Mike White, Veterinary Molecular Biology, Montana State University, Bozeman, MT.

*c* Macromolecular Resources, Colorado State University, Fort Collins, CO.

*d* Integrated DNA Technologies, Coralville, IA.

*e* United States Biochemical, Arlington Heights, IL.

**Table 13. Sequencing Filamentous Phage Clones**

1. Inoculate two ml of 2XYT (containing kanamycin at 75  $\mu\text{g/ml}$  for M13KBst vector or tetracycline at 40  $\mu\text{g/ml}$  for fd-tet vector) with a single isolated plaque (or colony of infected cells).
2. Incubate (in a 15 x 200 mm culture tube with a loose fitting cap) at 37°C for 12 hours with vigorous shaking.
3. Following incubation, decant 1.5 ml of turbid culture into a sterile 1.75 ml Eppendorf tube; microfuge at 12,000 RPM for five minutes.
4. Transfer ca. 1.25 ml of the supernatant to a new microfuge tube and add 138  $\mu\text{l}$  40% PEG-8000 and 138  $\mu\text{l}$  of 5 M NaOAC, pH 7.0, MIX WELL, and ice one to twenty-four hours.
5. Label tube containing remaining supernatant. Record on the tube the clone number, experiment number and experiment step number, and keep at 4°C indefinitely in case you need to grow more of that particular clone.
6. Microfuge phage 12,000 RPM for 15 minutes, aspirate supernatant, being careful to avoid the phage (should see a small white pellet), let sit a few minutes, and aspirate again to collect any residual liquid.
7. Add 20  $\mu\text{l}$  10 mM TE pH 7.5 (pH 8.0 seems to be OK), let soak 5-60 minutes, mix well until dissolved.
8. Immerse in boiling water bath five minutes, spin briefly to collect, mix, transfer 7  $\mu\text{l}$  to a fresh tube.
9. To the 7  $\mu\text{l}$  of material in the fresh tube (step #8 above), add one  $\mu\text{l}$  of sequencing primer such as #J140,12 (1 pmol/ $\mu\text{l}$ ), and 2  $\mu\text{l}$  of Sequenase RXN buffer (NOT Sequenase dilution buffer), mix well.
10. Put DNA-primer-buffer mixture (step #9 above) in a 65°C water bath for two minutes, then transfer tubes to a container of water at 65°C (about one liter of water, and a depth of about 3 cm), and let cool slowly to <30°C, over the period of about 30-45 minutes. Try to do steps 11-15 while the water bath is cooling.
11. Label a set of four tubes for each sample with A, T, G, or C.
12. Dispense 2.5  $\mu\text{l}$  of the appropriate termination mix (dideoxynucleotide) to each of the four tubes, cap, and keep in refrigerator until just before use (step #17,

below).

(The following volumes should be enough for 24 clones.)

13. Prepare the diluted labeling mix by adding 8.5  $\mu$ l of labeling mix to 74  $\mu$ l of sterile distilled water, mix well, hold on ice.
14. Prepare the diluted enzyme by adding 8.5  $\mu$ l Sequenase ver. 2.0 enzyme (enzyme is never allowed to warm above  $-20^{\circ}\text{C}$  until you dilute the small amount at this time) with 71  $\mu$ l ice cold enzyme dilution buffer, mix well, keep on ice.
15. Prepare the sequencing mixture by combining:
  - 40  $\mu$ l 0.1 M DTT (from kit)
  - 79  $\mu$ l diluted labeling mix (step #13 above)
  - 84  $\mu$ l diluted enzyme (step #14 above)
  - 3  $\mu$ l  $^{35}\text{S}$ -dATP (catalog #NEG-034H from NEN)mix well, hold on ice.
16. When the water bath has cooled to  $<30^{\circ}\text{C}$ , microfuge annealed DNA samples a few seconds to collect liquid, and hold on ice until ready to use.
17. Put the four tubes containing the termination mixes (step #12 above) in a  $37^{\circ}\text{C}$  water bath.
18. Add 5.25  $\mu$ l of the sequencing mix (step #15 above) to the 10  $\mu$ l of annealed DNA (step #16 above), incubate at room temperature for five minutes.
19. After five minutes, transfer 3.5  $\mu$ l of the DNA-enzyme mix (step #18 above) to each of the four termination mixtures which are now warmed to  $37^{\circ}\text{C}$  (step #17 above), continue incubation at  $37^{\circ}\text{C}$  for five more minutes.
20. At the five minute incubation of step #19 above, add four  $\mu$ l of stop solution, mix well, and either run sample on sequencing gel, or store at  $-20^{\circ}\text{C}$  for up to two weeks.

**Table 14. Procedure for Producing "Starved" K91 Cells.**

1. Inoculate two ml of LB broth with a single colony of K91 cells from a fresh LB agar plate and incubate overnight at 37° C with strong aeration.
2. Dilute one ml of stationary culture into 35 ml of LB broth, and continue incubation in a sterile 250 ml flask as before until OD<sup>600</sup> reaches 0.4, then slow rotations of shaker to about one revolution per second to avoid shearing the F pili, continue incubation for about five minutes.
3. Pellet cells from 25 ml of the culture in a sterile tube at about 2000 xG for about 10 minutes, 23° C.
4. Resuspend the pellet in 25 ml of 80 mM NaCl solution and continue incubation at 37° C for 45 minutes with moderate aeration.
5. Pellet cells as described in step #3.
6. Resuspend cells in one ml of 80 mM NaCl, 50 mM NaPhosphate, pH 6.8. The cells can be kept at 4° C in this buffer for one week.

MONTANA STATE UNIVERSITY LIBRARIES



3 1762 10246824 4